Lung localized protective responses to heterosubtypic influenza challenge

Daniel Hyunwook Paik

Submitted in partial fulfillment of the
requirements for the degree of
Doctor of Philosophy
under the Executive Committee
of the Graduate School of Arts and Sciences

COLUMBIA UNIVERSITY

2020

Abstract

Lung localized protective responses to heterosubtypic influenza challenge

Daniel Hyunwook Paik

Influenza A virus (IAV) is one of the most ubiquitous respiratory viruses in the world, causing significant disease burden in the United States and abroad. Current vaccination strategies that target the generation of humoral immunity offer limited heterosubtypic protection; T cells offer cross-strain protection and the promise of universal immunity against IAV. Local tissue immunity plays a key role in pathogen clearance and tissue protection, particularly in the form of tissue resident memory T cells (TRM), which are a non-circulating memory T cell subset that have been shown in a variety of tissue sites to be superior mediators of protection compared to circulating memory T cells. At the same time, T cell immunity has been associated with inflammatory processes that may also lead to lung immunopathology. How lung tissue localized T cell immunity mediates its protection during a recall response to IAV challenge is not well understood.

Using the lymphocyte sequestering drug FTY720, we show that primary infection with H3N2 IAV strain X31 provides tissue localized heterosubtypic immunity independently of humoral immunity against an H1N1 PR8 IAV strain. Within the lung resident niche, the recall response drives faster $CD4^+$ and $CD8^+$ T cell expansion compared to a primary infection. This rapid T cell expansion resulted from *in situ* TRM proliferation that was augmented by the migration of peripheral T cells. By tracking a naïve T cell population specific for the IAV strain used in secondary challenge, we demonstrate that influenza-specific T cells, including those specific for newly introduced antigens, migrate to the lung niche from the local mediastinal

lymph node (medLN) where both $CD4^+$ and $CD8^+$ T cells experience enhanced priming and proliferation. We further show that primary infection fortifies the medLN with persistently increased numbers of T cells as well as both $CD103^+$ and $CD103^-$ conventional dendritic cells (cDCs) that are transcriptionally similar to cDCs in an infection naïve mouse. By depleting $Zbtb46^+$ cDCs, we determine that cDC fortification is a crucial mechanism for enhanced T cell priming and expansion in the medLN during a recall response.

We also found that lung localized $CD4^+$ T cell responses exhibit significant immunomodulatory function. Polyclonal lung $CD4^+$ TRM generated by influenza infection as well as lung OT-II TRM exhibit increased production of antiviral inflammatory cytokines in addition to enhanced IL-10 family cytokine production compared to splenic $CD4^+$ effector memory T cells (TEM). During a heterosubtypic challenge, we further observed that lung niche non-TRM $CD4^+$ T cells produce significantly more *in situ* IL-10 compared to a primary infection, which modulated airway IFN-ɣ and TNF-α production without any depreciation in viral clearance. Immunomodulatory characteristics of a recall response was reflected in lung tissue-wide transcriptional downregulation of innate responses such as type I IFN responses compared to a primary infection. This work demonstrates the dual antiviral and immunomodulatory protective role of enhanced tissue-localized T cell responses during the recall response to IAV challenge.

Table of Contents

List of Figures and Tables iii
List of Abbreviations v
Acknowledgments vi
Chapter 1: Introduction 1
1.1: Overview of influenza A virus infection 1
1.2: Influenza virus 2
Figure 1.1: Influenza A viral structure 5
1.3: Innate signaling responses to influenza A 7
1.4: Innate cellular response to influenza 9
Figure 1.2: Innate cellular responses to influenza A 13
Figure 1.3: DC lineage development 15
1.5: Adaptive response to primary IAV infection 17
Figure 1.4 T cell priming 21
1.6: Memory T cells 23
Figure 1.5 Memory T cell migratory characteristics 27
1.7: Tissue resident memory T cell antiviral protective capacity 29
Figure 1.6: TRM protective antiviral function 34
1.8: Trained innate immunity 36
1.9: Thesis Aims 37
Chapter 2: Materials and Methods 40
2.1: Influenza virus preparation and murine infection 40
2.2: Influenza viral titer determination 40
2.3: Proliferation dye labeling and transgenic T cell isolation and transfer 41
2.4: Mouse tissue digestion and cellular isolation 41
2.5: In vivo labeling 42
2.6: Flow cytometry staining protocol 43
Table 2.1: List of antibodies used for flow cytometry 44
2.7: FTY720 treatment 45
2.8: OT-II RAG$^{-/-}$ memory mouse generation 45
2.9: *In vitro* T cell peptide stimulation and cytokine analysis 45
2.10: αIL-10R antibody blockade 46
2.11: Generation of zbtb46-DTR bone marrow chimeras 46
2.12: Diphtheria toxin preparation and administration 46
2.13: RNA Sequencing and Analysis 46
2.14: Mouse strains 49
2.15: Statistical Analysis 49
Chapter 3: Influenza infection imprints local lymphoid sites to promote lung resident heterosubtypic immunity 50

3.1: Abstract....50
3.2: Introduction....51
3.3: Results....53
Lung niche T cells mediate protective responses to heterosubtypic influenza infection independent of B-cells....53
Expansion of CD103$^-$ negative T cells within the lung resident niche and medLN during recall....63
Enhanced T cell priming to new epitopes in the secondary response drives effector migration to the lung resident niche....73
Prior influenza infection fortifies local lymph nodes for T cell priming....79
Increased numbers of conventional dendritic cells persist in the medLN following influenza infection....84
Lymph node DC are required for protection and enhanced CD4$^+$ and CD8$^+$ T cell priming in the recall response....89
3.4: Discussion....95
Chapter 4: Local lung tissue immunoregulation during heterosubtypic influenza challenge....98
4.1: Abstract....98
4.2: Introduction....99
4.3: Results....101
Enhanced lung TRM cytokine production is modulated by tissue antigen-presenting cells....101
Lung environment undergoes globally attenuated innate immune response during heterosubtypic challenge....108
Enhanced IL-10 production by lung niche CD4$^+$ T cells during heterosubtypic influenza challenge....113
IL-10 signaling modulates Th1 responses but preserves heterosubtypic immunity....117
4.4: Discussion....120
Chapter 5: Conclusions....123
Figure 5.1: Proposed model of lung-localized T cell immune responses to heterosubtypic IAV challenge....126
References....132
Appendix A: Accepted Abstracts....144
Appendix B: Abstracts of contributing author manuscripts....145

List of Figures and Tables

Chapter 1

Figure 1.1: Influenza A viral structure

Figure 1.2: Innate cellular responses to influenza A

Figure 1.3: DC lineage development

Figure 1.4: T cell priming

Figure 1.5: Memory T cell migratory characteristics

Figure 1.6: TRM protective antiviral function

Chapter 2

Table 2.1: List of antibodies used for flow cytometry

Chapter 3

Figure 3.1: Influenza infection generates memory $CD4^+$ and $CD8^+$ T cells in the lung tissue niche and draining lymph node.

Figure 3.2: Primary infection generates influenza-specific local memory T cells

Figure 3.3: T cell-mediated protection to heterosubtypic challenge is tissue-localized and independent of B cells.

Figure 3.4: Local resident memory persists after FTY720 treatment

Figure 3.5: Heterosubtypic recall promotes rapid accumulation and proliferation of lung niche CD103- T cells

Figure 3.6: FTY720 treatment does not block T cell migration to lung niche

Figure 3.7: The recall response enhances accumulation and proliferation of medLN T cells

Figure 3.8: Lymphoid T cell expansion during recall response

Figure 3.9: Recall response enhances local lymph node T cell priming and migration to the lung tissue niche

Figure 3.10: Enhanced medLN T cell priming in B cell-deficient mice

Figure 3.11: FTY treatment does not affect IAV-specific T cell lung migration

Figure 3.12: Enhanced naïve T cell recruitment, activation and proliferation in the medLN during the recall response

Figure 3.13: Influenza infection promotes long-term quantitative increases in cDC in the medLN

Figure 3.14: MedLN cDC are required for enhanced T cell priming and protection during the recall response

Chapter 4

Figure 4.1: Cytokine profile of αCD3/28 bead stimulated CD4 lung niche and splenic memory T cells

Figure 4.2: Tissue specificity of lung CD4 TRM cytokine production dependent on antigen-presenting cells type

Figure 4.3: Enhanced lung niche CD4 IL-10 production during recall response

Figure 4.4: Recall response IL-10 signaling modulates Th1 responses while maintaining antiviral protection

Figure 4.5: Early recall response modulates early innate response of the total lung transcriptome

Chapter 5

Figure 5.1: Model of fortified medLN enhancement of local T cell priming and tissue migration

List of Abbreviations

IAV: Influenza A virus

TRM: Tissue resident memory T cells

TEM: Effector memory T cells

TCM: Central memory T cells

LN: Lymph node

MedLN: Mediastinal lymph node

FRT: Female reproductive tract

DC: Dendritic cell

cDC: Conventional dendritic cell

MoDC: Monocyte-derived dendritic cell

pDC: Plasmacytoid dendritic cell

NK cell: Natural killer cell

AM: Alveolar macrophage

IM: Interstitial macrophage

DT/DTR: Diphtheria toxin/diphtheria toxin receptor

BAL: Bronchoalveolar lavage

RNAseq: RNA sequencing

TCR: T cell receptor

Acknowledgments

I would like to thank my thesis advisor, Dr. Donna Farber, who has been so important not only for the work I present here, but also for my progression as a scientist. She gave me the opportunity to freely explore the ideas that I chose to pursue. Even my ideas and decisions led to a host of failures, Dr. Farber offered me encouragement and patiently guided me through my scientific hurdles so that I could achieve my goals. I feel extremely fortunate to also have a mentor who is not only great at her job, but also invested in her the well-being of her trainees.

I would also like to thank my thesis committee members Dr. Sankar Ghosh, Dr. Anthony Ferrante, and Dr. Anne Moscona, who have provided invaluable feedback and advice throughout the course of my PhD ever since my qualifying exam. I would also like to thank Dr. Andrew Yates for being an outside examiner for the defense, as well as his wonderful insight for the collaboration between our labs (as well as his great coffee).

I am grateful to the MD/PhD directors Dr. Patrick Spitalnik, Dr. Ronald Liem, and Dr. Steven Reiner not only for offering me the opportunity to pursue my medical and scientific dreams at Columbia University, but also for all their hard work and support in ensuring the success of the program. I must also thank Jeffrey Brandt, Rebecca Spurr, and Kaitlyn Matthews as well for all their essential work behind the scenes for the MD/PhD program. In addition, I would like to thank Ms. Zaia Sivo of the Integrated Graduate Program without whom the graduate program would cease to function.

My research would not be possible without the people of the flow cytometry core in the Columbia Center for Translational Immunology, particularly former manager Dr. Siu-Hong Ho, as well as current managers Dr. Caisheng Lu, Dr. Wei Wang, and associates Sean Chen and Jie Fu. Their technical assistance and expertise in flow cytometry and cell sorting was invaluable.

I would also like to thank two former mentors Dr. Michael Lenardo of the NIAID Lab of Immunology as well as Dr. Raymond Samuel of Hampton University. Their enthusiasm and guidance in my early experiences in biomedical research spurred me to seek more of it.

My current and former lab members have also played a critical aspect of my growth and development as a scientist, and much of my own studies is built upon the work of those that came before me. I would in particular like to recognize Dr. Kyra Zens who was a former graduate student that taught me many laboratory techniques and protocols that I used for much of my own work. I would also like to recognize my classmate Dr. Brahma Kumar who was a great friend and offered me great scientific (and non-scientific) discussion. I would also like to thank Dr. Puspa Thapa for her insight and discussion of scientific and technical issues specific to our work on murine influenza models.

I must recognize my wonderful family – my mother, father, and brother. Life is unimaginable without family, and their support and values make me who I am. And finally, I would like to thank my wonderful wife, Dr. Apiradee Sanglimsuwan, for her continual love and support.

Chapter 1: Introduction

1.1: Overview of influenza A virus infection

Influenza A virus (IAV) is an enveloped RNA virus of the family *Orthomyxoviriade* and can be either spherical or filamentous in shape, at sizes of approximately 100 nm in diameter or 300 nm in length, respectively [1]. It is a tropic virus that infects humans who are exposed to droplets containing viral particle, typically in the upper respiratory tract, eventually spreading to the lower respiratory tract where it infects the epithelial cells of the airway and alveoli, inducing acute respiratory distress syndrome (ARDS) in the most severe clinical cases. Although influenza virus consists of several subtypes, influenza epidemics are mainly caused by influenza A (>75%) [2].

The innate immune response immediately responds to IAV infection, producing a host of soluble antiviral mediators and triggering a tissue-wide antiviral state. These include interferons (IFN-α, IFN-β, IFN-λ) as well as pro-inflammatory cytokines (IFN-γ, TNF-α, IL-6, IL-1β) that may be produced by a wide variety of cells, including epithelial cells as well as specialized innate immune cells such as dendritic cells, macrophages, neutrophils, and natural killer cells [3]. Innate immune cells may kill infected cells, clear debris, or present viral antigen to T and B cells to activate the adaptive immune system, a function classically performed by dendritic cells.

Both $CD4^+$ and $CD8^+$ T cells mount a specialized and effective immune response that ultimately peaks several days after the initial viral exposure. $CD4^+$ and $CD8^+$ perform essential roles in IAV clearance through robust cytokine and chemokine production as well as cytotoxic killing of virus-infected cells [4]. Activated B cells produce neutralizing immunoglobulins that clear virus and are critical to disease resolution and host recovery. Upon resolution, long-lived plasma cells and memory T cells provide long-term adaptive immunity against the encountered

strain of IAV. Here, we seek to better understand the mechanisms that contribute to T cell-mediated immunity to IAV infection during a memory response.

1.2: Influenza virus

IAV is among the most prevalent infectious respiratory disease-causing viruses in the world, estimated by the Center of Disease Control to contribute to roughly 50,000 deaths and 500,000 hospitalizations per year in the United States alone. Epidemiologically, influenza is characterized by outbreaks in the northern and southern latitudes as the basic reproductive number (R_0) increases during colder and drier winter months. On the other hand, influenza prevalence tends to be more consistent in equatorial regions that have less seasonal climate variance. The proliferation of international air travel has not only connected countries and people with one another, but also the diseases that they harbor, leading to a perpetual circulation of newly emerging strains of influenza. New strains of influenza virus arise from minor genetic mutations of surface antigens known as antigenic drift, which allows the virus to elude immunity raised against prior iterations of the virus. Although humans are a primary reservoir of pathogenic strains, influenza virus is widely circulated among many other animal species. Strains of zoonotic origin contain particularly diverse and novel strains, most notably from wild avian reservoirs, which pass on to humans through domesticated poultry intermediates [5]. More dramatic alterations, known as antigenic shift, is typically caused by genomic reassortment between viral strains from different animal hosts. Antigenic shift is associated with greater disease spread and severity due to significant immune evasion and contain increased pandemic risk; most recently, the pandemic 2009 H1N1 strain emerged from a reassortment of human, avian, and swine flu genomic segments [6].

The viral structure consists of three major components: the viral envelope, matrix protein (M1), and its viral ribonucleocapsid (vRNP) core (Fig. 1.1). The viral envelope is a phospholipid bilayer containing the major surface glycoproteins hemagglutinin (HA) and neuraminidase (NA), as well as the M2 ion channel (BM2 in influenza B), all of which play major roles in host cell entry and exit. Surface glycoproteins NA and HA are the primary antigenic determinants of the adaptive immune response, and variations in these two proteins define the viral subtype. The HA structure is composed of a cylindrical head, which is a trimeric, globular structure composed of three identical polypeptide chains that is connected to a stalk-like polypeptide stem. HA comprises ~80% of the viral envelope proteins and forms the spikes of the viral surface; HA mediates viral binding and fusion with the lipid membrane of target cells. NA is a mushroom shaped tetrameric enzyme that is critical in catalyzing the release of sialic acid residues to facilitate both viral linkage and release. Matrix protein M1 maintains and controls the structure of the viral particle. The genomic core consists of eight distinct genomic RNA segments and its bound viral ribonucleocapsid (vRNP) core which consists of its trimeric RNA polymerase (PB1, PB2, and PA) and nucleoprotein (NP), which binds to RNA segments and facilitates full-length gene replication and transcription [7].

At the cellular level, the IAV infectious cycle begins when viral HA binds to sialic acid residues on host cell glycoproteins and glycolipids, which initiates IAV internalization through receptor mediated endocytosis. IAV sialic acid binding is highly specific and a determinant of species tropism. Because human respiratory epithelial cells mostly contain α(2, 6) linkages, IAV originating from different species such as birds, which are specific for α(2, 3) sialic acid residues, must mutate or acquire genetic material from other viruses in order to adapt to human sialic acid residues [8]. Upon endocytic fusion, the pH and K^+ environment of the endosome lead to M2

channel activation and subsequent H^+ influx and K^+ efflux, leading to exit from the endosome. Newly released vRNP then enter the host cell nucleus and initiate transcription of positive sense RNA which is exported to the cytoplasm for protein translation. Newly translated surface glycoproteins HA and NA localize and cluster at the assembly site, located on the apical side of the host epithelial cell membrane. Along with M1, these proteins alter the viral structure to initiate budding and further recruit M2 protein and vRNPs which are necessary for a complete viral particle [9, 10]. As the virus buds from the cell, NA cleaves the sialic acid – glycoprotein bonds to release the viral particle from the host cell and propagate the cycle once again.

Figure 1.1: Influenza A viral structure

Influenza is a spherical or filamentous structure (spherical structure depicted) composed of a plasma membrane envelope that contains eight negative-sense RNA genomic segments. Nucleoprotein (NP) proteins are bound to the genomic segments which are read by RNA polymerases PA, PB1, and PB2. M1 matrix protein maintains the structural integrity of the viral particle. The M2 proton channel plays a key role in regulating viral pH to mediate viral component release after host cell entry. Hemagglutinin (HA) and neuraminidase (NA) are the primary surface glycoproteins that recognize sialic acid residues and play key roles in host cell fusion and budding. Both proteins are the primary antigenic sources for humoral immune responses.

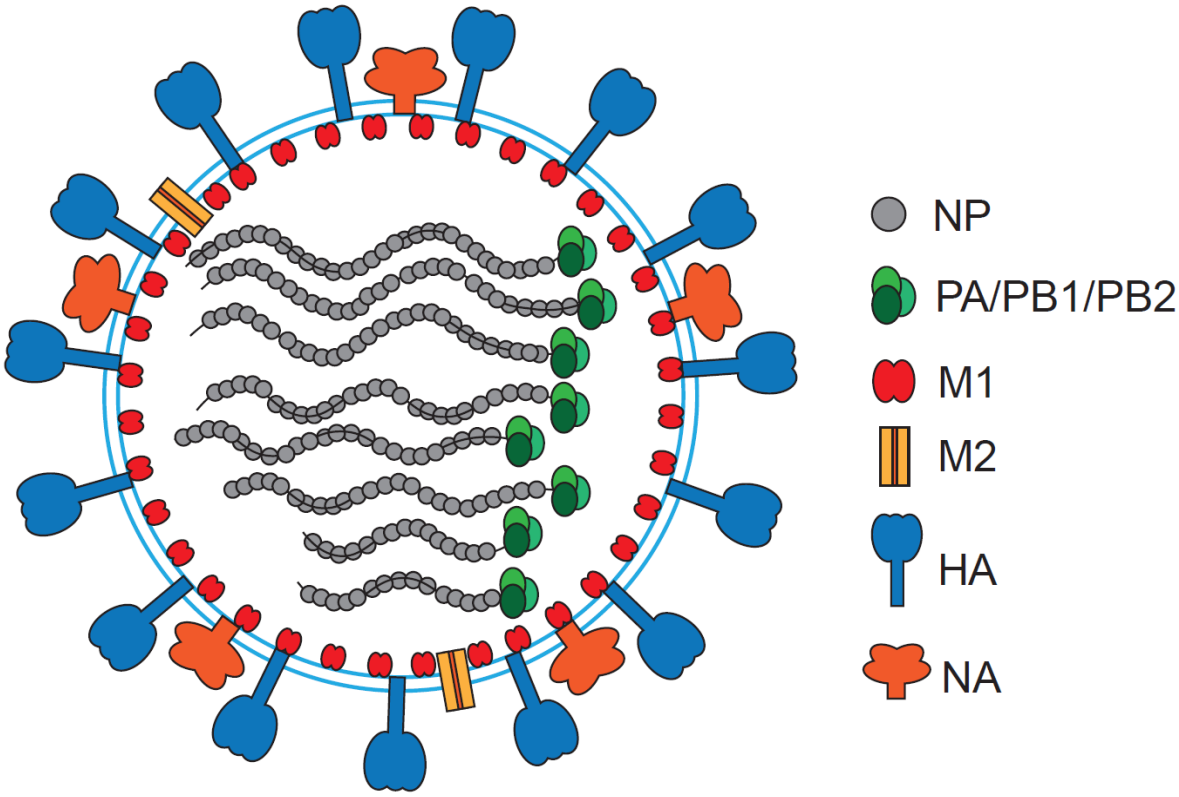
NP
PA/PB1/PB2
M1
M2
HA
NA

1.3: Innate signaling responses to influenza A

The innate immune response provides a multifactorial defense against pathogen infection that determine the outcome of disease progression. The first line of defense are physical barriers such as the epithelial cell layer, which lines the respiratory tract and physically prevents pathogens from penetrating into the body. At the physical barrier layer, epithelial and immune cells also secrete antimicrobial peptides including defensins and cathelicidins [11], whose mechanism of action is based upon their disruption of bacterial membranes. Mucus production provides an additional barrier layer by preventing the attachment of the pathogen to the epithelium, and ciliary motion continuously clears mucus and trapped pathogen and debris. However, because IAV directly infects epithelial cells, additional innate mechanisms are necessary for protection.

Early IAV infection and proliferation triggers antiviral responses to enhance host cell viral resistance and inhibit viral replication. Pathogen recognition receptors (PRRs) on host cells recognize pathogen associated molecular patterns (PAMPs), which are molecular motifs such as such as certain nucleic acids, protein structures, lipids, and carbohydrate structures that are unique for various pathogen classes (viruses, bacteria, fungi, and helminths). The triggering of these receptors by influenza leads to the activation of many antiviral responses, including the secretion of cytokines and chemokines.

The internalization of IAV and IAV-infected host cells introduces viral RNA that is sensed by Toll-like receptors (TLR) 3 and 7 in the endosome [12, 13] and retinoic acid-induced gene I-like receptor (RIG-I) [14] in the cytoplasm, which comprise the two major sensor types that induce robust type I interferon (IFN) production [15, 16]. Type I interferons are produced by a wide range of immune and non-immune cells in the lung, including epithelial cells, dendritic cells, and macrophages. Type I IFN bind to IFNAR and suppress viral replication by activating the

JAK/STAT pathway to upregulate interferon stimulated genes (ISG), which include hundreds of differentially expressed genes [17]. The orthomyxovirus resistance gene (MX) was one of the earliest discovered ISGs, and its lack of function in most laboratory mice strains are a key determinant for their susceptibility to influenza infection which demonstrates the importance of ISGs in anti-IAV immunity. ISGs also inhibit viral replication through RNA cleavage [18], translational block [19], and viral cycle inhibition [20, 21] among many other mechanism. While type I IFNs have broad effects on nearly all cell types, type III IFNs, specifically IFN-λ, perform similar functions but act specifically on epithelial cells including those in the respiratory tract [22]. Influenza viruses evade the IFN system through their production of NS1, NEP, PB-F2, and PA-x to neutralize type I IFN signaling by suppressing downstream kinases and transcription factors [23], enabling a productive infection to take hold.

Innate immune cytokines and chemokines also play a major role in protection by increasing inflammation and the recruitment of additional leukocytes. Activation of the NLRP3 inflammasome by macrophage and dendritic cell-derived IL-1 has been demonstrated to be essential for anti-IAV resistance [24, 25], although NLRP3 does not induce direct antiviral function. TNF-α and IL-6 are further mediators of inflammation that are highly upregulated in bronchoalveolar lavage samples from patients [26] and are critical for antiviral protective effects [27, 28]. Chemoattractants are also produced at high levels to recruit immune cells as part of both the adaptive and innate responses. IP-10, RANTES, and MCP-1 is secreted by epithelial cells to attract monocytes, DCs, macrophages, and effector T cells [29]. IL-8 production attracts neutrophils, while playing important roles in influenza protection and recovery. However, while inflammatory cytokines and chemokines are essential for antiviral protection, increased production is correlated with IAV strain pathogenicity and worse clinical outcomes [30].

1.4: Innate cellular response to influenza

The innate immune response to IAV is not confined to soluble mediators; neutrophils, macrophages, dendritic cells, and NK cells play diverse roles in early antiviral immunity such as environmental surveillance, cytokine production, cytolytic effector activity, debris clearance, tissue repair, and antigen presentation (Fig. 1.2). Early in the course of infection, natural killer (NK) cells kill infected host cells early in the course of infection prior to the development of adaptive immunity. NK cells utilize a combination of perforin and granzyme release, Fas mediated apoptosis, and antibody-dependent cellular cytotoxicity (ADCC) to kill infected cells. Defective NK function leads to impaired viral clearance and increased morbidity and mortality in mouse models [31]. PMNs, also known as neutrophils, are the most abundant leukocyte in the blood and rapidly respond to bacterial threats through mechanisms such as phagocytosis and release of anti-bacterial enzymes [32]. Though excess neutrophilia is associated with increased morbidity, neutrophil function remains crucial for both protection and resolution of influenza infection [27, 33] Dendritic cells (DCs) and macrophages also play critical effector and maintenance roles and are the primary professional antigen-presenting cells (APCs) in the IAV response, representing a bridge to adaptive immunity.

Macrophages

Macrophages are primarily phagocytic cells which engulf bacteria and cellular debris upon PRR stimulation. Macrophages are present in virtually all tissue sites and are important not only for host defense but also tissue maintenance and equilibrium, particularly in anti-inflammatory and tissue repair functions [34-36]. In the lung, two major macrophage populations are present:

alveolar macrophages (AM) and interstitial macrophages (IM). IM express high levels of CD11b expression and low levels of CD11c. IM are found in the lung parenchyma and are thought to play an immunomodulatory role because of their high IL-10 production [37, 38]. Located within the airway lumen, AMs can be identified by high surface expression of CD11c and Siglec-F as well as low expression of CD11b. Of the two lung macrophage populations, AM have been found to be most critical for host defense due to their highly phagocytic nature and secretion of inflammatory, anti-pathogen factors such as nitric oxide (NO), IFN-ɣ, TNF-α, and IL-6. Furthermore, AM have also been shown to reduce inflammation and repair damaged tissue through phagocytosis of apoptotic cells in a process known as efferocytosis its byproduct prostaglandins [39]. Aberrant AM phagocytosis has been implicated in human disease such as asthma [40, 41], chronic obstructive pulmonary disease [42], and interstitial lung disease [43].

Dendritic Cells

Dendritic cells are a cornerstone of innate immunity, performing early innate effector function as well as antigen presentation to activate the adaptive immune response. Dendritic cells are critical immune sentinels and highly responsive to environmental cues. DC patrol and sample the local milieu for antigen to present and prime T cells, bridging the innate and adaptive immune responses. DCs are among the earliest responders to influenza and are represented by a heterogeneous population that includes conventional DCs (cDCs), monocyte-derived DCs (moDCs), and plasmacytoid DCs (pDCs). Though these subtypes all derive from common bone marrow progenitors [44], their lineages (Fig. 1.3) and function have distinct differences.

Plasmacytoid dendritic cells are functionally distinct from other DC subsets, offering little in the way of antigen presentation but playing an outsized role in early interferon and cytokine

production. They are characterized by their antiviral function and low expression of CD11c, myeloid markers, and MHC class II, which corresponds with less efficient antigen presentation [45]. pDCs express very high levels of TLR7 and TLR9 [46] and rapidly produce antiviral cytokines such IFN-α in the presence of viral nucleic acids [47, 48]. Upon exposure to IAV, pDCs rapidly release large quantities of type I IFN and other cytokines, playing a major role in early antiviral immunity (Fig. 1.2). Impaired pDC activity has been linked to significantly impaired antiviral function [49]. However, pDCs have also been shown to be dispensable in a sublethal IAV infection [50], suggesting that their contributions to anti-IAV immunity are not well defined.

Monocyte-derived DCs derive from blood-borne monocytes and are phenotypically similar to cDCs due to their efficient antigen presentation capabilities and high CD11c expression, but are distinct in lineage and lack cDC markers *FLT3* and *ZBTB46*. IAV-induced inflammation recruits monocytes to the lung tissue as well as draining lymph nodes where they differentiate into moDCs. However, their role in mediating protective immunity is unclear as IAV-induced lymph node moDC have poor T cell priming function [51].

Conventional DCs are superior antigen presenters compared to other DC subsets and exhibit the ability to cross-present antigen on MHC class I. Respiratory cDCs are primarily comprised of $CD11b^{-}$ $CD103^{+}$ and $CD11b^{+}$ $CD103^{-}$ subsets which localize to the airway mucosa and the lung parenchyma, respectively [52]. These cDCs continuously sample their environment through constitutive macropinocytosis [53]. After exposure to IAV, lung and airway DCs acquire IAV antigen through a combination of receptor-mediated endocytosis of viral particles as well as phagocytosis of host infected cells (Figure 1.2) [54, 55]. cDCs may also acquire antigen by becoming infected themselves; *in vitro* studies show that cDCs may be infected by IAV [56, 57], although animal studies have suggested that DC infection is not a necessary requirement for

antigen acquisition and transport. Upon transport to the lymph nodes, migratory DC transfer antigen to lymph node DC as well, providing a mechanism for the efficient distribution of IAV antigen to all LN DC and increasing the number of APCs that can activate the anti-IAV T cell response [58].

IAV infection also produces inflammatory signals (e.g. PRR activation, cytokine signaling) and activates cDCs which then undergo rapid maturation which manifests in increased expression of co-stimulatory molecules such as CD80 and CD86 as well as homing receptors such as CCR7 [59]. Upon antigen acquisition, the $CD11b^{-}CD103^{+}$ subset, also known as the migratory subset, more rapidly and efficiently migrates to the draining mediastinal lymph node (medLN) [60]. Ultimately, both $CD11b^{+}$ and $CD103^{+}$ respiratory cDCs subsets eventually migrate to the medLN along the CCL21 gradient to the afferent lymphatic vessels of local lymph nodes [61]. An intra-nodal CCL21 gradient further directs activated cDCs into the T cell rich zone where they can effectively initiate the adaptive immune response [62]. Conventional DCs have been shown to be essential to T cell responses and the depletion of $CD11c^{+}$ DCs during IAV infection significantly impairs viral clearance and clinical severity in a murine model [51, 63]. Although innate and adaptive responses are distinct from one another, their interactions are critical to maintaining host protection.

Figure 1.2: Innate cellular responses to influenza A

A constellation of innate cells rapidly responds to IAV infection. Plasmacytoid dendritic cells (pDC) rapidly produce large quantities of type I interferons to promote tissue-wide antiviral function. Natural killer cells (NK) kill infected host cells through both the release of soluble mediators and receptor-ligand mediated cell death. Alveolar macrophages (AM) and polymorphonuclear cells (PMN) phagocytose cellular debris to maintain tissue homeostasis and produce cytokines that amplify the immune response. Interstitial macrophages (IM) are present in lower levels but also produce cytokines. Conventional and monocyte-derived dendritic cells (DC) acquire viral antigen through host cell phagocytosis and receptor-mediated endocytosis of IAV particles and migrate to local lymph nodes to present IAV antigen to initiate T cell responses

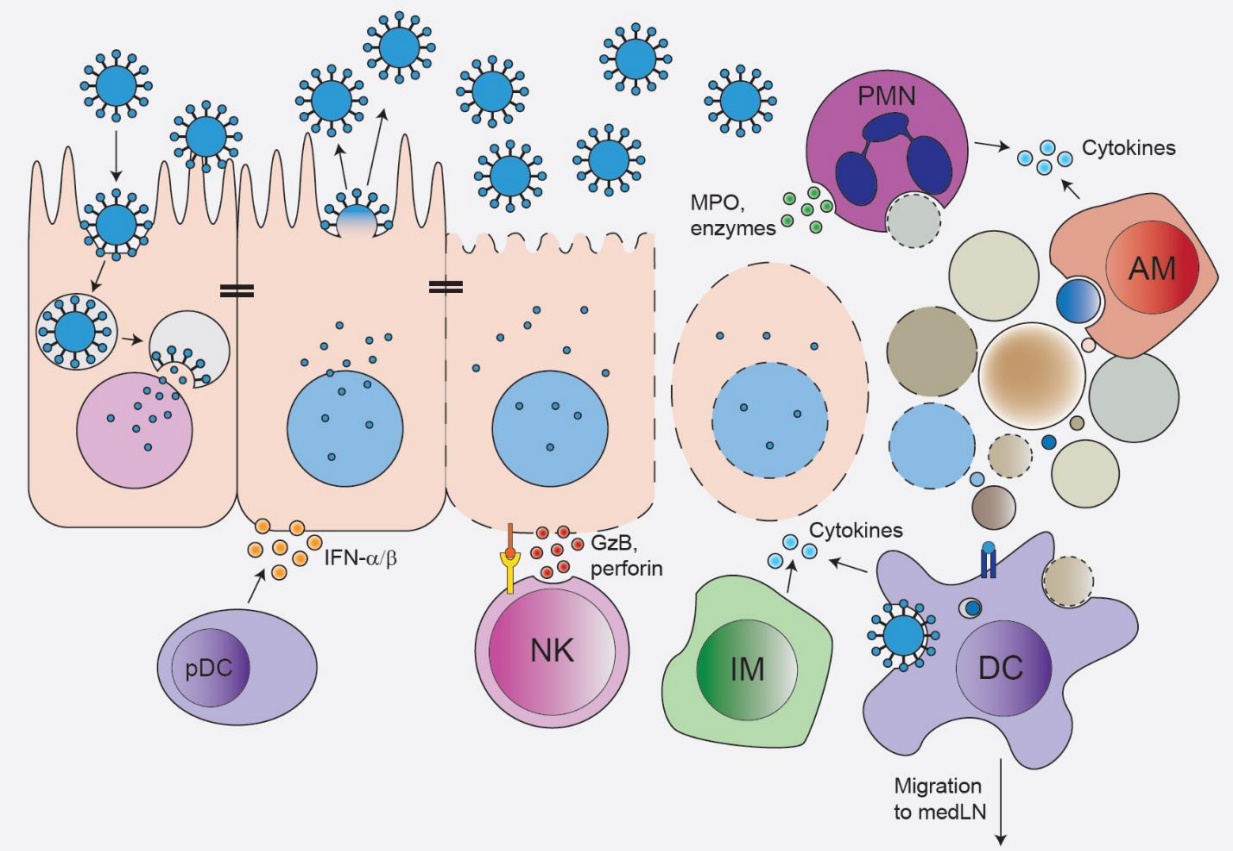
PMN
Cytokines
MPO,
enzymes
AM
IFN-α/β
GzB,
perforin
Cytokines
pDC
NK
IM
DC
Migration
to medLN

Figure 1.3: DC lineage development

All dendritic cell subsets derive from monocyte-dendritic cell progenitors (MDP) which ultimately derive from hematopoietic stem cells (HSC) in the bone marrow. These MDPs may yield monocytes or common dendritic precursors (CDP). Monocytes exit the bone marrow to circulate throughout the body and under certain conditions, may differentiate into monocyte-derived dendritic cells (moDC) at the tissue site. In the bone marrow, CDPs may differentiate into plasmacytoid dendritic cells, which circulate throughout the body, or into pre-dendritic cells (pre-DC), which also circulate throughout the body. Conventional dendritic cells may then derive from these circulating pre-DCs in peripheral tissue or lymphoid sites.

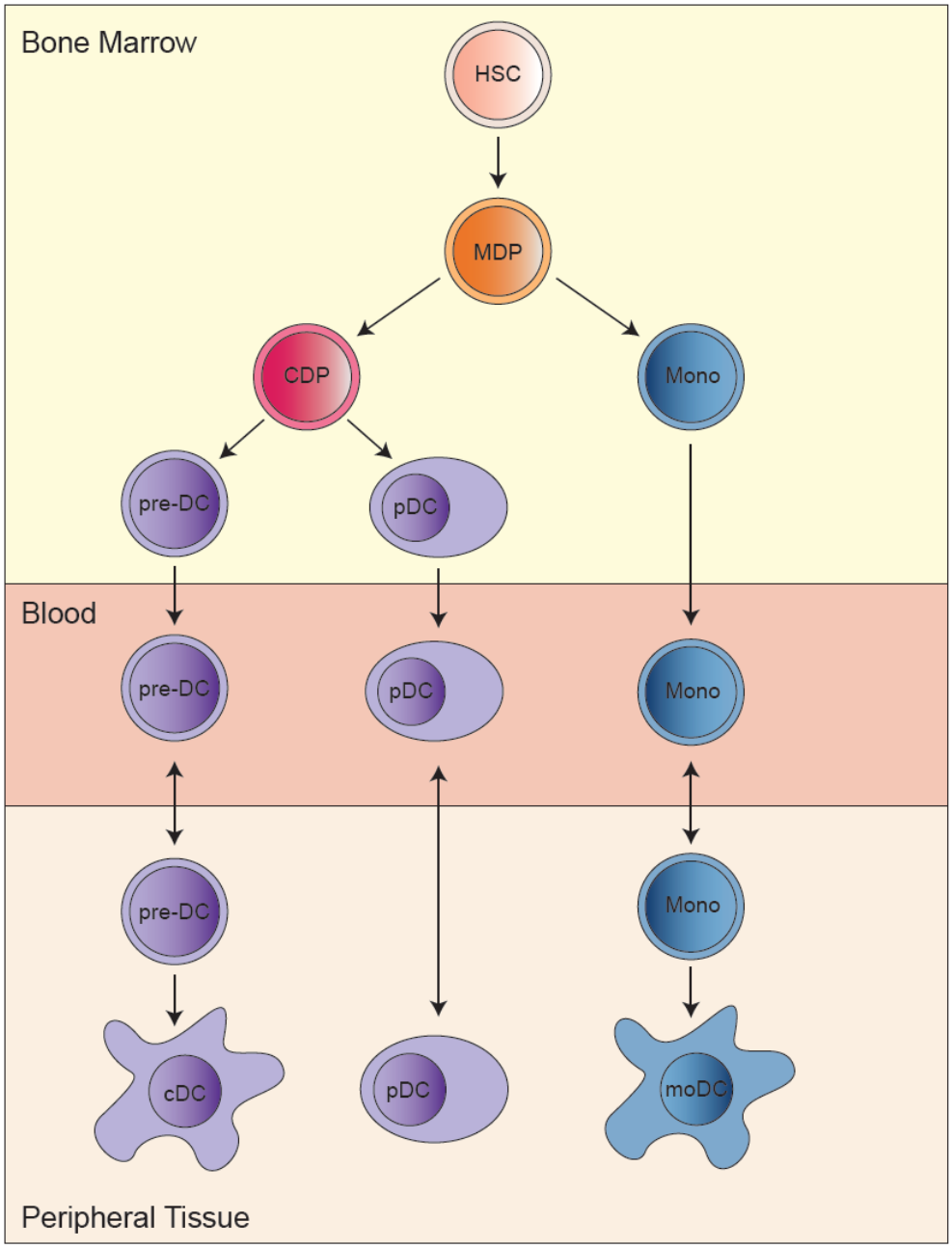
Bone Marrow
HSC
MDP
CDP
Mono
pre-DC
pDC
Blood
pre-DC
pDC
Mono
pre-DC
Mono
cDC
pDC
moDC
Peripheral Tissue

1.5: Adaptive response to primary IAV infection

Humoral immunity

The adaptive immune response is essential to mounting protective immunity to influenza infection. Early animal studies demonstrated that recovered animals developed transferrable, efficacious humoral immunity [64], and antibody titers remain the gold standard to test influenza immunity today. Antibodies target the surface of the IAV particle and so antibody specifies are dominated by the major surface glycoproteins HA and NA though minor levels of antibodies can be detected against NP and matrix proteins. During exposure to IAV strains, humoral immunity protects the host to varying degrees based upon prior exposures by infection or vaccination [65]. In the absence of complete protection, naïve B cells are activated by viral antigen and CD4 help, differentiating into plasmablasts to produce low affinity decavalent IgM which peaks about a week after initial infection and provides a low level of humoral protection during the course of infection [66]. Bivalent, high affinity IgG antibodies are not produced until weeks after initial infection, but are critical to complete viral clearance and maintaining long-term immunity. B-cell deficient mice exhibit significantly greater susceptibility to and poorer recovery from primary IAV infection compared to B-cell competent mice [67]. Upon the resolution of infection, long-lived plasma cells continue to produce IgG that provides lifelong protection.

Cellular immunity

T cell immunity is another branch of adaptive immunity that can confer broad, cross-strain protection against influenza. In addition to HA and NA, a significant proportion of $CD4^+$ and $CD8^+$ T cell epitopes are also derived from proteins NP and M1; $CD8^+$ T cell epitopes have been found that derive virtually every influenza protein [68]. This broader antigenic response provides

T cell responses against highly conserved, internal proteins that enable efficacious cross-strain immunity that is not possible for humoral immunity.

Naïve T cells continuously circulate between lymphoid organs, entering lymph nodes (LN) from the blood, and spend about 8-12 hours within the LN cortex, probing for their cognate antigen [69]. Like activated DCs which migrate to LNs, naïve T cells express high levels of CCR7 that guide their migration from lymphatic and blood to the LN where CCL19 and CCL21 are expressed in the high endothelial venules and especially the T cell cortex [70]. In order to exit the lymph node, naïve T cells follow a sphingosine 1-phosphate (S1P) gradient that is elevated in the blood and lymph. S1P is produced in nearly all tissues, and its gradient is generated by S1P lyase which degrades S1P in the peripheral tissue [71]. Activated T cells temporarily upregulate the marker CD69 which blocks the S1P signaling pathway by suppressing S1P receptor function which arrests migration of newly activated T cells [72]. This mechanism blocks the egress of newly actively T cells which allows them to remain with their cognate antigen as the T cell response develops. S1P blockade has been shown to prevent the LN egress of lymphocytes based upon experiments using the drug FTY720 [73], although its efficacy during an active IAV infection is less clear.

The T cell activation process is comprised of 3 distinct "signals" that dictate the outcome. The first signal is the TCR engagement with the cognate antigen peptide-MHC complex, known as the immunological synapse. In addition to a sustained TCR signal, studies determined that T cells activated without a costimulatory second signal were rendered anergic, unable to respond to future TCR signaling [74]. Classically, CD28 is the major costimulatory protein on T cells that engages with CD80 and CD86 (B7.1/B7.2) on the surface of APCs by reducing the number of TCRs required in the SMAC [75], lowering the activation threshold and activating downstream pathways that promote T cell proliferation and survival [76]. Finally, T cell activation requires a

third cytokine signal that is typically provided by antigen presenting cells and the priming environment. T cells that do not receive this signal fail to develop effector function. APC cytokine production is dependent on the infectious agent and may include the production of general inflammatory signals or even more immunomodulatory signals [77], suggesting that dendritic cells prime T cells to generate the optimal subtype of effector T cells necessary to resolve the original stimulus.

Effector T cells consist of several functionally distinct, non-overlapping subsets that are specialized to combat different pathogen classes. While $CD8^+$ T cells generally differentiate into cytotoxic T cells (CTLs), $CD4^+$ T cells exhibit significant plasticity and may differentiate into Th1, Th2, Th17, and T regulatory cells (Treg), among other subsets. Th1 cells are characterized by their cytokine effector function, producing IFN-ɣ and TNF-α that is critical for antiviral immunity. On the other hand, Th2 cells mediate immunoglobulin production as well as allergic and antiparasitic function. Th17 cells are involved in inflammatory process and often associated with autoimmunity, while Treg produce IL-10 and TGF-β and have strong immunosuppressive function.

During IAV infection, DC production of IL-12 during T cell priming induces Type 1 polarization to produce high numbers of CTLs as well as Th1 $CD4^+$ T cells in the lung draining lymph nodes where effector T cells downregulate CCR7 and upregulate CXCR3 and CCR4, mediating their migration to IAV-infected lung [78]. Effector $CD4^+$ cells and CTLs that migrate to the lung and airways produce a broad range of cytolytic compounds (granzyme B, perforin) and cytokines (IFN-g, TNF-a, IL-2) that are critical to IAV clearance. Secreted IFN-ɣ is the most prominently produced antiviral cytokine and leads to tissue-wide upregulated interferon signaling. TNF-α, also robustly secreted, leads to broad proinflammatory responses which triggers greater

cell death amplifies inflammatory and chemokine signaling that enhance antiviral responses but may also mediate tissue damage as well [79]. T cells also coordinate the greater immune response by producing the chemokine macrophage inflammatory protein (CCL3) which recruits monocytes, lymphocytes, DCs, and neutrophils to clear IAV from the site of infection [80]. $CD4^+$ T cell-mediated protection is abrogated in the absence of B cells and $CD8^+$ T cells [81], suggesting, that coordination with other immune cells is essential for $CD4^+$ protective function. $CD4^+$ T cells also offer more diverse function, differentiating into T follicular helper cells that are critical to the formation of germinal centers and immunoglobulin class switching that produces neutralizing IgG [82]. Additionally, the loss of $CD4^+$ or $CD8^+$ T cell responses led to impaired viral clearance and increased mortality, although the presence of other immune cells is sufficient for protection in less virulent challenges. [83, 84], In addition to pro-inflammatory mediators, both $CD4^+$ and $CD8^+$ effector T cells have also been shown to produce IL-10 in IAV mouse models, suggesting that T cell responses also provide tissue protective mechanisms via immunomodulation [85].

Figure 1.4 T cell priming

Naïve T cells are primed in secondary lymphoid sites by conventional dendritic cells that present peptide on major histocompatibility complex (MHC). Naïve T cells require 3 signals in order to properly differentiate into effector T cells. (1) Naïve T cells which possess the TCR specific for the presented peptide will receive signal 1 which is dependent on TCR engagement. (2) Activated dendritic cells contain costimulatory molecules such as CD80 and CD86 which engage with CD28 on the T cell in order to provide signal 2. (3) Finally, dendritic cells produce cytokines that provide a third signal to the naïve T cell that induces full differentiation.

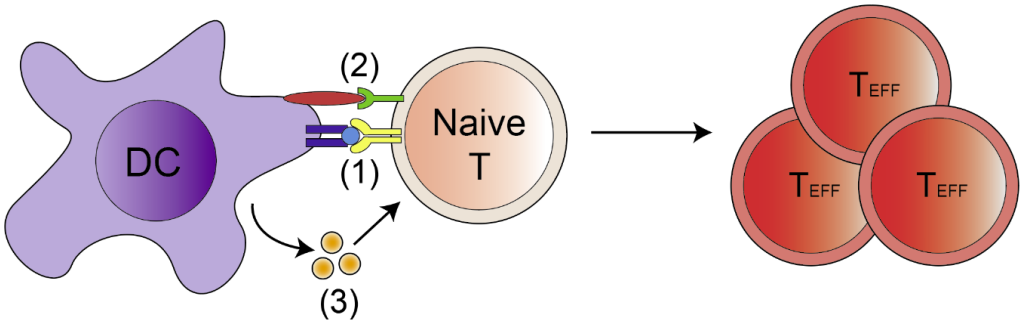

(1) TCR engagement
(2) Costimulation
(3) Cytokine stimulation

1.6: Memory T cells

Memory T cells are a heterogenous subset of T cells that are distinct from naïve T cells due to their ability to respond more rapidly and effectively upon antigen exposure. The precise mechanisms of memory T cell generation are not fully understood, as to memory T cells may also develop memory-like characteristics in the absence of foreign antigen [86]. Canonically, memory T cells are generated after a primary exposure from the expanded effector T cell pool which contains memory T cell precursors. After pathogen clearance, the effector T cell pool contracts to leave behind a small, long-lived subset that persists as so-called "memory" for their ability to remember the primary infection by rapidly responding to the same pathogen.

Heterogeneity of memory T cell migration patterns are a major determining factor in their functional characteristics. Studies in blood identified circulating populations memory T cells that migrate between either peripheral tissue or secondary lymphoid organs. Central memory T cells (TCM) are a circulating subset of memory T cells which localize to secondary lymphoid sites including lymph nodes as well as the spleen. TCM are identified by surface markers that define both their memory status as well as their migratory characteristics. In humans, these cells can be defined by the upregulation of chemokine receptor CCR7, and in mice, the upregulation of CD62L, surface proteins that facilitate their localization to lymphoid sites. Mouse models have demonstrated that TCM exhibit functional differences including enhanced IL-2 production and cellular proliferation after T cell antigen stimulation which augments lymphoid T cell responses [87]. Effector memory T cells (TEM) comprise the other major subset of circulating memory T cells and migrate between peripheral tissues and the blood. Unlike TCM, TEM at steady state are characterized by low expression of CCR7 in humans and low expression of CD62L in mice, which facilitates their migration to peripheral tissue rather than lymphoid sites. TEM possess enhanced

cytolytic function and effector cytokine production [88], which corresponds to their localization in peripheral tissue sites, which are most likely to be sites of pathogen exposure.

Tissue resident memory T cells

In addition to the TEM and TCM memory T cell subsets, another subset known as tissue resident memory T cells (TRM) has become more recently appreciated for its role in protection and rapid response. In contrast to TEM and TCM which circulate between the blood and peripheral tissue or secondary lymphoid organs (SLO), respectively, TRM are a memory T cell population that resides in tissues without recirculating throughout the body (Fig. 1.5) [89, 90]. Parabiosis experiments in mice have functionally demonstrated that TRM are non-circulating [91]. TRM comprise the largest subset of memory T cells in the body, residing in a wide range of tissues such as barrier sites like the lung, skin, and gut, and female reproductive tract (FRT), lymphoid sites, and other non-lymphoid tissue such as the brain, liver, and kidneys [92-100]. As they tend to persist within peripheral tissue sites, TRM also share phenotype characteristics with TEM, upregulating CD44 and downregulating CD62L in mouse models and downregulating both CD45RA- and CCR7 in humans. TRM exhibit transcriptional signatures distinct from circulating memory T cells [101, 102], and murine TRM as a collective group share a common transcriptional core mediated by the transcriptional factors *Hobit* and *Blimp1* [97]. A number of approaches such as intravascular labeling [103, 104], parabiosis [91], and tissue transplantation [105] have shown that TRM permanently reside within tissue niches without recirculating into the blood or lymph and are associated with surface proteins such as CD69, CD103, and CXCR6 which mediate tissue retention and migration. However, such markers are not always expressed by TRM nor are they wholly unique to TRM as well. Therefore, tissue residency is functionally defined by a lack of

migration to the blood and other tissue sites [91, 106]. Therefore, the term TRM describes a collective, heterogenous group of tissue-retentive, non-circulating memory T cells with distinct functional characteristics.

The mechanisms driving lung TRM generation and maintenance have not been fully elucidated. Local infection is a key driver of TRM generation, but the relative contributions of generalized inflammation and *in situ* antigen recognition are unclear. Recent work has found that T cells may can be conditioned for a TRM fate by cytokine signaling during the priming step [107, 108]. In the lung, the persistence of antigen may be critical to maintaining T_{RM} upregulation of chemokine receptors has been shown to regulate TRM localization to airways [109]. At steady state, evidence suggests that lung TRM are replenished from T cells within the lung interstitium rather than being replenished from sources outside of the resident niche [110]. Lung TRM generated by IAV infection have been known to decline in number over time unlike other tissue TRM which experience longer persistence, and this diminishment is associated with declining protection as well [111]. This may be partially explained by the fact that lung TRM, and especially airway TRM, are limited in their access to blood borne nutrients and experience amino acid starvation, promoting cell death and contributing to the long-term loss of TRM numbers [112]. By repeated pathogen exposure, TRM numbers and durability can be boosted [113], suggesting that lung T_{RM} persistence may depend on the continually environmental exposure experienced under normal physiologic conditions.

While $CD4^+$ and $CD8^+$ TRM share many similarities, including a core transcriptional signature [101], several key differences exist in their functional capacity and roles. $CD4^+$ TRM represent a more heterogenous population in clonal diversity, likely reflective of the functional plasticity and heterogeneity of $CD4^+$ T cells, which can differentiate into many helper T cell

subsets. In addition to Th1 polarized TRM, Th2 and Th17 polarized TRM have also been discovered to play roles in allergic immunity in a house dust mite model [114] as well as antibacterial function in a *Klebsiella pneumonia* model of infection [115]. As such, $CD4^+$ TRM can produce a diverse range of Th1, Th2, and Th17 cytokines, whereas $CD8^+$ TRM tend to primarily produce cytotoxic mediators as well as Th1 cytokines such as IFN-ɣ and TNF-α cytokines. $CD4^+$ and $CD8^+$ have also been shown to occupy different tissue niches that optimize their differing function. $CD8^+$ TRM tend to localize within the epithelial layers of tissue sites which optimizes their rapid cytotoxic function, whereas $CD4^+$ TRM tend to localize in clusters [116] below the epithelial layer where they are better position to provide supporting cytokine production to coordinate the immune response and interact with APCs [117]. Both $CD4^+$ and $CD8^+$ TRM occupy overlapping, but distinct roles and tissue niches to optimize host defense responses.

Figure 1.5 Memory T cell migratory characteristics

T cells subsets are defined by their migratory characteristics. Naïve T cells migrate in the blood and lymph to various lymphoid sites until cognate antigen encounter. Effector (TEM) and central (TCM) memory T cell subsets are migratory memory T cells that can be found in the blood. TCM primarily localize to secondary lymphoid sites whereas TEM migrate to peripheral tissue. Tissue resident memory T cells (TRM) are a non-migratory subset that resides primarily in peripheral tissue.

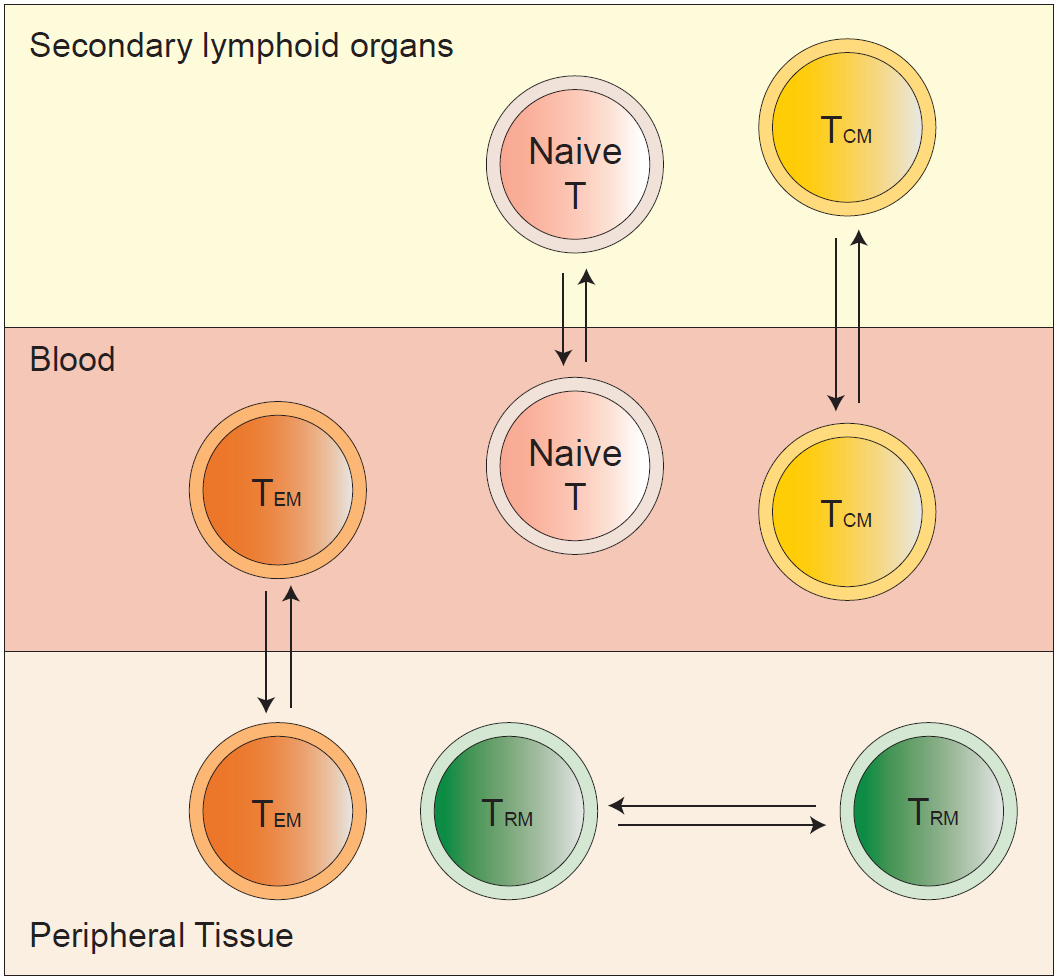
Secondary lymphoid organs
Naive T
TCM
Blood
TEM
Naive T
TCM
TEM
TRM
TRM
Peripheral Tissue

1.7: Tissue resident memory T cell antiviral protective capacity

TRM localized patrol function

TRM mediate protection in several viral infection models including not limited to, influenza [94, 100, 118, 119], HSV [116, 120, 121], vaccinia [122, 123], and LCMV [124] and provide superior protection compared to circulating memory T cells. Located at the site of infection, T_{RM} patrol the tissue milieu to respond to invading pathogens with rapid cytolytic and cytokine function.

TRM at steady state are relatively fixed within their niche and do not migrate to other locations within the tissue [125]. However, despite their restrictive localization, TRM are hardly sessile. Significant evidence has shown that at steady state, TRM demonstrate motile features within their tissue site as a part of their sentinel function (Fig. 1.6). Intravital imaging showed that murine skin $CD8^+$ TRM slowly (~1-2 μM/min), but efficiently crawl within the epidermis in order to expand their patrol function and exhibited dendritic features while scanning for antigen [126, 127]. Upon antigen stimulation, skin $CD8^+$ TRM retract their dendritic extremities and arrest their motility, lending credence to the hypothesis that TRM motility supports a sentinel role that is fulfilled upon pathogen encounter. Using an *ex vivo* fluorescent labeling and culture system with human skin biopsies, recent imaging studies corroborated past animal studies and showed that human $CD8^+$ TRM actively migrate within both dermal and epidermal skin layers and arrest upon antigen exposure [128]. Another recent study showed that $CD8^+$ TRM do not preferentially migrate toward infected cells, suggesting that TRM cellular density may be crucial toward increasing the odds of a chance encounter [129]

TRM motility is highly tissue dependent, where differences in architecture may account for discrepancies in local TRM migratory patterns. Hepatic $CD8^+$ TRM which reside within

sinusoids showed track speeds ~5 μM/min, several times faster than epidermal TRM [96]. Unlike skin TRM, FRT TRM exhibited relatively high speeds of ~10 μM/min within the FRT stroma and motility remained high after viral clearance [130]. FRT TRM speeds were dependent on the type of uterine connective tissue layer, in which collagen-dense regions were correlated with slower speeds compared to collage poor areas. $CD8^+$ TRM in the small intestine also exhibited motility that varied depending on which tissue layer of the small intestine they were located [131], further suggesting that architectural constraints of the tissue are a key determinant of TRM motility.

TRM are also thought to permanently reside within their tissue site without migration into blood or lymph, offering local protection against future pathogen exposures. Challenging this dogma, recent work revealed that activated TRM exhibit developmental plasticity and re-enter the circulating pool by differentiating into central and effector memory T cells (Fig. 2) [132]. Furthermore, these differentiated circulating memory T cells retain their TRM origins and are able to re-differentiate back into TRM upon appropriate cytokine stimulation. These findings offer new mechanisms for TRM generation and protection, in which TRM may supply a bloodborne reservoir for the influx of effector and memory T cells to the site of infection as well. Recent corroborating work in human samples discovered the presence of $CD4^+$ $CD103^+$ TRM cells in blood that were both functionally and transcriptionally similar to $CD4^+$ $CD103^+$ TRM in the skin [133]. Using a human skin xenograft model in mice, the authors determined that $CD4^+$ $CD103^+$ cutaneous TRM were able to reseed distal skin sites without needing to differentiate into a circulating memory subset unlike the previous murine study. These results demonstrate an additional mechanism of protection that allows for seeding of distal, pathogen naïve tissue sites by differentiation into circulating memory subsets. TRM entry into circulation may also underly findings from a recent study in which lung donor recipients experienced greater clinical

complications when donor lung TRM numbers diminished in the tissue site [106]. However, it is unclear whether TRM in other than the skin sites also exhibit the same migratory capabilities, as the vast majority of TRM remain restricted within their tissue site.

Rapid TRM effector response

Situated at the site of infection, TRM are poised to rapidly respond to pathogens through the release of cytotoxic and inflammatory compounds which are essential to $CD8^+$ TRM mediated protection (Fig. 2). Enhanced cytolytic function underlies their superior protective capacity. $CD8^+$ TRM have been shown in various murine models to constitutively express enhanced levels of cytotoxic proteins granzyme B and perforin [124, 134-136]. TRM cytolytic activity may also be dependent on anatomical location: $CD8^+$ airway TRM offered little cytolytic activity in contrast to their parenchymal counterparts in the lung [119]. Yet, studies in human TRM have not necessarily recapitulated these same results in mouse models; TRM isolated from post-mortem human brain and lung express minimal protein levels of perforin or granzyme B [137-140]. Inhibitory proteins including PD-1, CTLA-4, and Tim-3 are highly expressed in TRM, suggesting that expression of cytolytic proteins may be purposefully low as part of an overarching immunoregulatory program to minimize T_{RM}-mediated tissue damage. $CD4^+$ and $CD8^+$ TRM have also been found to upregulate inhibitory proteins such as PD-1 in various other tissues including the spleen, pancreas, and skin, [95, 101, 141], suggesting that immunoregulation may be a universal hallmark of TRM and associated with their long-term persistence in tissue sites. A recent study highlights the pathologic potential of TRM, demonstrating in an aspergillus model that that lung $CD103^{lo}$ $CD69^+$ $CD4^+$ TRM cause lung inflammation and fibrosis [142]. While human TRM may express low protein levels of cytotoxic mediators at baseline, granzyme and perforin mRNA are highly

expressed, are rapidly produced upon stimulation. These studies have found that TRM are poised to quickly abandon their immunoregulated state to rapidly upregulate cytolytic activity upon antigenic stimulation or type I IFN signaling within the tissue milieu [138, 139, 143].

TRM produce robust levels of Th1 cytokines and chemokines in order broadly enhance tissue-wide antiviral responses and mediate leukocyte recruitment which are critical for protection and viral clearance (Fig. 2) [118, 119, 144, 145]. At rest, both $CD4^+$ and $CD8^+$ TRM exhibit elevated levels of preformed IFN-ɣ transcript that aids in the immediate and robust IFN-ɣ production upon restimulation [101, 138, 139]. Recent work on lung $CD4^+$ $CD103^+$ TRM found that Actinomycin D treatment, which blocks *de novo* transcription, dramatically reduced IFN-ɣ production which indicates that much of superior TRM cytokine production was due to enhanced transcription, suggesting that TRM may perhaps contain a more accessible IFN-ɣ locus [143]. Recent work on $CD8^+$ TRM in human skin found that $CD49a^+$ identifies IFN-ɣ producers whereas $CD49a^-$ TRM produced IL-17A [146]. $CD49a^+$ TRM preferentially localize to the epithelial layer, where enhanced effector function is best suited. Within several hours of stimulation with cognate antigen, TRM produce IFN-ɣ which induces a tissue-wide antiviral state that is reflected by broad transcriptional changes, including the upregulation of type I IFN signaling and chemokine genes [125]. Murine studies in an FRT model found that IFN-ɣ produced by TRM created a state of alert in the tissue that activated natural killer cells and dendritic cells and directed the recruitment of not only effector T cells, but also unstimulated memory T cells and B cells to the site of infection via chemokine release and the upregulation of adhesion molecules on vascular endothelium [144, 147]. early protective responses by activating the antiviral innate responses response and initiating leukocyte recruitment.

In situ TRM proliferation

In addition to leukocyte recruitment, TRM proliferation also contributes to the expanding immune effector pool in the tissue niche (Fig. 2) [129, 130, 148]. In the skin and FRT, recent studies demonstrated that TRM proliferated within the tissue niches to produce additional TRM that continue to reside within the original tissue site [129, 130, 149]. This proliferation dominates cellular expansion during the early recall response to both pathogen and peptide challenge. Using parabiotic mice, cellular expansion was dominated by host cell responses, indicating that circulating T cells were not significant contributors [130]. Non-specific bystander T cells from the circulation also contributed to the generation of *de novo* TRM, suggesting that the initiation and maintenance of a TRM program is not dependent on cognate antigen recognition. Newly generated TRM did not displace existing TRM, supporting recent studies which demonstrate that TRM numbers can be continually increased with repeated pathogen or antigen exposures [113, 150, 151]. *In situ* TRM proliferation may also provide an expanded T cell pool that migrates to distal infection sites. While proliferating T_{RM} can differentiate into circulating memory cells that may migrate to tissue sites [132], recent work using a heterosubtypic influenza infection model determined that lymphoid TRM rapidly proliferated within the lung draining mediastinal lymph node which coincided with rapid expansion of lung effector T cells [152]. On the other hand, a recent study of skin T_{RM} in a peptide challenge model did not find evidence to support *in situ* TRM proliferation as the dominant source of TRM expansion [150]. $CD8^+$ TRM expansion after peptide stimulation was eliminated with systemic anti-CD8 antibody treatment, suggesting that circulating T cells were the dominant source of TRM mediated secondary TRM expansion.

Figure 1.6: TRM protective antiviral function

TRM mediate their protective antiviral function through a variety of mechanisms. TRM patrol their respective tissue niches and arrest their motility upon pathogen encounter. In order to control viral infection, TRM rapidly produce cytotoxic mediators such as granzyme B and perforin as well as effector cytokines such as IFN-ɣ, which induces a tissue wide antiviral state. TRM may also proliferate *in situ* in order to magnify their protective response. TRM-induced chemokine production mediates rapid leukocyte recruitment including memory T cells and B cells. TRM may also differentiate into circulating TEM and TCM memory subsets and migrate, providing a mechanism for providing effector function in distal infection sites.

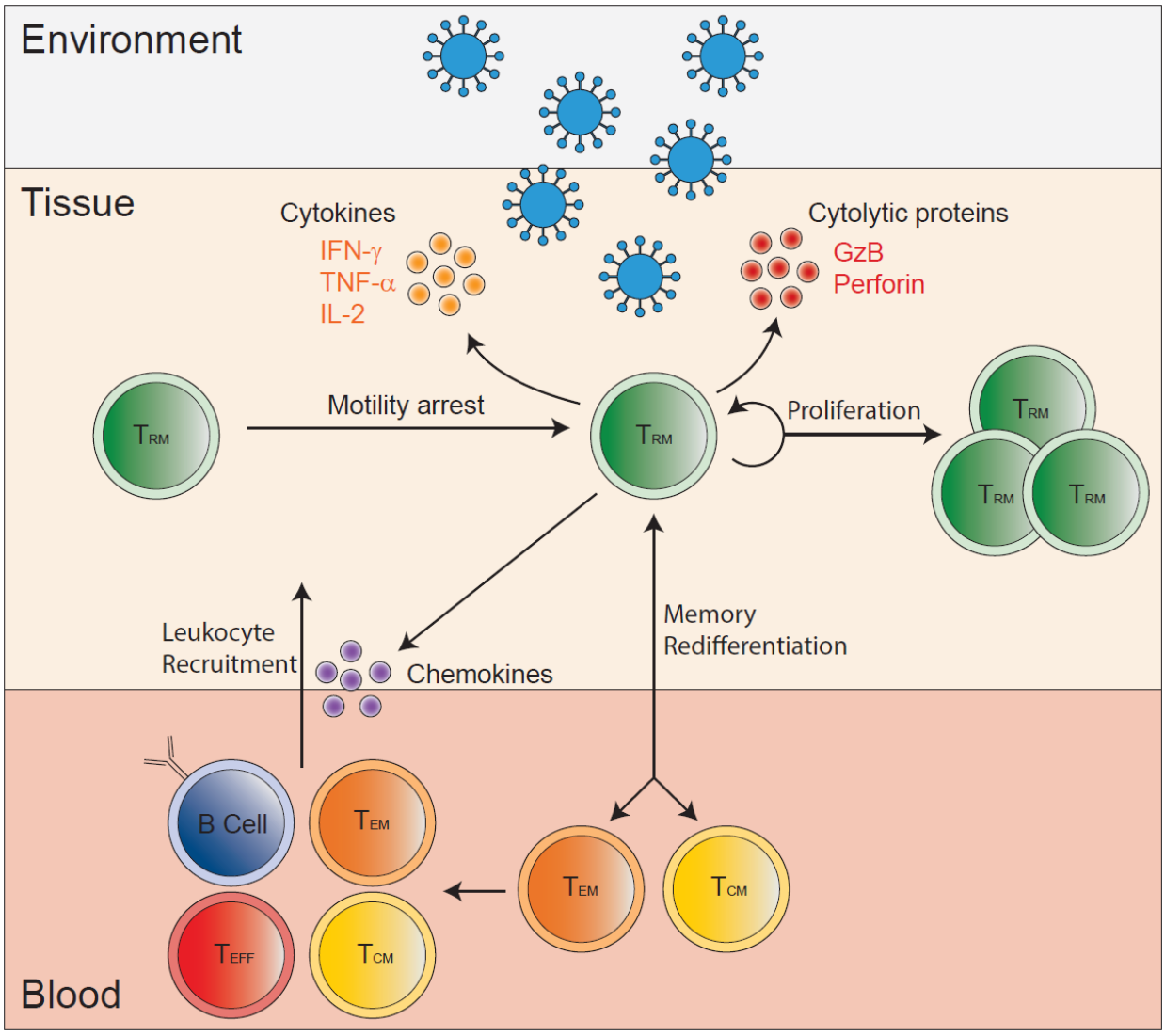
Environment
Tissue
Cytokines
IFN-γ
TNF-α
IL-2
Cytolytic proteins
GzB
Perforin
TRM
Motility arrest
TRM
Proliferation
TRM
TRM
TRM
Leukocyte
Recruitment
Chemokines
Memory
Redifferentiation
B Cell
TEM
TEFF
TCM
TEM
TCM
Blood

1.8: Trained innate immunity

Though immunological memory is largely thought to be the purview of the adaptive immune system, recent evidence suggests that innate immune cells also have the capacity to optimize their responses against subsequent pathogen exposures, in a phenomenon known as trained immunity. While adaptive immunity is thought to provide lifelong protection, trained immunity tends to reversible, persisting only on the order of months to years [153]. Even in the absence of T and B lymphocytes, RAG1 mice are protected against subsequent re-exposure to *C. albicans*; primary infection epigenetically reprogrammed monocytes to enhanced further cytokine production [154]. Prior respiratory viral exposure has also been shown to induce long-lived memory alveolar macrophages which coordinate neutrophil responses to *S. pneumoniae* challenge in a cytokine and chemokine dependent fashion, suggesting that innate immune immunity may provide protection against an incredibly broad range of pathogens [155]. It has been observed that vaccinations in humans may also provide non-specific protective benefits such as in the case of BCG, measles, and oral polio vaccine, in which the reduction in overall mortality cannot solely be attributed to elimination of those specific pathogens [156] and include concurrent enhancement of T cell immunity [157].

Though the underlying mechanisms of trained immunity remain to be fully elucidated, it is clear that epigenetic reprogramming underlies many instances of innate memory. Myeloid cell stimulation durably increases the acetylation and RNA polymerase recruitment at inflammatory gene loci, long after the resolution of inflammatory stimuli [158]. Trained immunity also derives from changes to cellular metabolism that modulate epigenetic profiles [159]. Activation of the mTOR/Akt pathway by β-glucan from *C. albicans* was shown in human monocytes and mouse models to underly trained monocyte immunity [160]. These immunological changes are not

limited to protective responses, but can also induce tolerization as well [161]. The long-term effects of primary pathogen exposure on innate cells cannot be discounted when considering the ramifications of immunological memory.

1.9: Thesis Aims

Aim 1: Assess the lung localized antiviral T cell responses that contribute to heterosubtypic protection during an influenza infection

T cell-mediated immune responses offer the promise of universal protection against influenza A virus. Much evidence has emerged that tissue-localized T cell responses provide optimal protection against a host of viral pathogens, particularly in the form of TRM, which have been shown in several murine models to provide heterosubtypic immunity against IAV [94]. However, tissue resident memory T cells are not the only driver of local tissue memory responses; circulating memory T cells as well as innate cells also contribute to protective immunity. How these different aspects of T cell responses coordinate to mediate lung localized cross-strain protection against influenza has not yet been fully elucidated. **Our objective is to determine the difference between a recall and primary infection's lung tissue localized T cell responses that contribute to protective immunity and investigate those underlying mechanisms.**

Here we demonstrate that prior IAV infection generates tissue localized immunity that protects against heterosubtypic influenza challenge in a B cell independent manner. By sequestering blood lymphocytes with the drug FTY720, we investigated tissue-localized immunity and discovered that compared to a primary infection, the recall response initiates a more rapid expansion of lung niche T cells that partially results from *in situ* proliferation $CD4^+$ and $CD8^+$ TRM, consistent with recent studies of TRM in other tissue sites [129, 130]. But unlike other

tissue sites, we also observed significant proliferation of non-TRM in the lung niche. By tracking an influenza specific, naïve T cell population, we demonstrated that peripheral T cells migrate into the lung niche to contribute to the rapid T cell proliferation during a recall response. Further, this migration was antigen-specific rather than being due to non-specific inflammation and chemoattraction.

Increased lung T cell migration resulted from enhanced priming and proliferation within the lung-localized medLN. During a recall response, we found that both naïve $CD4^+$ and $CD8^+$ T cells experienced more rapid priming and enhanced proliferation within the medLN, leading to enhanced migration of T cells to the lung niche, including T cells specific for novel antigen. Underlying this enhancement were persistent changes to the medLN, which led to increased numbers of T cells and cDCs that persisted for at least several weeks after a primary IAV infection. Through the depletion of $Zbtb46^+$ cDCs, we find that the increased number of dendritic cells are key drivers of the enhanced T cell priming phenomenon observed in the recall response. Together, these data suggest that a primary influenza infection leads to durable changes in innate immunity, specifically in dendritic cell numbers that enhance the adaptive T cell response, including T cell responses to novel antigen, which are necessary for heterosubtypic immunity.

Aim 2: Assess immunomodulatory responses of the recall response to influenza viral challenge

Although a robust immune response to respiratory infection is paramount to viral clearance and a return to tissue homeostasis, associated inflammatory processes represent an altogether separate threat to tissue integrity and host health. The virulence of a given influenza strain is highly correlated with the hyperinduction of proinflammatory cytokine production, also known as a cytokine storm [162]. Immunomodulatory cytokines are produced by a variety of immune cells,

including T cells, in order to dampen inflammatory responses. During an influenza infection, T cells, including both effector and T_{reg} cells, have been demonstrated to be major producers of anti-inflammatory cytokines. However, the role of anti-inflammatory T cell responses during a memory response have not been well studied. **Our second objective is to assess the contributions of T cells to the immunomodulatory function of the lung localized immune response during a recall infection**

Our work found that *in vitro* stimulation of tissue resident memory T cells led to the superior production of both immunomodulatory IL-10 family and pro-inflammatory cytokines compared to their circulating counterparts. Further, lung-derived APCs promoted T cell production of immunomodulatory cytokines, suggesting that the lung tissue environment itself may contribute to immunoregulatory T cell responses. The study of T cells during a heterosubtypic challenge revealed enhanced *in situ* IL-10 production by $CD4^+$ T cells in the lung resident niche. The blockade of IL-10 signaling during IAV secondary challenge led to increased IFN-ɣ and TNF-α levels in the airway, demonstrating that IL-10 signaling plays an important role in the suppression of inflammatory immune responses. Whole lung tissue transcriptional analysis was performed for primary and secondary infections compared to their uninfected baselines; secondary innate immune responses were significantly dampened, particularly for type I interferon responses, and upregulated significantly fewer genes. Our findings suggest that lung localized T cell responses produce increased levels of immunomodulatory cytokines to minimize immunopathology during a recall response to IAV challenge.

Chapter 2: Materials and Methods

2.1: Influenza virus preparation and murine infection

PR8, PR8-OTII, PR8-OTI, and X31 influenza virus were grown using chicken eggs. Fresh and fertilized specific pathogen-free (SPF) chicken eggs (Charles River laboratories) were incubated at 37C at 40-60% humidity for 10 days. Eggs were inspected for viable embryos using an egg candler. Under sterile conditions, a hole was made in the shell above the air space using an 18 gauge needle. 200 μL of influenza virus diluted in PBS (10^3-10^4 pfu/mL) were injected into the allantoic cavity, and the hole was covered with masking tape. Eggs were then returned to the incubator and incubated for 48 hours at 37 ºC. After 48 hours, eggs were moved to 4 ºC overnight. The shell covering the air space was cut away, and allantoic fluid was collected, aliquoted, and stored at -80 ºC for long term storage.

To prepare influenza virus for infection, frozen aliquots were thawed on ice and diluted in ice cold PBS as determined by the stock concentration and desired infection titer, which is determined as described below in Section 2.2. Diluted influenza virus stock was used soon as possible for murine inoculation. Mice were anesthetized in 3.5% isofluorane using a rodent anesthesia machine and inoculated with 30 μL of viral solution by allowing mice to breathe in the fluid from a pipette tip.

2.2: Influenza viral titer determination

In order to determine the viral concentration of a given sample, influenza virus was quantified using a Madin-Darby canine kidney (MDCK) cell line culture assay. MDCK cells are an adherent kidney epithelial cell line that is susceptible to influenza virus and provide a mammalian cellular substrate for viral propagation. Viral samples were serially diluted five-fold

in a U-bottom 96 well plate in 100 µL of Dulbecco's Modified Eagle Medium (DMEM) containing 5% heat-inactivated fetal bovine serum (FBS) and 500 µg/mL of L-glutamine-penicillin-streptomycin supplement. Three to four replicates per dilution were plated. MDCK cells were detached from culture plates with trypsin and resuspended at a concentration of 2.5×10^5 cells/mL. 100µL of MDCK cells were added to each well and plates were incubated in 37 ºC for 18-24 hours. Media was aspirated from the plates and replaced with 200 µL/well of serum-free DMEM with 0.0002% trypsin, whose protease activity supports the internalization of virus into MDCK cells.

After 4 days of 37 ºC incubation, 50 µL of 0.5% washed chicken red blood cells diluted in PBS were added to each well and allowed to incubate at room temperature for 1 hour. The presence of influenza virus leads to HA-mediated hemagglutination of red blood cells that is manifested by an absence of a pellet in the bottom of the well. The median tissue culture infectious dose ($TCID_{50}$) was determined from these results using the Reed-Muench method.

2.3: Proliferation dye labeling and transgenic T cell isolation and transfer

In order to label donor T cells with eFluor 450 proliferation dye (ThermoFisher), whole splenocytes were isolated and labeled with the dye as outlined in the manufacturer's directions. T cells were then isolated from labeled and rinsed splenocytes using magnetic $CD4^+$ or $CD8^+$ T cell negative isolation (Stemcell Technologies). 5×10^4 transgenic T cells were adoptively transferred into each mouse by retroorbital injection one day prior to PR8-OTI or PR8-OT-II challenge.

2.4: Mouse tissue digestion and cellular isolation

Lung tissue was enzymatically digested in order to isolate both lymphocyte and myeloid cell populations. Digestion media was 20 ug/mL Liberase TM (Roche) in DMEM. Lung lobes

were minced into chunks and added to gentleMACS C tubes (Miltenyi) containing 10 mL of digestion media where they were physically dissociated using gentleMACS Spleen 4.01 program. The resulting cell suspension was incubated in a 37 ºC shaker for 45 min – 1 hour and then mechanically dissociated again using gentleMACS Spleen 4.01 program. The resulting cell suspension was then passed through a 70 µM filter.

To process lymph nodes, lymph nodes were minced using a blade and incubated in 2 mL of digestion media for 20 minutes in a 37 ºC shaker. Lymph node suspension was pipetted up and down using a 1 mL pipette in order to further physically dissociate cells. After allowing undigested cellular debris to settle, supernatant was removed and added to 10% FBS DMEM on ice. Remaining cellular debris was resuspended in 1 mL of digestion media and added back to a 37 ºC shaker and the process was repeated until lymph nodes were completely digested. Spleen was minced and incubated in digestion media in a 37 ºC shaker for 30 minutes and mechanically dissociated through a 70 µM filter. If only T cells were needed, lymph nodes and spleen were passed through a 70 µM filter by manual mechanical dissociation technique in complete DMEM.

2.5: In vivo labeling

In order to distinguish tissue resident from circulating leukocytes, 2.5 µg of fluorescent antibody was injected into mice 3-5 minutes prior to sacrifice. Antibody used was specific for either CD45.2 or CD90.2 antigen in order to stain all cells depending on the congenic markers being studied.

2.6: Flow cytometry staining protocol

Fluorescent antibodies, TruStain FcX (Biolegend), and BD Horizon™ Fixable Viability Stain 700 (BD Biosciences) were diluted in FACS buffer (1% fetal bovine serum in PBS). Surface antigen staining of cells was performed in FACS buffer for 30 minutes at room temperature. Cells were rinsed in FACS buffer and then fixed for 10 minutes in Cytofix buffer (BD Biosciences) before resuspension in FACS buffer and storage at 4C away from light sources. Cells were analyzed within 72 hours of fixation. In the case of staining for BrdU, Phaseflow BrdU kit (Biolegend) was used according to the manufacturer's protocol and recommendations. Staining for surface molecules was also performed for 30 to 45 min at room temperature in the dark. Stained cells were analyzed using a BD LSRII (BD Biosciences) flow cytometer and analyzed using FlowJo V10 (Tree Star, Inc., Ashland, OR).

For cell sorting, staining was performed similarly, but in sorting buffer which was composed to FACS buffer with 5 mM EDTA. Cells were sorted using a BD Influx high-speed sorter and into 5 mL tubes containing 1 mL of DMEM with 10% FBS. List of fluorescently-conjugated antibodies used are listed in Tables 2.1.

Table 2.1: List of antibodies used for flow cytometry

Antigen	Manufacturer	Fluorophore	Clone
CD90.2	Biolegend	Alexa 647/Alexa 488	30-H12
BrdU	Biolegend	Alexa 647	3D4
CD3	Biolegend	BV421	145-2C11
CD4	BD Biosciences	BUV395	GK1.5
CD8	Biolegend	BV650	53-6.7
CD44	Biolegend	APC/Fire™ 750	IM7
CD62L	Biolegend	PE/APC	MEL-14
CD69	Biolegend	PE/Dazzle™ 594	H1.2F3
CD103	Biolegend	PE/Cy7	2E7
CD45.2	Biolegend	BV421	104
CD45.1	Biolegend	BV605	A20
CD45	BD Biosciences	BUV395	30-F11
I-A/I-E (MHC II)	Biolegend	APC/Fire™ 750	M5/114.15.2
CD11b	Biolegend	BV650	M1/70
CD11c	Biolegend	PE/APC	N418
CD86	Biolegend	BV421	GL-1
Influenza A NP	MBL Intl	PE	

2.7: FTY720 treatment

FTY720/Fingolimod (Sigma) was diluted in normal saline and injected intraperitoneally daily into mice (200 µL/mouse) at a dose of 1mg/kg body weight. FTY720 treatment was initiated 2 days prior to heterosubtypic challenge and maintained throughout secondary infection.

2.8: OT-II RAG$^{-/-}$ memory mouse generation

Whole splenocytes were isolated from OT-II mice and purified for OT-II cells using a magnetic CD4^{+} T cell negative isolation kit (Stemcell Technologies). T cells were cultured with $OVA_{323-339}$ peptide (1 µg/mL) in complete RPMI (10% FBS) in U-bottom 96 well plates (5×10^4 cells/well) for 5 days. Resultant expanded T cells were adoptive transferred into RAG1$^{-/-}$ mice (10^6 OT-II cells/mouse) by intraperitoneal injection. After 4 weeks, lung and spleen cells isolated for antigen-specific memory T cell responses

2.9: *In vitro* T cell peptide stimulation and cytokine analysis

In order to stimulate OT-II lung TRM, whole lung cells were isolated as described and cultured in complete DMEM (10% FBS) with varying concentrations of $OVA_{323-339}$ for 24 hours in 10^5 cells/well in a 96 well U-bottom plate. To activate OT-II lung TRM and spleen TEM with antigen presenting cells, CD4^{+} CD44^{+} CD62L^{-} T cells were sorted from the lung or spleen of OT-II RAG1$^{-/-}$ memory mice. 5×10^4 sorted memory T cells were co-cultured with equal numbers of lung or spleen cells from RAG1$^{-/-}$ mice in a 96 well U-bottom plate in complete DMEM with varying concentrations of $OVA_{323-339}$ for 24 hours. Supernatant was stored at -80C and analyzed using a LEGENDPlex^{TM} Mouse Th Cytokine Panel (Biolegend) cytometric bead array. Data was acquired on a BD LSRII or Fortessa flow cytometer.

2.10: αIL-10R antibody blockade

One day prior to influenza challenge, mice were intraperitoneally injected with 0.4 mg and intranasally administered 0.2 mg of αIL-10R antibody (Bio X Cell). Two days after IAV challenge, αIL-10R antibody treatment was repeated. Bronchoalveolar lavage (BAL) washes were isolated for cytokine analysis five days after IAV challenge.

2.11: Generation of zbtb46-DTR bone marrow chimeras

CD45.1$^{+/+}$ C57BL/6 mice were irradiated with 1100-1200 rad by gamma irradiation in a secure CUMC facility. Bone marrow cells were isolated and filtered in HBSS from femurs and tibias of sex-matched CD45.2$^{+/+}$ zbtb46-DTR$^{-/+}$ mice, and 10^7 cells were i.v. injected into each irradiated mouse. Mice were maintained on water containing antibiotic (2mg/mL neomycin) for one week after irradiation, and allowed to recover for 10 weeks after irradiation for immune reconstitution.

2.12: Diphtheria toxin preparation and administration

Unnicked diphtheria toxin (List Biologicals) was reconstituted at 1mg/1 mL in PBS and aliquoted and stored at -80C. Mice were injected i.p. at a dose of 40 ng/g two days prior to secondary challenge, and administered i.n. 50µL (12ng/µL) one day prior to secondary challenge.

2.13: RNA Sequencing and Analysis

Zbtb46-GFP cDC RNA Sequencing and analysis

$CD45^+$ $Zbtb46^+$ $CD11c^+$ I-A/I-E^{hi} dendritic cells were FACS-sorted from the medLN cells of either naïve and memory mice. However, the number of medLN cDCs from uninfected naïve was extremely low. Therefore, each biological replicate of naïve cDCs was sorted from the combined medLN cells of three different naive mice. On the other hand, medLN from memory mice contained significantly more cells, so an individual mouse was sufficient to produce a single biological replicate. Sorted cells were spun down immediately in ice cold PBS and resuspended in Trizol. RNA was isolated from cell pellets using the RNeasy Mini Kit (Qiagen) and quantitated using an Agilent 2100 Bioanalyzer (Agilent Technologies).

For low input sequencing, RNA-Seq libraries were prepared and sequenced by the CUMC Genome Center using SMART-seq v4 Ultra Low Input RNA kit (Takara Bio USA) to create amplified cDNA and Nextera XT kit (Illumina) for library preparation. Libraries were sequenced on the Illumina Novaseq 6000 at the Columbia Genome Center. RNA-Seq reads were mapped using Kallisto (v.0.44.0) with default parameters to the mouse reference genome build GRCh38. Non-protein coding genes were filtered out, and then the bottom third of genes were filtered out by their gene counts. Differential gene expression analysis was then performed with DESeq2 using variance stabilized transformation to generate normalized gene expression data. Genes with $P_{adj} \leq 0.05$ and absolute value of fold change≥ 2 were considered to be differentially expressed. Heat map was generated from transcripts per million (tpm) counts generated from kallisto pseudoalignment. Data are available on Gene Expression Omnibus (GSE144755)

Whole lung tissue RNA Sequencing and analysis

Age-matched 12-16 week old C57BL/6 naïve and X31 memory mice were initiated daily FTY treatment. After two days of FTY treatment, half the mice were then challenged with

intranasal PR8 IAV ($TCID_{50}$ 2000). Two days later, all mice were euthanized and lungs were perfused with PBS. After blotting away excess water, the right lung lobe of each mouse was isolated and flash frozen in liquid nitrogen. RNA was extracted from frozen tissue using QIAsymphony (Qiagen) instrument and quantitated using an Agilent 2100 Bioanalyzer (Agilent Technologies) by the CUMC molecular pathology core. cDNA libraries were prepared by the CUMC Genome Center using a poly-A pulldown to enrich mRNA and subsequent Illumina TruSeq RNA prep kit. Libraries were sequenced using Illumina HiSeq 4000. RNA-Seq reads were mapped and quantified using Salmon (v.0.9.1) to the mouse reference genome build GRCh38. Differential gene expression analysis was performed with DESeq2 using variance stabilized transformation to generate normalized gene expression data. Heat map was generated using FPKM data of differentially expressed genes. Scatter plot generated using normalized counts with an average count greater than 10.

In order to analyze the functional relevance of differential expressed genes of both primary and secondary responses, Ingenuity Pathway Analysis (IPA) by Qiagen was used. A matrix containing differentially expressed genes as well as associated information such as fold changes, expression levels, p-values, and FDR values as determined by DESeq2 analysis was uploaded to the IPA software. We uploaded two matrices: one for primary infection and one for secondary infection. Pathway analysis was performed by proprietary IPA algorithms which reveal biological pathways that are enriched within the differentially expressed geneset.

Gene set enrichment analysis (GSEA) was performed using GSEA (v4.0.3) software provided by the Broad Institute [163, 164]. Gene lists for primary and recall responses were determined by DESEq2 analysis with a padj<0.05. Differentially expressed genes were inputted into .rnk files, listing gene names and their respective $\log_2$ fold changes. Gene lists were ranked

by their fold change. These gene lists were inputted into GSEA software using a weighted scoring scheme to an expression dataset c7.all.v7.1.symbols.gmt [Immunologic signatures] with 1000 permutations based upon the pathway phenotypes. The collapse parameter was selected during analysis. Chip platform "Mouse_ENSEMBL_Gene_ID_to_Human_Orthologs_MSigDB.v7.1" was used to assess the gene set enrichment of our findings to various transcriptional analysis in human cells. Significantly enriched gene sets were analyzed for their relevance to antiviral immunity.

2.14: Mouse strains

C57BL/6J (**B6 WT**, stain number 000664), B6.SJL-Ptprc^{a}Pepc^{b}/BoyJ (**CD45.1**, strain number 002014), C57BL/6-Tg(TcraTcrb)1100Mjb/J (**OT-I**, strain number 003831), B6.Cg-Tg(TcraTcrb)425Cbn/J (**OT-II**, strain number 004194), B6.129S2-Ighmtm1Cgn/J (**μMT**, strain number 002288), B6.129S6(C)-Zbtb46$^{tm1.1Kmm}$/J (**zbtb46-GFP**, strain number 027618), B6(Cg)-Zbtb46$^{tm1(HBEGF)Mnz}$/J (**zbtb46-DTR**, strain number 019506), B6.129S6-Il10^{tm1Flv}/J (**IL-10-GFP** tiger, strain number 008379), B6.129S7-Rag1$^{tm1Mom/J}$ (**Rag1 KO**, strain number 002216) mice were purchased from the Jackson Laboratory or bred and maintained under specific pathogen–free conditions in a BSL2 biocontainment room within Columbia University Medical Center (CUMC) animal facilities.

2.15: Statistical Analysis

Statistical analyses were performed in GraphPad Prism (v.8.0.0). Significance tests as well as cutoffs used are specified in each figure legend.

Chapter 3: Influenza infection imprints local lymphoid sites to promote lung resident heterosubtypic immunity

3.1: Abstract

Influenza infection generates tissue-resident memory T cells (TRM) that are maintained in the lung and can mediate protective immunity to heterologous influenza strains, though the precise mechanisms of local T cell-mediated protection are not well understood. In a murine heterosubtypic influenza challenge model, we demonstrate that protective lung T cell responses are independent of B cell responses, and derive from *in situ* activation of tissue resident memory T cell (TRM) and the enhanced generation of effector T cells from the local lung draining mediastinal lymph nodes (medLN). Primary infection fortified the medLN with an increased number of conventional dendritic cells (cDC) that mediate enhanced priming of T cells, including those specific for newly encountered epitopes; cDC depletion during the recall response diminished medLN T cell generation and heterosubtypic immunity. Our study shows that during a protective recall response, cDC in a fortified LN environment enhance the breadth, generation, and tissue migration of effector T cells to augment lung TRM responses.

3.2: Introduction

Diseases of the respiratory tract, triggered by diverse viral and bacterial pathogens that repeatedly infect individuals over their lifetimes, remain the leading cause of morbidity and mortality worldwide. Influenza virus is a major public health burden that globally causes up to 5 million cases of severe disease and 650,000 deaths each year, causing the most severe disease manifestations in children and the elderly [165]. Influenza vaccines target generation of strain-specific neutralizing antibodies and remain poorly efficacious, resulting in seasonal outbreaks of unpredictable severity. T cells however, can recognize invariant determinants of influenza present in all strains and mediate efficacious cross-strain protection in mouse models [166]. Moreover, T cell clones recognizing different influenza strains are readily detectable in human blood [167-169], indicating that promoting T cell-mediated immunity is a promising strategy for generating broad-based protection in the population.

Recent studies have shown that tissue localization is an important factor for T cell-mediated protective immunity, particularly in the respiratory tract. During a primary influenza infection, T cell responses are primed by dendritic cells (DC) that migrate from the lung to the draining lymph node (LN) and present influenza antigens to naïve T cells [60], resulting in the generation of lung-homing $CD4^+$ and $CD8^+$ effector cells to mediate viral clearance. Heterogenous subsets of memory T cells are generated from this initial infection and persist in multiple tissue sites, including non-circulating tissue resident memory T cells (TRM) within the lung [94, 104, 170]—a distinct subset that is present in multiple tissues in mice and humans and is transcriptionally and functionally distinct from circulating effector-memory (TEM) cells [97, 171, 172]. Lung $CD4^+$ and $CD8^+$ TRM mediate efficacious protection including lung viral clearance and reduced morbidity to heterosubtypic influenza strains [94, 104, 119, 173, 174]. Functionally, lung TRM can be activated

in situ in the presence of inhibitors of lymphoid egress [104], and TRM in the airways can mediate protection through effector cytokine production [119]. While these studies suggest that TRM in the tissue site of infection may dominate secondary responses, the contribution and requirements for circulating or lymphoid T cell populations during the recall response and specifically in the lung, are not clear.

Here, we demonstrate in a mouse model of heterosubtypic protection that lung T cells exhibit local protective responses to challenge with a heterologous viral strain, independent of B cells and humoral immunity. This local recall response involves both *in situ* lung TRM proliferation and recruitment of effector T cells from the periphery. Using a T cell tracking model, we demonstrate that in previously infected mice, priming of T cells in the medLN DC leads to rapid generation and trafficking of effector T cells to the lung resident niche, including those T cells specific for influenza antigens newly introduced during heterosubtypic challenge. We further demonstrate that enhanced T cell priming and generation was due to the fortification of medLN from the previous infection, marked by increased numbers of conventional DC (cDC). Preferential ablation of cDC in the medLN during heterosubtypic challenge abrogated enhanced T cell priming and inhibited the protective response. Therefore, the lung T cell-mediated recall response is comprised of robust effector generation from fortified local LN which coordinates with lung TRM to mediate efficacious protection against future infectious challenges.

3.3: Results

Lung niche T cells mediate protective responses to heterosubtypic influenza infection independent of B-cells

We assessed the differentiation and migratory state of T cells in the lung and draining mediastinal lymph node (medLN) from mice previously infected with influenza 3-4 weeks prior ("memory") mice compared to uninfected ("naïve") mice (Fig. 3.1 A). Intravenous antibody labeling was used to distinguish between T cells in circulation that become labeled by antibody from those cells in the tissues that are protected from antibody binding, as previously described [104]. Memory mice had significantly increased frequencies and numbers of protected $CD44^{hi}$ $CD4^{+}$ and $CD8^{+}$ T cells in the lung tissue niche (Fig. 3.1 A), which were enriched for influenza-specific T cells shown by tetramer staining of $CD8^{+}$ T cells (Fig. 3.2), consistent with our previous findings that lung niche T cells are a surrogate for antigen-specific responses [104]. Lung niche $CD44^{hi}$ memory T cells expressed CD69 (for CD4 and CD8) and CD103 (for CD8) (Fig. 3.1 B), consistent with a TRM phenotype [90, 101, 104, 174]. The lung-draining medLN also contained increased numbers of $CD44^{hi}$ $CD4^{+}$ and $CD8^{+}$ T cells compared to uninfected naive mice, and a minor subset also expressed TRM markers (Fig. 3.1 C). These results show a robust, quantifiable generation of lung TRM and local lymphoid memory T cells following influenza infection that is based on a polyclonal response.

Figure 3.1: Influenza infection generates memory $CD4^+$ and $CD8^+$ T cells in the lung tissue niche and draining lymph node.

T cells were isolated from the lung and lung-draining mediastinal lymph node (medLN) of uninfected "naïve" mice and "memory" mice (infected with X31 influenza 3-4 weeks previously), following intravenous administration of anti-CD45.2 antibody (see methods). (A) Analysis of lung T cells shown in representative flow cytometry plots of CD44 expression by circulating labeled (red) and lung tissue niche (blue) $CD4^+$ and $CD8^+$ T cells (*left*), and graphs of numbers of lung niche $CD44^+$ $CD4^+$ and $CD8^+$ T cells in individual naïve and memory mice (*right*). Data compiled from 2 groups, n=5-6 mice/group. (B) Lung niche T cells from memory mice express surface TRM markers. Expression of CD69 and CD103 expression by lung niche (blue) versus circulating (labeled, red) T cells shown as representative histograms (*left*) and graphs showing individual mice (*right*) treated with FTY720 for two days. Data compiled from two independent experiments, n= 7 mice/group. (C) Increased memory T cells in the medLN persist after primary influenza infection. *Left:* Representative flow cytometry plots of CD44 and CD69 expression by medLN $CD4^+$ and $CD8^+$ T cells from naïve and memory mice treated for 2 days with FTY720. *Right:* absolute numbers of medLN $CD44^+$T cells shown for individual naïve and memory mice. Data compiled from 2 independent experiments. n= 7 mice/group. Significance determined using student's unpaired t-test, **** $p<0.0001$; ** $p<0.01$. All error bars show mean ± SEM.

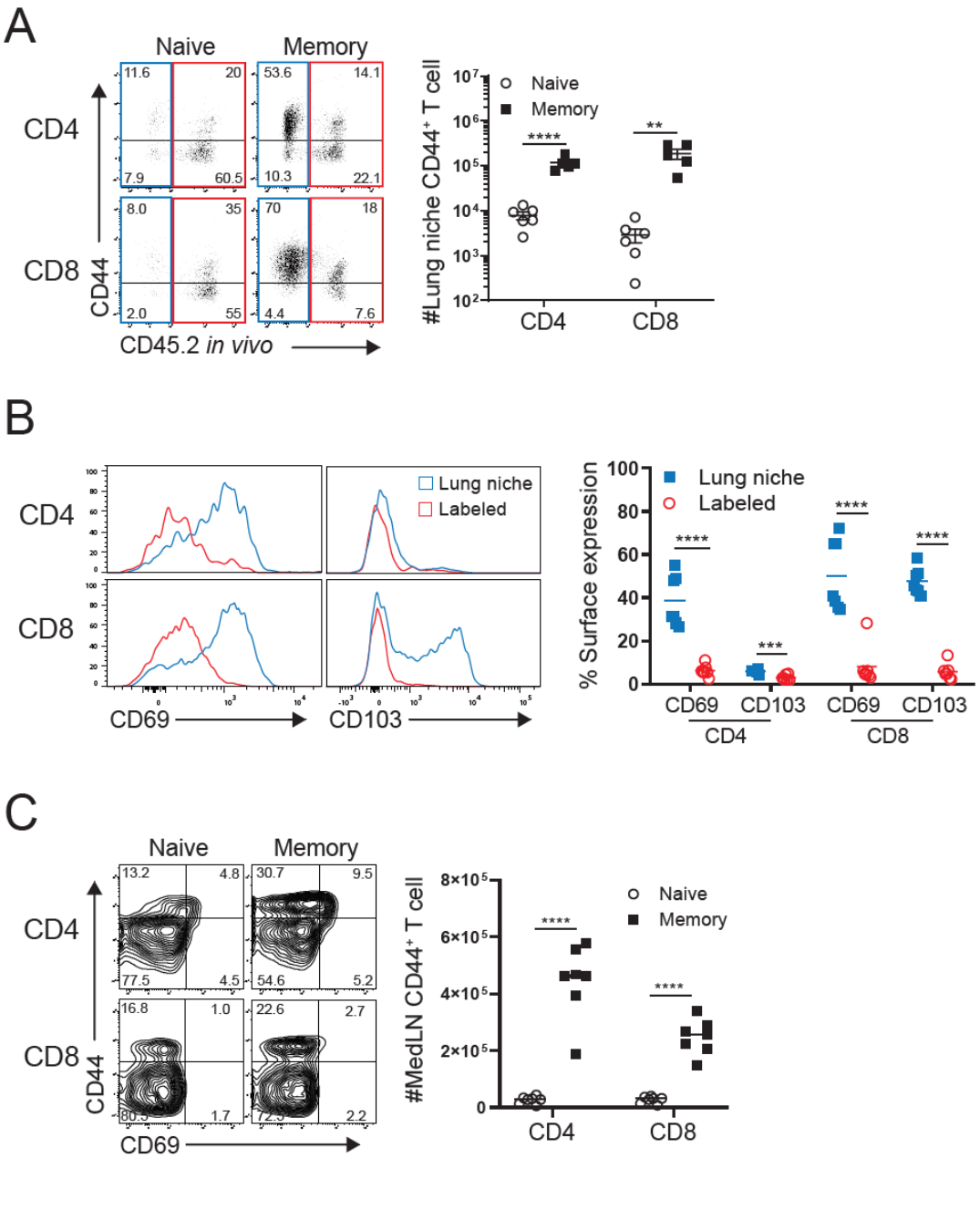
A
Naive
Memory
CD4
CD8
CD44
CD45.2 in vivo
11.6
20
7.9
60.5
53.6
14.1
10.3
22.1
8.0
35
2.0
55
70
18
4.4
7.6
#Lung niche CD44+ T cell
Naive
Memory
****
**
CD4
CD8
B
CD4
CD8
Lung niche
Labeled
CD69
CD103
% Surface expression
Lung niche
Labeled
****
***
CD69
CD103
CD69
CD103
CD4
CD8
C
Naive
Memory
CD4
CD8
CD44
CD69
13.2
4.8
77.5
4.5
30.7
9.5
54.6
5.2
16.8
1.0
1.7
22.6
2.7
2.2
#MedLN CD44+ T cell
Naive
Memory
****
****
CD4
CD8

Figure 3.2: Primary infection generates influenza-specific local memory T cells

Lung and medLN cells isolated from mice infected 3-5 weeks after primary infection. *Left*: Flow cytometry plots gated on lung $CD44^+$ $CD8^+$ showing NP-tetramer expression by lung niche (*blue*) and labeled (*red*) cells and graph showing number of lung $CD44^+$ $CD8^+$ $NP\text{-}Tet^+$ cells. *Right*: Flow cytometry plots gated on medLN $CD44^+$ $CD8^+$ showing CD103 and NP-tetramer expression and graph depicting absolute number of medLN $CD44^+$ $CD8^+$ $NP\text{-}Tet^+$ T cells. Data representative of 2 experiments, n=4 mice/group. Significance determined by student's unpaired t-test. ****, $p \leq 0.0001$, *, $p < 0.05$). Error bars are mean ± SEM.

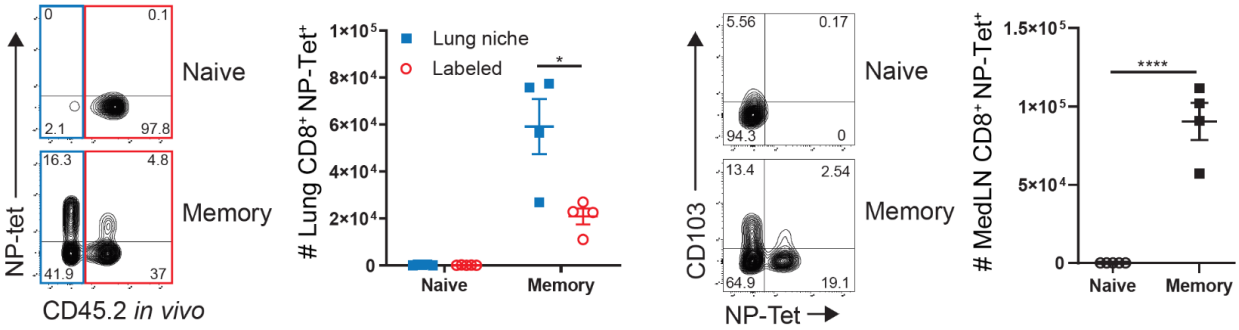
0
0.1
2.1
97.8
Naive
16.3
4.8
41.9
37
Memory
NP-tet
CD45.2 in vivo
Lung CD8+ NP-Tet+
1×10^5
8×10^4
6×10^4
4×10^4
2×10^4
0
Lung niche
Labeled
*
Naive
Memory
5.56
0.17
94.3
0
Naive
13.4
2.54
64.9
19.1
Memory
CD103
NP-Tet
MedLN CD8+ NP-Tet+
1.5×10^5
1×10^5
5×10^4
0
****
Naive
Memory

We used a modified mouse model of heterosubtypic immunity to assess mechanisms for T cell-mediated recall to influenza infection in the context of a polyclonal T cell response. Naïve and memory mice previously infected with the X31 (H3N2) strain of influenza virus were treated with the sphingosine-1-phosphate receptor (S1PR1) agonist FTY720 prior to and during challenge with the heterosubtypic PR8 (H1N1) strain of influenza in order to minimize the contributions of circulating cells at the time of challenge; protective immunity (morbidity and viral clearance) was measured at sequential timepoints post-challenge compared to primary influenza infection of naïve mice (Fig. 3.3 A, B). In the presence of FTY720 which selectively reduces the number of circulating (labeled) T cells in the lung but maintains TRM in the lung niche (Fig. 3.4 A) [104, 174], memory mice exhibited significantly reduced weight-loss morbidity over the course of infection compared to primary infection of naïve mice, and significantly lower lung viral load at 6 days post-infection (Fig. 3.3 B), the timepoint of peak viral load for primary infection [175]. The generation and localization of lung T cells in the lung tissue niche during maintenance with FTY720 treatment were similar in μMT mice which lack mature B cells [176] compared to WT memory mice (Fig. 3.4 B). Notably, reduced morbidity and near-complete viral clearance was also observed in μMT memory mice compared to primary infection of μMT naïve mice (Fig. 3.3 C). These data provide evidence that local T cell memory directs protective immunity with the canonical features of an enhanced and rapid recall response, independent of humoral immunity.

Figure 3.3: T cell-mediated protection to heterosubtypic challenge is tissue-localized and independent of B cells.

(A) Schematic diagram depicting heterosubtypic challenge model in which uninfected naïve mice, and memory mice, generated from prior X31 infection, are simultaneously challenged with PR8 (H1N1) virus with concurrent FTY720 treatment to compare primary and recall immune responses when systemic responses are inhibited. (B) *Left:* Weight loss morbidity at indicated times post-challenge during primary and recall infection. *Right:* Viral titers assessed in the bronchioalveolar lavage (BAL) on day 6 post-challenge. Data compiled from 2 independent experiments, n=10-12 mice/group. (C) Weight loss morbidity and BAL viral titers after PR8 challenge of B-cell-deficient (μMT) naïve and memory mice. Viral titers determined at Day 7 post-infection. Data compiled from 2 experiments, n=10-14 mice/group. Significance was determined by student's unpaired t-test. Log_{10} of viral titers $TCID_{50}$/mL was compared by t-test to determine significance. ****, $p \leq 0.0001$; ***, $p \leq 0.001$; ** $p \leq 0.01$; *, $p \leq 0.05$. All error bars show mean ± SEM.

A

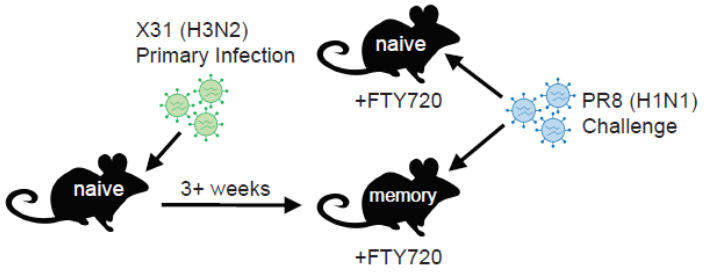
X31 (H3N2)
Primary Infection
naive
3+ weeks
naive
+FTY720
memory
+FTY720
PR8 (H1N1)
Challenge

B

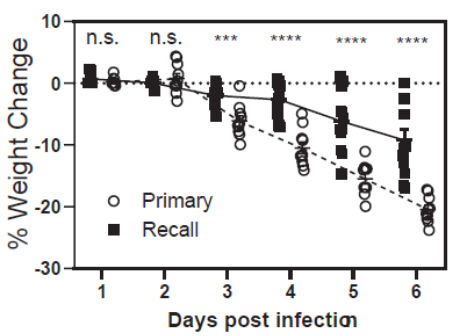
% Weight Change
Days post infection
Primary
Recall
n.s.
n.s.
***
****
****
****

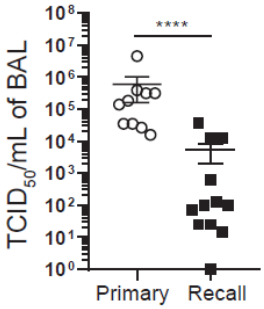
TCID50/mL of BAL
Primary
Recall
****

C

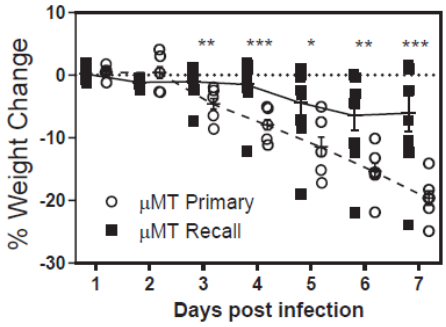
% Weight Change
Days post infection
µMT Primary
µMT Recall
**
***
*
**
***

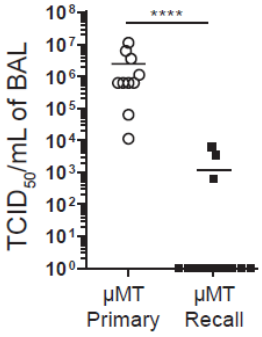
TCID50/mL of BAL
µMT Primary
µMT Recall
****

Figure 3.4: Local resident memory persists after FTY720 treatment

(A) Lung T cells isolated from wild type C57BL/6 mice after 3-4 weeks post-X31 infection and either treated with FTY720 or PBS control for two days and intravenously labeled with CD45.2 fluorescent antibody. Compiled from 4 independent experiments, n=5-7 mice/group. Significance determined by student's unpaired t-test. **, $p \leq 0.05$, *, $p < 0.05$. Error bars are mean ± SEM. (B) Representative FACS plot of lung (*left*) and medLN (*right*) T cells isolated from μMT memory mice after two days of FTY720 treatment.

A

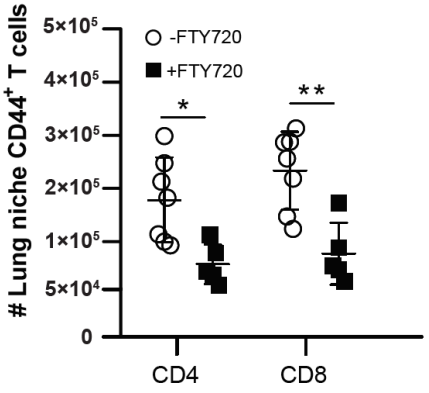
Lung niche CD44+ T cells
5×10^5
4×10^5
3×10^5
2×10^5
1×10^5
5×10^4
0
-FTY720
+FTY720
*
**
CD4
CD8

B

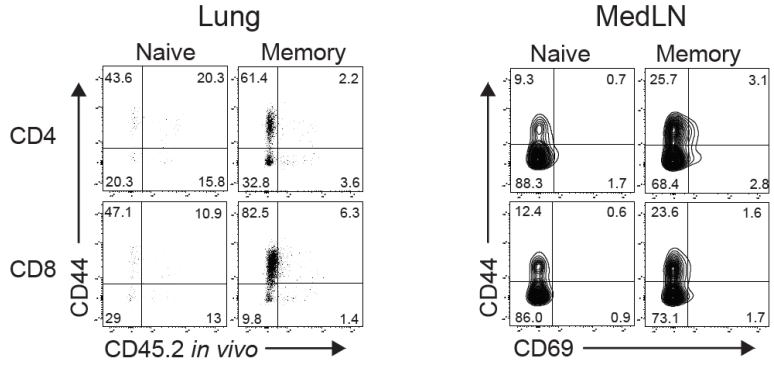
Lung
Naive
Memory
CD4
CD8
CD44
43.6
20.3
20.3
15.8
61.4
2.2
32.8
3.6
47.1
10.9
29
13
82.5
6.3
9.8
1.4
CD45.2 in vivo
MedLN
Naive
Memory
9.3
0.7
88.3
1.7
25.7
3.1
68.4
2.8
12.4
0.6
86.0
0.9
23.6
1.6
73.1
1.7
CD44
CD69

Expansion of CD103$^-$ negative T cells within the lung resident niche and medLN during recall

We investigated how the lung T cell dynamics in the recall response differed from that in the primary response. After PR8 challenge, the numbers of CD4$^+$ and CD8$^+$ CD44^{hi} T cells within the lung resident niche significantly increased at 4-5 days post-infection in memory mice (recall) to levels fivefold higher than the number of lung niche T cells in the primary response (primary) (Fig. 3.5 A). By contrast, circulating lung CD4$^+$ and CD8$^+$ T cells identified by *in vivo* Ab labeling did not increase in number after infection (Fig. 3.5 A), revealing that the enhanced and rapid T cell accumulation during recall is specific to the lung tissue niche. T cell proliferation during recall was further assessed by harvesting lung T cells two hours following *in vivo* BrdU administration. BrdU$^+$ CD4$^+$ and CD8$^+$ T cells were detectable 4-5 days post-challenge predominantly in the lung resident niche, and not within circulating (labeled) cells (Fig. 3.5 B) and were minimally affected by FTY720 treatment (Fig. 3.6). Together, these findings demonstrate that the increase in lung T cell numbers during the recall response was due, at least in part, to proliferating T cells localizing in the lung resident niche.

The accumulation of proliferating T cells in the lung tissue niche could derive exclusively from lung TRM, or also involve migration of T cells from the periphery during FTY720 treatment. We therefore assessed lung T cell numbers and BrdU incorporation based on CD103 expression as a TRM marker, as CD69 expression can vary during the course of infection [104]. Notably, CD103$^-$ and not CD103$^+$ T cells were the major subset accumulating in the lung resident niche for both CD4$^+$ and CD8$^+$ T cells, albeit lower frequencies of lung CD4$^+$ TRM express CD103 compared to CD8$^+$ TRM (Fig. 3.5 C). Furthermore, CD103$^-$ CD8$^+$ lung T cells incorporated BrdU to a greater extent than their CD103$^+$ TRM counterparts (Fig. 3.5 D), suggesting that enhanced

proliferation may underly their increased accumulation in the lung niche. (Similar BrdU analysis for $CD4^+$ cells was not performed due to low $CD103^+$ numbers). The predominant expansion of $CD103^-$ rather than $CD103^+$ lung T cells during recall suggested a potential influx of T cells from the periphery, prompting examination of proliferation within local lymphoid sites.

In the local medLN of memory mice, $CD4^+$ and $CD8^+$ T cells exhibited rapid accumulation at 3-4 days post-challenge, resulting in peak numbers 5 to 10-fold greater than during primary infection (Fig. 3.7 A, Fig. 3.8 A). Importantly, the expanded medLN T cells during recall were predominantly non-TRM, $CD44^{hi}CD62L^{lo}CD103^-$ (effector-memory) cells (Fig. 3.7 B). Accordingly, BrdU incorporation was significantly higher in the recall response compared to the primary response for proliferating medLN $CD44^{hi}CD62L^{lo}$ T cells and was largely observed in the $CD103^-$ TEM rather than the $CD103^+$ TRM subset (Fig. 3.7 C). No significant BrdU incorporation was observed in memory $CD4^+$ or $CD8^+$ T cells in the spleen at these timepoints, demonstrating this lymphoid-derived proliferation was locally regulated (Fig. 3.8 B). These data demonstrate robust local expansion of effector-memory T cells in the tissue-draining LN during recall.

Figure 3.5: Heterosubtypic recall promotes rapid accumulation and proliferation of lung niche CD103- T cells

Lung T cells were isolated from naïve and memory mice challenged as in Fig. 3.3, following administration of BrdU i.p. and i.n. 2 hrs prior to tissue harvest. (A) Accumulation of $CD44^+$ $CD4^+$(*upper*) and $CD8^+$ (*lower*) T cells in the lung niche following primary and recall challenge shown in representative flow cytometry plots (*left),* and in graphs depicting absolute numbers of lung niche (*middle*) and labeled (*right*) $CD44^+$ T cells. (B) Flow cytometry plots (*left*) gated on lung T cells showing BrdU incorporation by lung niche and labeled cells, and graphs depicting absolute numbers of $CD44^+$ $CD4^+$ (*middle*) and $CD8^+$ lung niche (*blue*) and labeled (*red*) $BrdU^+$ T cells. (C) Flow cytometry plots (*left*) depicting $CD103^-$ and $CD103^+$ $CD44^+$ $CD4^+$ and $CD8^+$ lung T cell accumulation during the recall response. Graphs show absolute numbers of lung niche $CD44^+$ $CD4^+$ (*middle*) and $CD8^+$ (*right*) T cells during recall response. (D) Lung $CD8^+$ T cell BrdU incorporation during the recall response, depicted by representative flow cytometry plot (*left*) of $CD44^+CD8^+$ lung niche T cell BrdU expression and a graph showing number of $BrdU^+$ lung niche $CD103^-$ and $CD103^+$ $CD44^+$ $CD8^+$ T cells. All data is representative of two independent experiments, n=2-5 mice/group/experiment. All error bars show mean ± SEM.

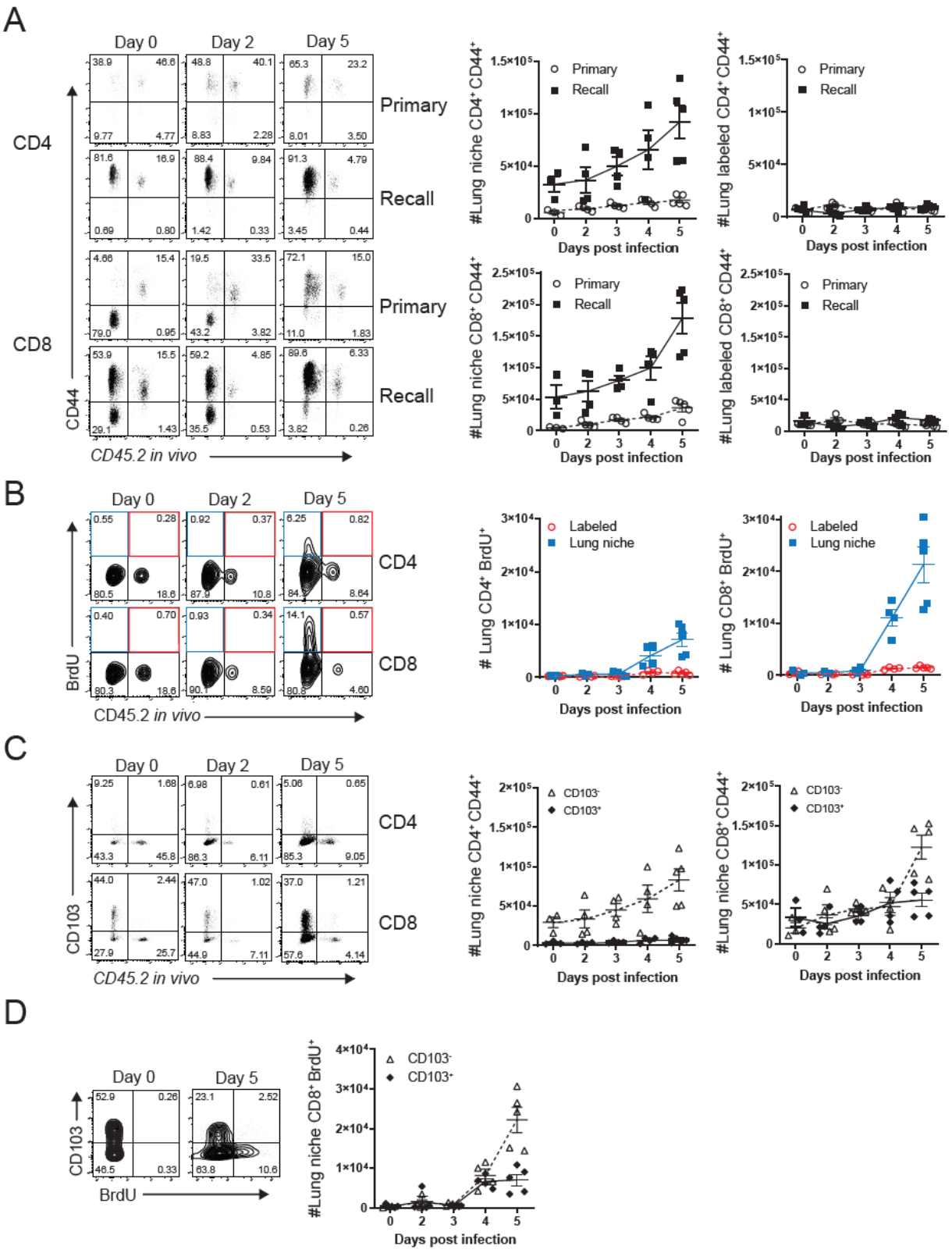
A
Day 0
Day 2
Day 5
CD4
CD8
Primary
Recall
CD44
CD45.2 in vivo
#Lung niche CD4+ CD44+
#Lung labeled CD4+ CD44+
#Lung niche CD8+ CD44+
#Lung labeled CD8+ CD44+
Days post infection
B
BrdU
Labeled
Lung niche
Lung CD4+ BrdU+
Lung CD8+ BrdU+
C
CD103
CD103-
CD103+
#Lung niche CD4+ CD44+
#Lung niche CD8+ CD44+
D
#Lung niche CD8+ BrdU+

Figure 3.6: FTY720 treatment does not block T cell migration to lung niche

T cells were isolated from the lungs of memory and naïve mice 5 days after PR8 challenge with or without daily FTY720 treatment. Left: Representative flow plot of $CD4^+$ and $CD8^+$ lung T cells showing CD44 expression plotted against *in vivo* injected CD45.2 expression. Right: Histograms depicting number of $CD44^+$ $CD4^+$ or $CD8^+$ T cells either labeled or protected by in vivo fluorescent antibody. Graphs show mean ± SEM (n=4-5 mice per group; significance between FTY720 treated and untreated groups determined by student's unpaired t-test, ***, $p \leq 0.001$; ** $p \leq 0.01$)

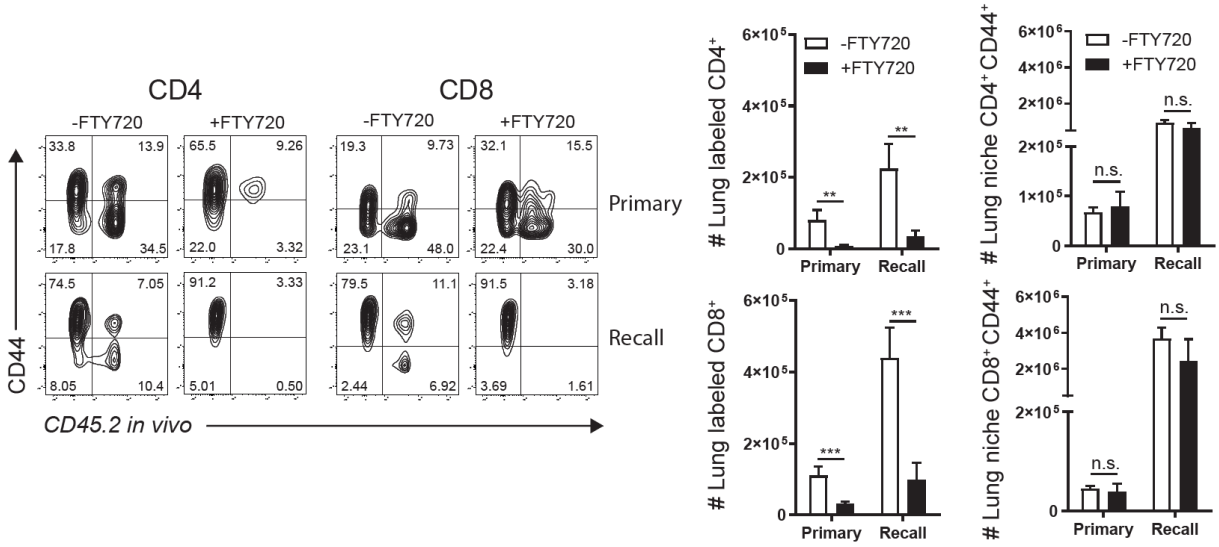
CD4
CD8
-FTY720
+FTY720
-FTY720
+FTY720
33.8
13.9
17.8
34.5
65.5
9.26
22.0
3.32
19.3
9.73
23.1
48.0
32.1
15.5
22.4
30.0
Primary
74.5
7.05
8.05
10.4
91.2
3.33
5.01
0.50
79.5
11.1
2.44
6.92
91.5
3.18
3.69
1.61
Recall
CD44
CD45.2 in vivo
Lung labeled CD4+
Lung labeled CD8+
Lung niche CD4+CD44+
Lung niche CD8+CD44+
-FTY720
+FTY720
6×10^5
4×10^5
2×10^5
0
6×10^6
4×10^6
2×10^6
1×10^5
**
***
n.s.
Primary
Recall

Figure 3.7. The recall response enhances accumulation and proliferation of medLN T cells

MedLN T cells were isolated from naïve and memory mice challenged and treated with BrdU during FTY720 treatment as in Figure 3.5. (A) Absolute numbers of medLN $CD44^+$ $CD4^+$ and $CD8^+$ T cells during primary and recall responses to PR8 challenge. (B) Similar to (A) except $CD44^+$ T cells during only the recall response were stratified into $CD103^+$ and $CD103^-$ cells. (C) BrdU incorporation by $CD103^+$ and $CD103^-$ $CD44^+CD62L^-$ $CD4^+$ (*top*) and $CD8^+$ (*bottom*) T cells in the primary and recall response shown in representative flow cytometry plots (*left*) and graphs (*right*) showing the percent BrdU incorporation from individual mice 4 and 5 days post-challenge. All data is representative of 2 independent experiments, n=2-4 mice/group. *, $p \leq 0.05$ as determined by student's t-test. All graphs show mean ± SEM.

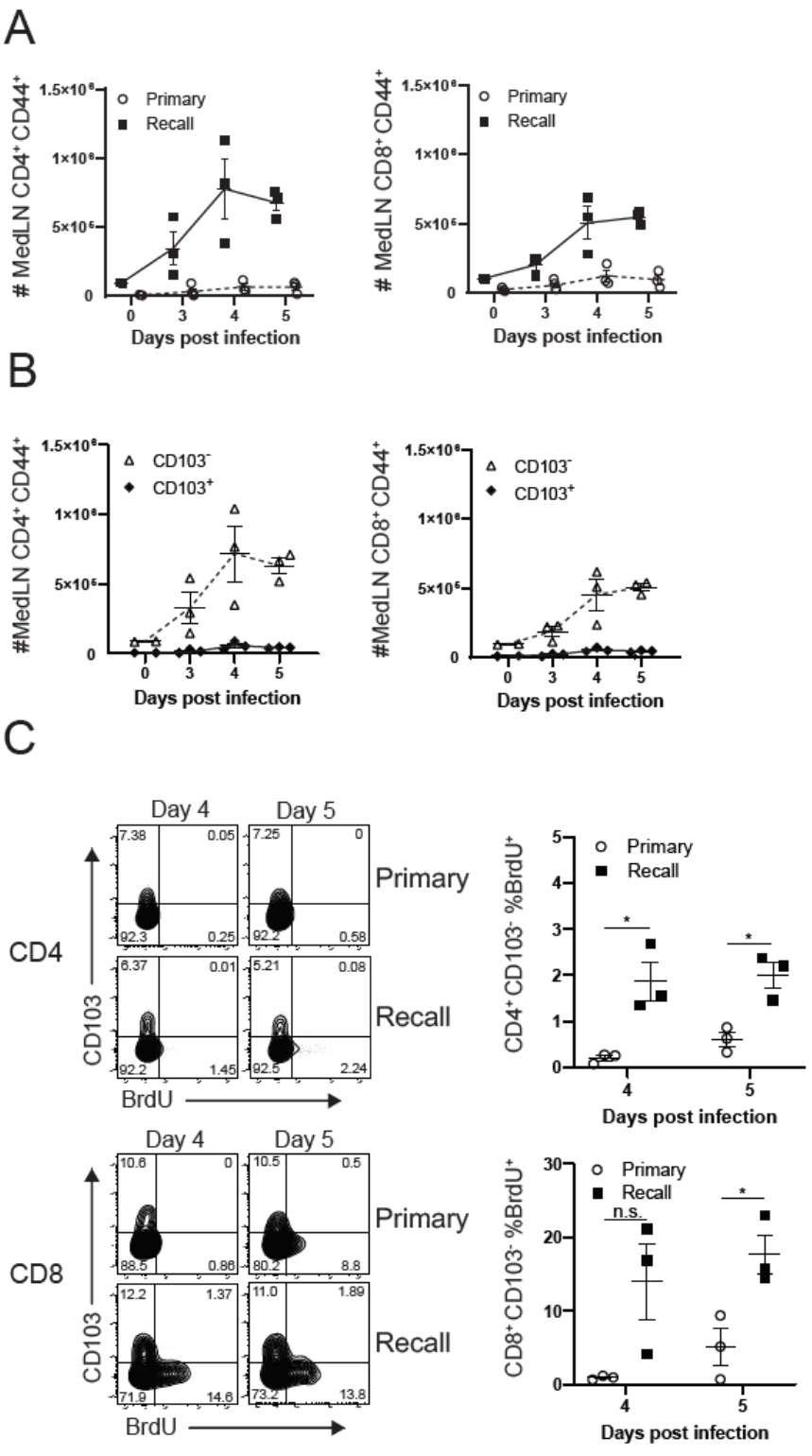
A
MedLN CD4+ CD44+
MedLN CD8+ CD44+
Primary
Recall
Days post infection
B
#MedLN CD4+ CD44+
#MedLN CD8+ CD44+
CD103-
CD103+
Days post infection
C
Day 4
Day 5
CD4
CD8
CD103
BrdU
Primary
Recall
CD4+ CD103- %BrdU+
CD8+ CD103- %BrdU+
n.s.
Days post infection

Figure 3.8: Lymphoid T cell expansion during recall response

(A) Total medLN $CD4^+$ and $CD8^+$ T cell counts (B) Spleen $CD4^+$ and $CD8^+$ $CD44^+$ $CD62L^-$ relative BrdU incorporation proportions. Data representative of two experiments, n=2-3 mice/group. Error bars show mean ± SEM.

A

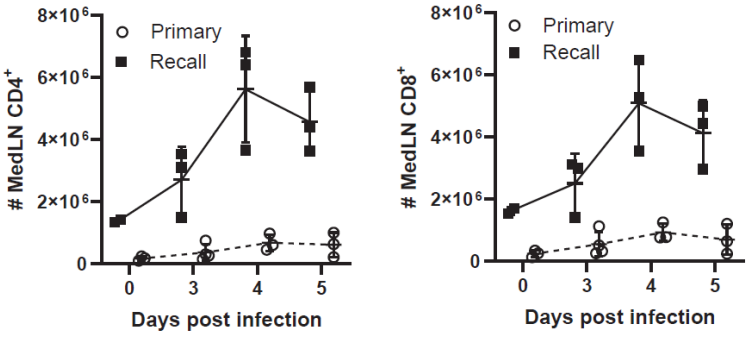
8×10⁶
6×10⁶
4×10⁶
2×10⁶
0
MedLN CD4⁺
Primary
Recall
0
3
4
5
Days post infection
8×10⁶
6×10⁶
4×10⁶
2×10⁶
0
MedLN CD8⁺
Primary
Recall
0
3
4
5
Days post infection

B

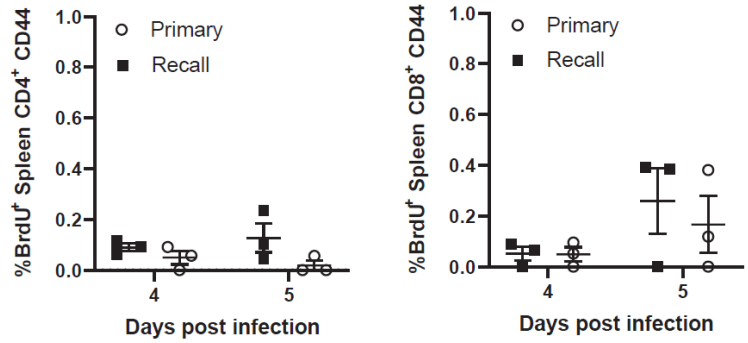
1.0
0.8
0.6
0.4
0.2
0.0
%BrdU⁺ Spleen CD4⁺ CD44
Primary
Recall
4
5
Days post infection
1.0
0.8
0.6
0.4
0.2
0.0
%BrdU⁺ Spleen CD8⁺ CD44
Primary
Recall
4
5
Days post infection

Enhanced T cell priming to new epitopes in the secondary response drives effector migration to the lung resident niche

In order to assess the contribution of peripheral T cell activation and migration to the lung-localized recall response, we adoptively transferred naïve $CD4^+$ $CD44^-$ $CD45.1^+$ OT-II cells expressing a transgene-encoded TCR specific for ovalbumin peptide (OVA) into naïve and memory mice which were subsequently challenged with recombinant PR8-OTII or PR8 as a control (Fig. 3.9 A). In response to PR8-OTII challenge, OT-II cells exhibited enhanced recruitment to the lung in memory compared to naïve hosts; there were increased frequencies and numbers of OT-II cells in the lung, lung resident niche, medLN, and spleen, at 5 days post-infection in memory mice compared to negligible-to-low numbers of OT-II cells during primary infection (Fig. 3.9 B). Minimal numbers of OT-II cells were detected in the inguinal lymph node (ILN) distal to the infection site in naïve or memory hosts following PR8-OTII challenge, indicating that priming of OT-II cells occurred local to the infection site. Moreover, OT-II cells were minimally present in tissues during primary or recall challenge with PR8 lacking the OVA epitope (Fig. 3.9 B), indicating that bystander migration was not sufficient to recruit and/or activate significant numbers of OT-II cells. During the recall response, lung OT-II cells incorporated more $BrdU^+$ compared to their polyclonal host $CD4^+$ T counterparts following PR8-OTII heterosubtypic challenge (Fig. 3.9 C), demonstrating robust activation and *in situ* proliferation of the OVA-specific T cells, similar to what was observed in the lung polyclonal T cell response (Fig. 3.5 B).

In addition, because we observed increased $CD8^+$ polyclonal T cell responses as well, we interrogated whether these same findings would apply to OT-I cells. We also transferred naïve OT-I $CD8^+$ T cells into naïve and memory mice and challenged mice with PR8-OTI in the same way as performed for OT-II cells (Fig. 3.9 B). Five days after challenge, we observed a significant

increase in $CD8^+$ OT-I numbers in the medLN, similar to what was observed for $CD4^+$ OT-II responses. However, we were also unable to find significant differences in the lung, perhaps due to differences in T cell migration kinetics using the PR8-OTI model. Together, these results show enhanced activation, proliferation and lung-specific migration of newly-primed, flu-specific $CD4^+$ and $CD8^+$ effector cells in the presence of an ongoing recall response to influenza.

Because B-cells are a major antigen presenting cell, we investigated whether expansion and migration of OT-II cells during the recall response also occurred in μMT memory mice. Similar to results in B-cell competent WT hosts, OT-II cells were present in the lung resident niche, medLN, and spleen in significantly greater numbers in memory μMT mice compared to naïve μMT mice at 4-5 days post-challenge with PR8-OTII (Fig. 3.10 A and B). OT-II cells were present in greater numbers in the medLN compared to the spleen at day 4 post-infection, suggesting that the medLN is the primary initiating priming site (Fig. 3.10 A). Moreover, OT-II expansion and migration occurred independently of FTY720 treatment (Fig. 3.11), suggesting that while FTY720 treatment may reduce non-specific bystander T cell migration (Fig. 3.9 B), migration from local lymphoid sites is unaffected. These results show that local recall responses are associated with enhanced generation of effector T cells from the local draining lymph node independent of B cell-mediated priming, including T cells specific for newly encountered influenza epitopes

Figure 3.9: Recall response enhances local lymph node T cell priming and migration to the lung tissue niche

(A) Experimental schematic for tracking new effector and circulating T cell responses: $CD44^{lo}$ $CD45.1^{+}$ OT-I or OT-II T cells were transferred into naïve and memory mice (WT or μMT), which were subsequently challenged with PR8 or recombinant PR8-OTI/OT-II in the presence of FTY720 treatment, and tissues were harvested day 4-5 post-infection following intravenous administration of anti-CD45.2 Ab. (B) T cells isolated from lung, medLN, spleen, and ILN of the indicated hosts and challenge conditions were assessed for the presence of OT-II ($CD45.1^{+}$) $CD4^{+}$ T cells shown in representative flow cytometry plots (*left*, OT-II containing quadrants outlined in green), and in graphs depicting total numbers of OT-II cells in each tissue site for individual mice. Data are representative of two independent experiments, n=3-5 mice/group/experiment. (C) BrdU incorporation by lung OT-II cells and $CD45.1^{-}$ host polyclonal cells 5 days after recall challenge with PR8-OTII. Data representative of two independent experiments, n=3-5 mice/group/experiment. (D) OT-I cells in the lung and medLN of wild type hosts following primary or recall challenge with PR8-OTI shown in representative flow cytometry plots (left), and graphs depicting total numbers of OT-I cells in each tissue site in primary or recall responses. Data are representative of 2 independent experiments, n=3-5 mice/group/experiment. Significance in (B) and (D) between primary and recall groups determined by student's unpaired t-test. Significance in (C) determined by paired t-test between OT-II and polyclonal cells. ****, $p \leq 0.0001$, ***, $p \leq 0.001$; *, $p \leq 0.05$). All error bars show mean ± SEM.

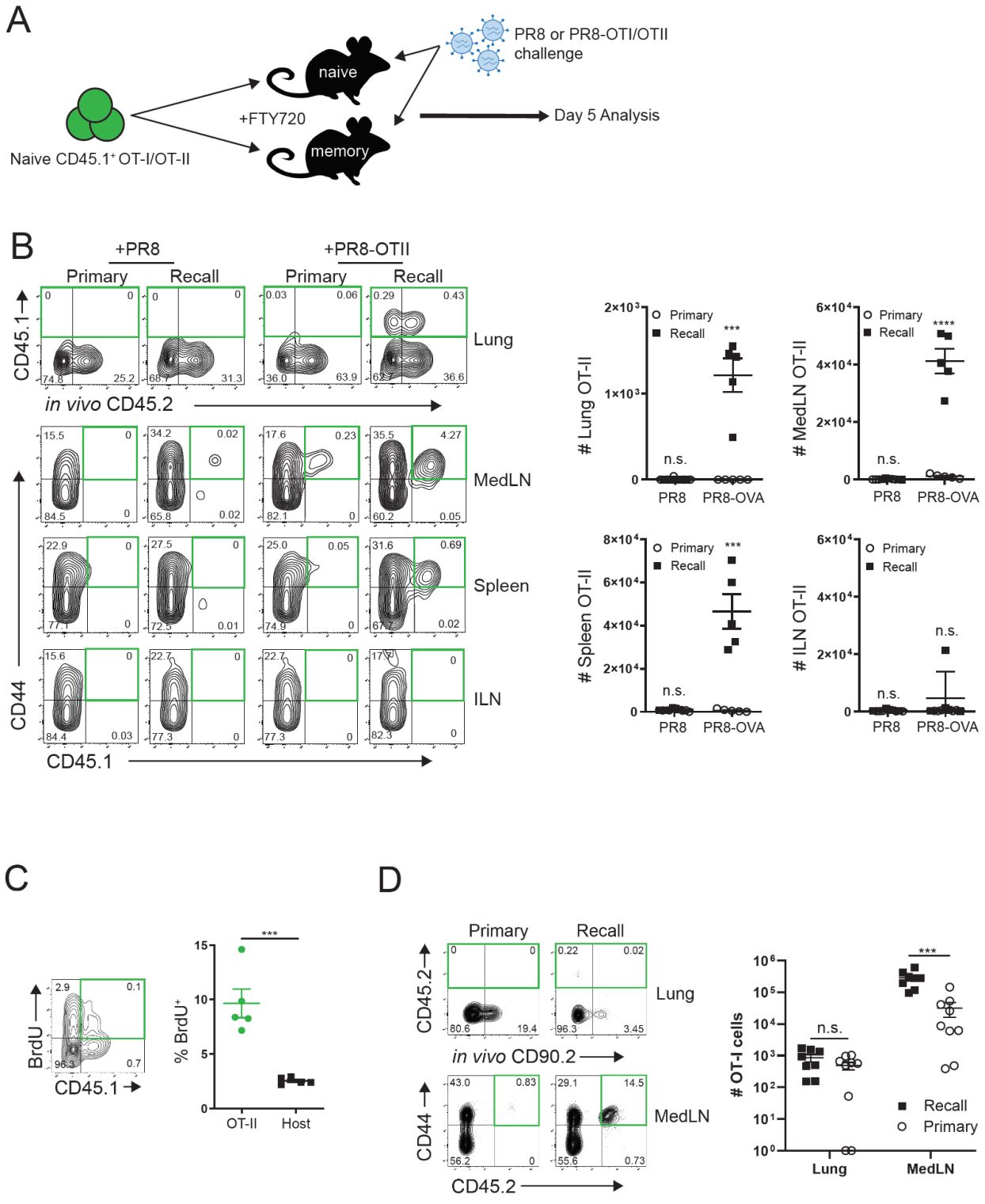
A
naive
memory
+FTY720
Naive CD45.1+ OT-I/OT-II
PR8 or PR8-OTI/OTII challenge
Day 5 Analysis
B
+PR8
+PR8-OTII
Primary
Recall
CD45.1
in vivo CD45.2
Lung
MedLN
Spleen
ILN
CD44
CD45.1
Lung OT-II
MedLN OT-II
Spleen OT-II
ILN OT-II
PR8
PR8-OVA
n.s.
C
BrdU
CD45.1
% BrdU+
OT-II
Host
D
CD45.2
in vivo CD90.2
CD44
OT-I cells
Lung
MedLN

Figure 3.10: Enhanced medLN T cell priming in B cell-deficient mice

$CD44^{lo}$ $CD45.1^{+}$ OT-II indicator population is transferred into both naïve and memory μMT mice, and PR8-OTII challenge performed, and cells were isolated from lung, medLN, and spleen T cells after (A) 4 and (B) 5 days. (A, B) *Left*: Representative flow cytometry plots gated on $CD4^{+}$ T cells. *Right*: Graph depicting number of OT-II cell in lung, medLN, and spleen. Representative of 2 independent experiments, n=3-5 mice/group. Significance determined by student's unpaired t-test ***, $p \leq 0.001$; ** $p \leq 0.01$. Error bars show mean ± SEM.

A

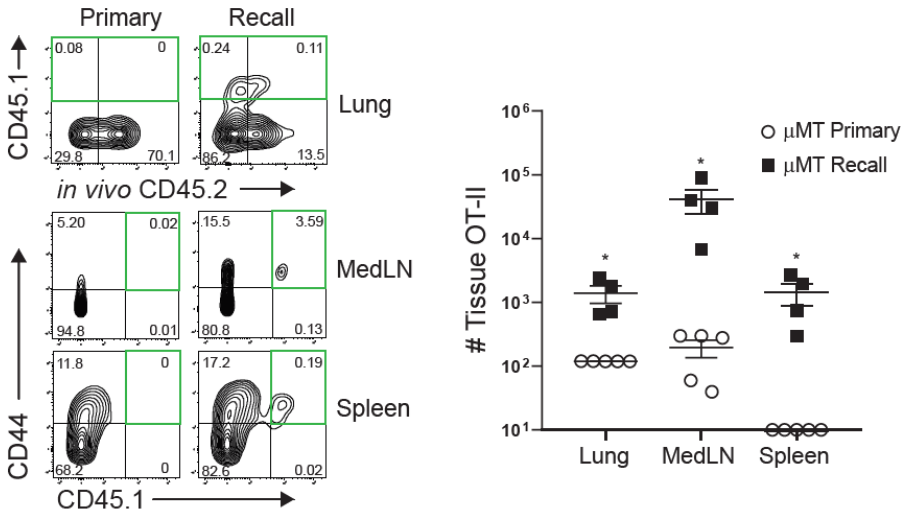
Primary
Recall
CD45.1
0.08
0
29.8
70.1
0.24
0.11
86.2
13.5
Lung
in vivo CD45.2
5.20
0.02
94.8
0.01
15.5
3.59
80.8
0.13
MedLN
11.8
0
68.2
0
17.2
0.19
82.6
0.02
Spleen
CD44
CD45.1
Tissue OT-II
µMT Primary
µMT Recall
Lung
MedLN
Spleen

B

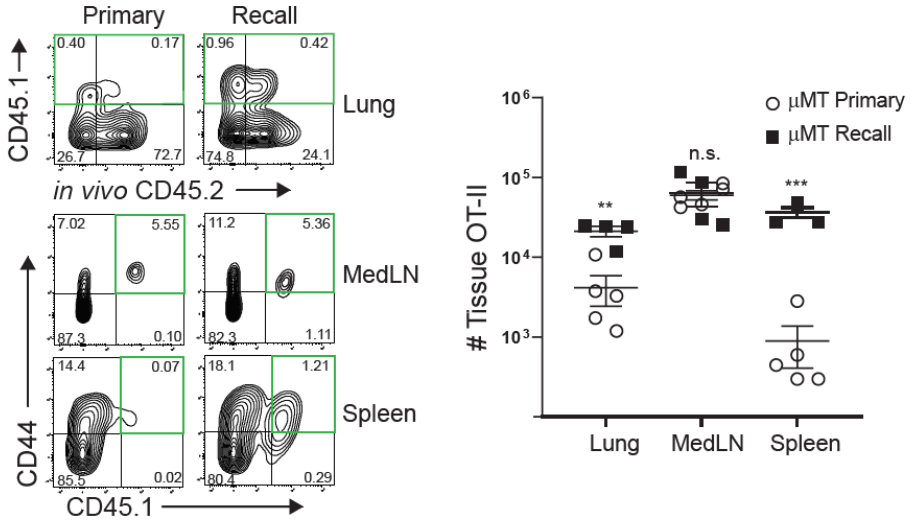
Primary
Recall
CD45.1
0.40
0.17
26.7
72.7
0.96
0.42
74.8
24.1
Lung
in vivo CD45.2
7.02
5.55
87.3
0.10
11.2
5.36
82.3
1.11
MedLN
14.4
0.07
85.5
0.02
18.1
1.21
80.4
0.29
Spleen
CD44
CD45.1
Tissue OT-II
µMT Primary
µMT Recall
n.s.
Lung
MedLN
Spleen

Prior influenza infection fortifies local lymph nodes for T cell priming

We hypothesized that the local LN environment in memory mice promoted activation and priming of new flu-specific effector cells. Following previous influenza infection, there was a marked increase in T cell numbers—both naïve and memory—even at 35 days post-infection (Fig. 3.12 A), suggesting that local infection may confer preferential homing or retention of T cells in the medLN. Indeed, transfer of equal numbers of naïve OT-II cells into the different hosts, resulted in greater numbers of OT-II retained in medLN of memory compared to naïve mice (Fig. 3.12 B), indicating that the environment of medLN in previously infected mice enabled increased retention of T cells compared to uninfected mice.

We then sought to clarify the degree to which the significantly increased medLN OT-II expansion during the recall response was due to a larger precursor population or enhanced activation and proliferation. At day 2 post-challenge with PR8-OTII, nearly all of the OT-II cells in the medLN of memory mice expressed the early TCR activation marker Nur77 (known to be induced several hours after TCR signaling [177, 178]), while OT-II cells in the spleen did not express Nur77 at this early timepoint (Fig. 3.12 C), demonstrating that the medLN is the initial site of influenza-specific T priming. By day 3 post-challenge, there was already extensive proliferation of medLN OT-II cells during the recall response compared to a significantly lower proliferation (and greatly reduced numbers) of medLN OT-II cells in the primary response (Fig. 3.12 D). These data demonstrate that prior influenza infection fortifies the local medLN to promote TCR-mediated signaling and proliferation during heterosubtypic challenge.

Figure 3.11: FTY treatment does not affect IAV-specific T cell lung migration

$CD44^{lo}$ $CD45.1^{+}$ OT-II indicator population is transferred into both naïve and memory mice and challenged with PR8-OTII. Lung cells were isolated after 5 days post PR8-OTII challenge. Graph depicts number of lung $CD4^{+}$ $CD45.1^{+}$ OT-II T cells during the primary and recall responses with or without FTY720 treatment. Data compiled from 2 independent experiments, n=4-9 mice/group.

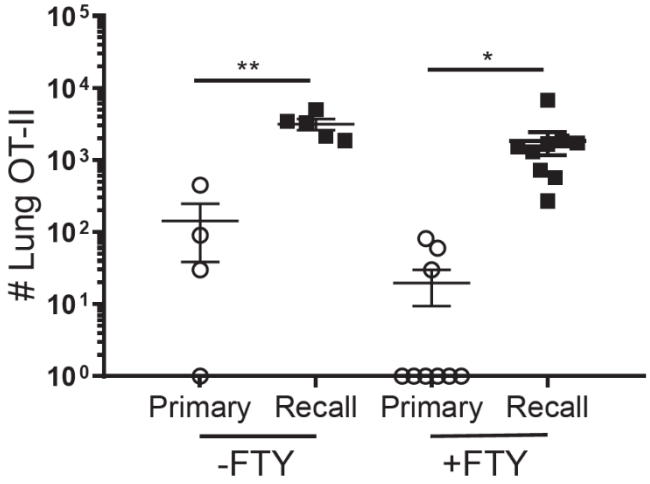
10^5
10^4
10^3
10^2
10^1
10^0
Lung OT-II
**
*
Primary
Recall
Primary
Recall
-FTY
+FTY

Figure 3.12: Enhanced naïve T cell recruitment, activation and proliferation in the medLN during the recall response

(A) Prior influenza infection results in increased numbers of naïve and memory T cells in the medLN. Graphs show numbers of indicated $CD4^+$ and $CD8^+$ T cell subsets (T-naïve, $CD44^{lo}$ $CD62L^{hi}$; TEM, $CD44^{hi}$ $CD62L^{lo}$; TCM, $CD44^{int}$ $CD62L^{hi}$) in the medLN of uninfected (naïve) mice and memory mice 3-5 weeks post-infection. Data representative of 2 experiments, compiled from 3-5 mice per group. (B) Recruitment and/or retention of naïve OT-II $CD4^+$T cells in medLN 2 days following transfer of equal numbers (50k cells/mouse) into naïve and memory congenic mice as assessed by representative flow cytometry plots of transferred $CD45.1^+$ $CD4^+$ T cells (*left*), and by graph (*right*) showing absolute numbers of OT-II cells in naïve and memory mouse hosts. compiled from 4-5 mice/group. (C, D) Enhanced priming in the medLN of memory mice during recall. Proliferation dye labeled OT-II/Nur77-GFP cells were transferred into naïve and memory mice hosts, and mice were subsequently challenged with PR8-OTII one day later. (C) Expression of the early TCR signaling molecule Nur77 as indicated by GFP expression by T cells isolated from medLN and spleen 2 days post-challenge shown in representative flow cytometry plots gated on OT-II cells (*left*), and graphs (*right*) showing frequency of GFP^+ cells in the recall response. Data representative of 2 experiments, n= 3-5 mice/group. (D) Enhanced proliferation in the recall response. Same setup as in (C) except T cells were isolated from medLN 3 days after PR8-OTII challenge. *Left:* Representative flow cytometry plots gated show dilution of proliferation dye by OT-II cells. Graphs depict percentage of OT-II cells divided (*middle*)and total number of OT-II cells (*right*). Data shown are representative of two independent experiments, n=3 mice/group. Significance determined by student's unpaired t-test, ***, $p \leq 0.001$; **, $p \leq 0.01$; *, $p \leq 0.05$). Error bars show mean ± SEM.

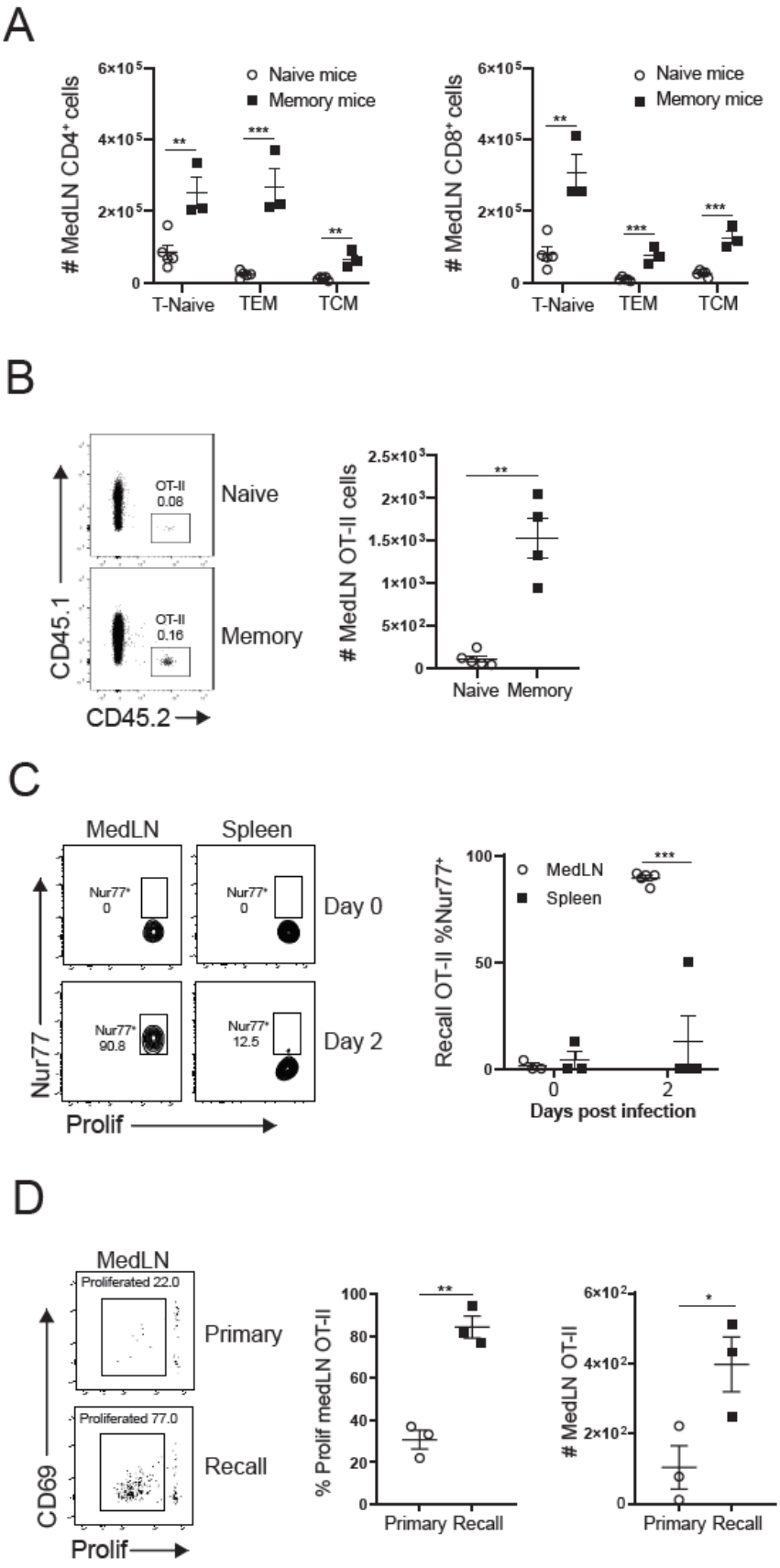
A
MedLN CD4+ cells
MedLN CD8+ cells
Naive mice
Memory mice
T-Naive
TEM
TCM
B
CD45.1
CD45.2
OT-II 0.08
OT-II 0.16
Naive
Memory
MedLN OT-II cells
C
MedLN
Spleen
Nur77+ 0
Nur77+ 90.8
Nur77+ 12.5
Day 0
Day 2
Nur77
Prolif
Recall OT-II %Nur77+
Days post infection
D
Proliferated 22.0
Proliferated 77.0
Primary
Recall
CD69
% Prolif medLN OT-II
# MedLN OT-II

Increased numbers of conventional dendritic cells persist in the medLN following influenza infection

The more rapid priming of OT-II in the medLN of memory mice suggested that conventional dendritic cells (cDC), which prime naïve T cells, were altered in the medLN of memory compared to naïve mice. The number of medLN cDCs ($CD45^+$ $CD11c^+$ I-A/I-E^{hi}) increases within four days following primary infection, and both $CD11b^+$ $CD103^-$ and $CD11b^-$ $CD103^+$ cDCs are present in increased numbers up to 35 days after primary challenge (Fig. 3.13 A). To better identify cDCs between sites, as CD11c can also be expressed by tissue macrophages [179], we assessed expression of the transcription factor zbtb46, which is specifically expressed by cDCs [180, 181], using zbtb46-GFP reporter mice [181]. Consistent with the CD11c results, zbtb-46^+cDCs are present in greater numbers specifically within the medLN of memory mice compared to naïve (uninfected) mice, while cDC numbers in the non-draining ILN are unchanged between naïve and memory mice (Fig. 3.13 B). Numbers of Lung cDC are also not significantly different between naïve and memory mice (Fig. 3.13 B). This quantifiable increase in cDC content that is induced from prior influenza infection, is therefore specific to the local lung-draining LN and not within the tissue site of infection.

We examined the augmented medLN cDC population for qualitative functional changes, including markers of migration and activation. $Zbtb46^+$ cDCs from both the lung and medLN of memory mice contained higher proportions of $CD11b^-$ $CD103^+$ migratory cells (Fig. 3.13 C), which also express higher levels of the costimulatory ligand and DC activation marker CD86 (Fig. 3.13 D). (There was no change in the level of CD86 expression by either cDC subset between naïve and memory mice). In an unbiased approach to identifying potential changes in medLN cDCs between naïve and memory mice, we analyzed the transcriptome profile of $CD45^+zbtb46^+$

cDCs from the medLN of naïve and memory mice by RNAseq (Fig. 3.13 D). Gene expression between the two cDC populations was highly similar with only 61 genes differentially expressed (Fig. 3.13 E) including the tissue residence marker *Cxcr6*, and chemokines *Ccl6* and *Ccl24*, but without a clear signature of increased cDC activation or antigen presentation. These data show increased numbers and migration of zbtb46^{+} cDC populations in the medLN of memory mice that are transcriptionally similar to their naïve counterparts, suggesting that the enhanced T cell priming during the recall response derives from greater numbers of cDC.

Figure 3.13: Influenza infection promotes long-term quantitative increases in cDC in the medLN

(A) Number of lung-migratory cDCs in the medLN increases during influenza infection and persists. *Left:* Flow cytometry plots show frequency of cDC ($CD11c^+$MHC Class II^+) and lung-migratory ($CD103^+CD11b^{lo}$) cDC in the medLN at indicated timepoints after primary X31 infection. *Right:* Graph depicting absolute numbers of $CD11b^+CD103^-$ and $CD11b^-CD103^+$ cDC in the medLN over the course of primary infection from 3-4 mice per group. (B) Quantification of cDC using zbtb46-GFP reporter mice. *Left:* Flow cytometry plots show GFP expression in lung, medLN, and ILN $CD45^+$ cells isolated from naïve or memory zbtb46-GFP mice. *Right:* Graphs showing total number of $zbtb46^+$ $CD11c^{hi}$I-A/I-E^{hi} cDC and proportion of $zbtb46^+$ expressing $CD45^+$ cells in lung, medLN, and ILN of naïve or memory mice, compiled from 4 experiments, n=6-12 mice/group. (C) CD103 expression of cDC using zbtb46-GFP reporter mice. *Left:* Flow cytometry plots of CD103 and CD11b expression by zbtb46-GFP^+ cDCs from lung, medLN or ILN of naïve and memory mice. *Right:* Graphs showing proportion of $CD11b^-CD1103^+$zbtb46-GFP^+ cDCs compiled from 4 experiments, n=6-12 mice/group. (D) CD86 and CD103 expression by medLN zbtb46-GFP^+ cDC isolated from naïve and memory mice compiled from 3 experiments, n=9 mice/group. (E) Whole transcriptome profiling by population RNA sequencing (RNAseq) of $CD45^+$ zbtb46-GFP^+ $CD11c^+$ I-A/I-E^+ cDCs sorted from medLN of naïve and memory mice as in (B). Reads were mapped using Kallisto and DESeq2 was used to determine significantly differentially expressed genes by memory cDC compared to naïve cDC. *Left*: Volcano plot depicts genes by the absolute value of $Log_{10}P_{adj}$ and the relative fold change comparing memory cDC against naïve cDC. Genes that show differential gene expression of at least twofold change show in green, and genes with an absolute value of $Log_{10}P_{adj}$ greater than 4

shown in red. *Right*: Heat map of top differentially expressed genes between naïve and memory cDCs based on transcripts per million (TPM) and determined by $P_{adj} \leq 0.05$ and mean fold difference ≥2. Z-score based on standard deviation from mean TPM value per gene. N=3 mice/group. For all experiments, significance between naïve and memory mice determined by student's unpaired t-test. ****, p≤0.001; ** p≤0.01). Error bars show mean ± SEM.

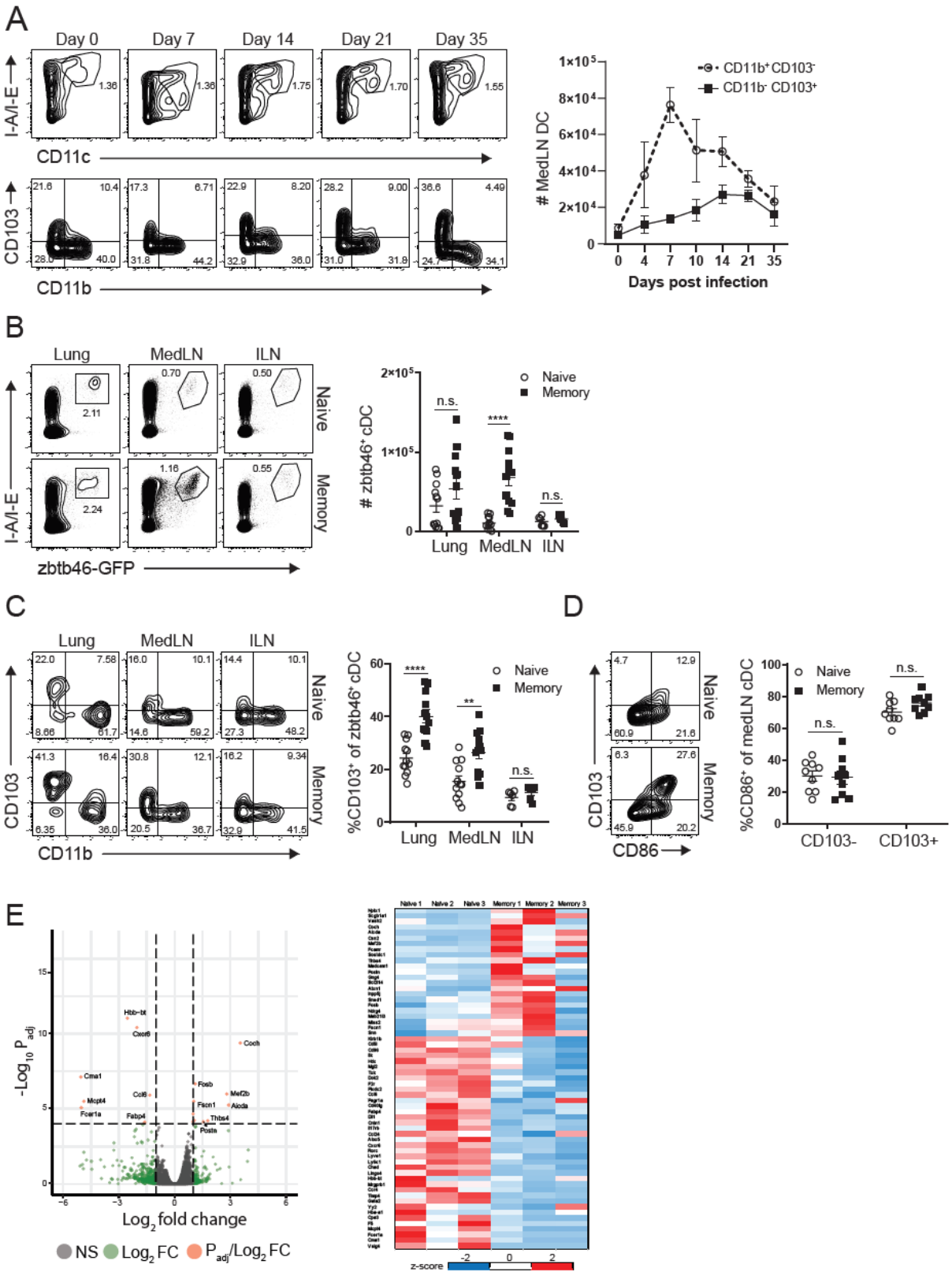
A
Day 0
Day 7
Day 14
Day 21
Day 35
I-A/I-E
CD11c
CD103
CD11b
1.36
1.36
1.75
1.70
1.55
21.6
10.4
28.0
40.0
17.3
6.71
31.8
44.2
22.9
8.20
32.9
36.0
28.2
9.00
31.0
31.9
36.6
4.49
24.7
34.1
MedLN DC
CD11b+CD103-
CD11b- CD103+
Days post infection
B
Lung
MedLN
ILN
Naive
Memory
zbtb46-GFP
0.70
0.50
2.11
1.16
0.55
2.24
zbtb46+ cDC
n.s.
****
Naive
Memory
C
D
%CD103+ of zbtb46+ cDC
**
22.0
7.58
8.66
61.7
16.0
10.1
14.6
59.2
14.4
10.1
27.3
48.2
41.3
16.4
6.35
36.0
30.8
12.1
20.5
36.7
16.2
9.34
32.9
41.5
4.7
12.9
60.9
21.6
6.3
27.6
45.9
20.2
CD86
%CD86+ of medLN cDC
CD103-
CD103+
E
-Log10 Padj
Log2 fold change
NS
Log2 FC
Padj/Log2 FC
Hbb-bt
Cxcl6
Ccl4
Cma1
Mcpt4
Fcer1a
Ccl6
Fabp4
Fosb
Fscn1
Thbs4
Postn
Mef2b
Aloda
Naive 1
Naive 2
Naive 3
Memory 1
Memory 2
Memory 3
z-score

Lymph node DC are required for protection and enhanced $CD4^+$ and $CD8^+$ T cell priming in the recall response

To assess the role of increased cDC numbers in key features of the recall response, including protective immunity and enhanced $CD4^+$ and $CD8^+$ T cell priming within the medLN, we used a Zbtb46-DTR mouse model to deplete cDCs *in vivo* by diphtheria toxin (DT) administration. Due to broad expression of $zbtb46^+$ in non-hematopoietic cells [181], we generated bone marrow chimeras (B6.zDTR) using bone marrow cells derived from $CD45.2^{+/+}$ zbtb46-DTR mice transferred into lethally irradiated $CD45.1^{+/+}$ host mice (Fig. 3.14 A, see methods). B6.zDTR mice were infected with X31 to generate memory mice as in Fig. 3.3 and treated with DT to deplete cDC; OT-I or OT-II $CD45.1^+/CD45.2^+$ cells were subsequently transferred into both DT-treated and untreated B6.zDTR memory mice which were challenged with PR8-OTI or PR8-OTII (Fig. 3.14 A). In this way, we could assess the contribution of cDC numbers to enhanced priming and the overall recall response.

Following OT-II transfer and PR8-OTII challenge, the frequency and numbers of cDC were significantly reduced in the medLN of DT-treated compared to untreated mice; however, cDC numbers in the lung were comparable in infected hosts +/- DT (Fig. 3.14 B). This medLN-localized cDC depletion was associated with significant weight loss in DT-treated compared to the untreated group (Fig. 3.14 C), demonstrating a loss of memory T cell-mediated protection. The accumulation and proliferation of OT-II cells in the medLN was significantly reduced in DT-treated compared to untreated mice (Fig. 3.14 D). At the same time, OT-II cells did not proliferate in the spleen, demonstrating that the enhanced antigen-specific T cell priming is locally regulated (Fig 3.14 D). We also tested whether cDC depletion would diminish the enhanced medLN priming of IAV-specific $CD8^+$ T cell responses by transferring OT-I cells into DT treated and untreated

memory mice and challenging those mice with PR8-OTI. Like OT-II cells, OT-I cells also exhibited significantly abrogated proliferation within the medLN (Fig. 3.14 E), suggesting that increased cDC numbers enhance both $CD4^+$ and $CD8^+$ influenza-specific T cell priming and proliferation. Consistent with transgenic flu-specific T cell responses, the total number of both polyclonal medLN $CD4^+$ and $CD8^+$ T cells also significantly decreased with DT depletion (Fig. 3.14 F). Together, these results demonstrate that cDCs in the medLN are required for enhanced priming and proliferative expansion of influenza specific $CD4^+$ and $CD8^+$ T cells observed during the recall response that are critical for optimal protective immunity in the lung.

Figure 3.14: MedLN cDC are required for enhanced T cell priming and protection during the recall response

(A) Schematic for cDC depletion experiments: B6 CD45.1$^{+/+}$ mice were lethally irradiated and reconstituted with 10^7 CD45.2$^{+/+}$ zbtb46-DTR bone marrow cells to create B6.zDTR bone marrow chimeras. After 10 weeks, B6.zDTR chimeras were infected with X31 to generate B6.zDTR memory mice. B6.zDTR memory mice were treated with FTY720 and either treated with i.p. DT (40mg/g body weight) or PBS as a vehicle control. One day later, mice were administered i.n. DT (20mg/g body weight) or PBS vehicle control and eF450 proliferation dye labeled CD45.1$^+$CD45.2$^+$ OT-I or OT-II cells were transferred into FTY720 treated B6.zDTR memory mice. One day later, mice were challenged with PR8-OTI or PR8-OTII (see methods), and recall protection and OT-I/OT-II priming was assessed 3 days post-infection. (B) Preferential reduction in medLN cDC following DT treatment in B6.zDTR memory mice depicted in representative flow cytometry plots (*left*) gated on CD45$^+$ cells showing CD11c$^+$ cDC in the MedLN and lungs of PR8-OTII challenged mice, and in graphs of cDC numbers in each site (*right*). Data representative of 2 independent experiments, n=3-4 mice/group. (C) Weight loss morbidity DT-treated and untreated memory mice at indicated times after PR8-OTII challenge. Data compiled from 2 independent experiments, n=6 mice/group. (D) DT treatment abrogates enhanced priming of medLN OT-II cells. *Left:* Flow cytometry plots show medLN and spleen OT-II proliferation and CD69 expression with and without DT treatment. *Right:* MedLN and spleen OT-II counts and proportion of OT-II cells that fully diluted proliferation dye. Data are compiled from of two independent experiments (n=3-7 mice/group). (E) DT treatment also abrogates enhanced priming of medLN OT-I cells. *Left*: Flow cytometry plots show medLN OT-I proliferation and CD69 expression with and without DT treatment three days after PR8-OTI challenge. *Right*: Plots

depicting proportion of medLN OT-I cells that express diluted levels of proliferation dye. N=5 mice/group. (F) DT treatment abrogates medLN polyclonal T cell responses. Graph depicts absolute number of medLN $CD4^+$ and $CD8^+$ T cells with and without DT treatment. Data compiled from 2 independent experiments, n=7 mice/group. Significance determined by student's unpaired t-test. ***, $p \leq 0.001$, **, $p < 0.05$; *, $p < 0.05$). Error bars are mean ± SEM.

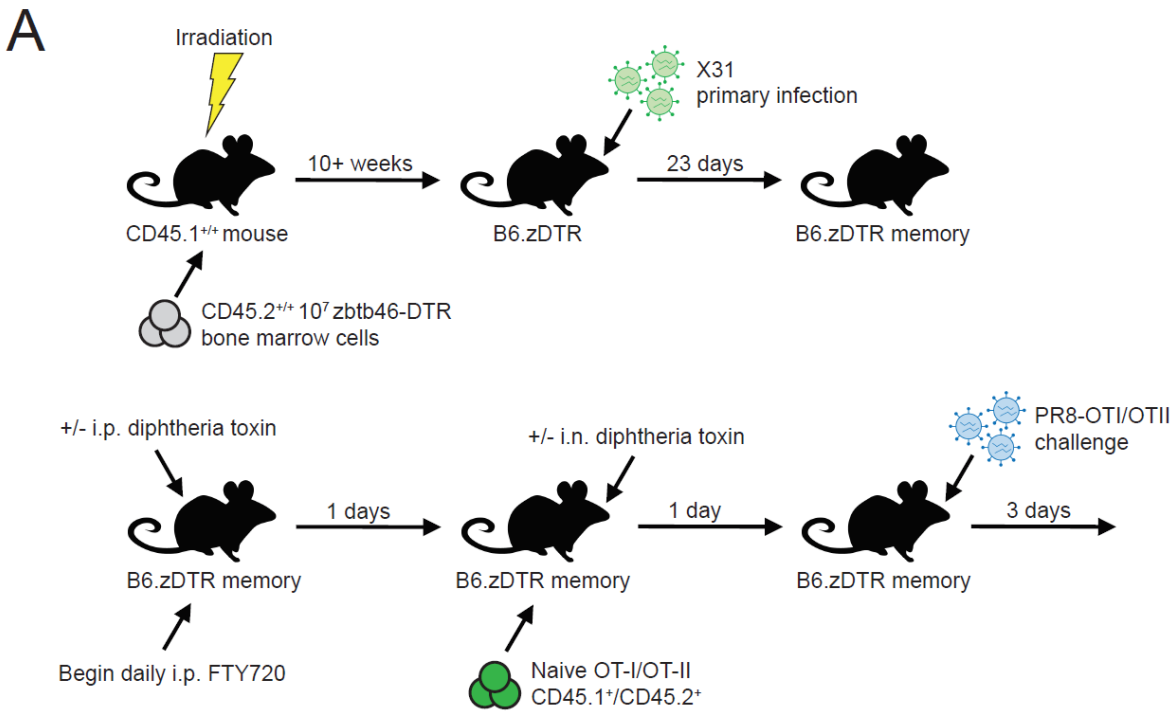
A
Irradiation
CD45.1+/+ mouse
10+ weeks
B6.zDTR
X31
primary infection
23 days
B6.zDTR memory
CD45.2+/+ 10^7 zbtb46-DTR
bone marrow cells
+/- i.p. diphtheria toxin
B6.zDTR memory
1 days
B6.zDTR memory
+/- i.n. diphtheria toxin
1 day
B6.zDTR memory
PR8-OTI/OTII
challenge
3 days
Begin daily i.p. FTY720
Naive OT-I/OT-II
CD45.1+/CD45.2+

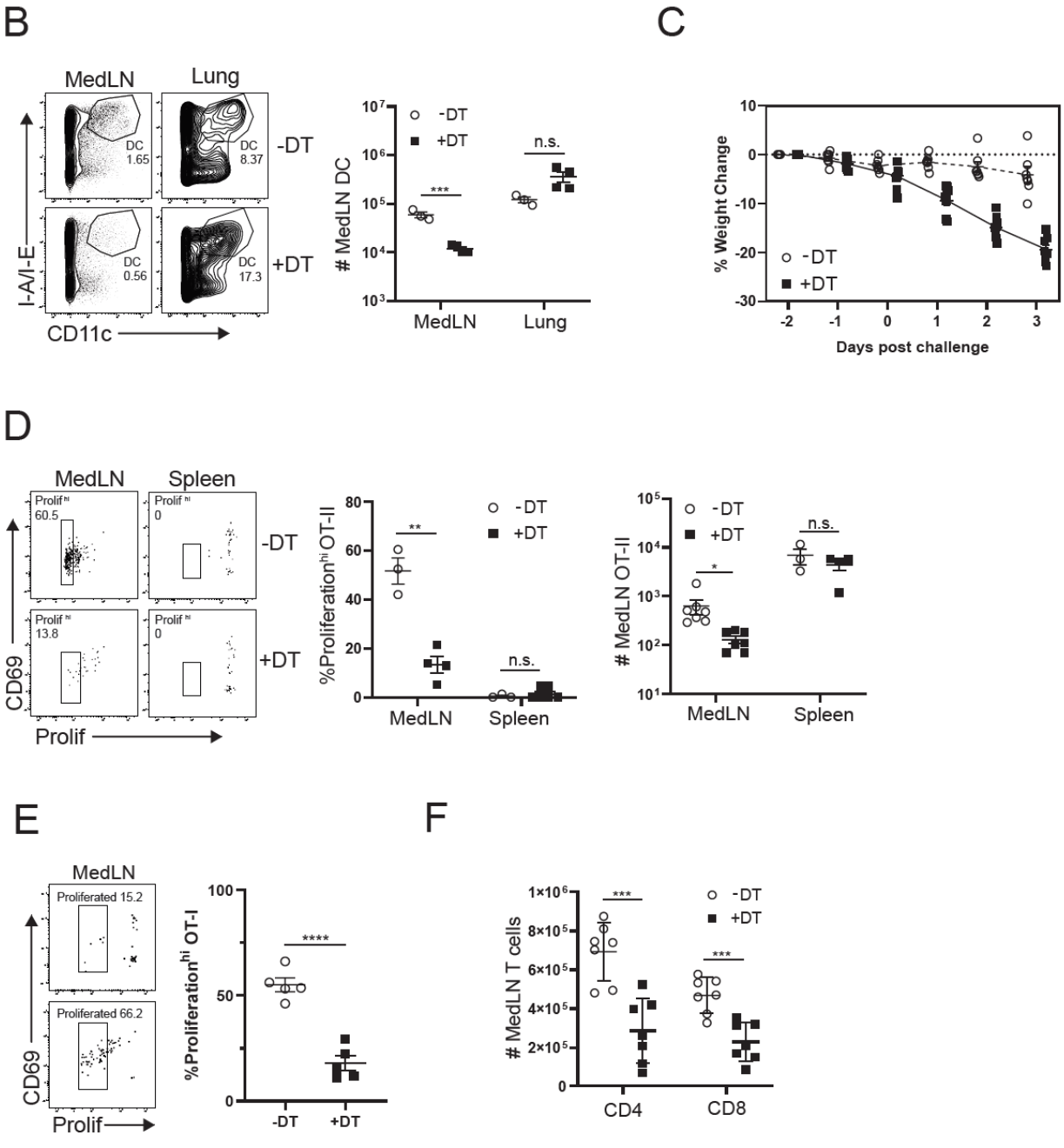
B
MedLN
Lung
DC 1.65
DC 8.37
DC 0.56
DC 17.3
-DT
+DT
I-A/I-E
CD11c
MedLN DC
-DT
+DT
***
n.s.
MedLN
Lung
C
% Weight Change
-DT
+DT
Days post challenge
D
MedLN
Spleen
Prolif hi 60.5
Prolif hi 0
Prolif hi 13.8
Prolif hi 0
-DT
+DT
CD69
Prolif
%Proliferation hi OT-II
**
n.s.
MedLN
Spleen
MedLN OT-II
*
n.s.
E
MedLN
Proliferated 15.2
Proliferated 66.2
CD69
Prolif
%Proliferation hi OT-I
****
-DT
+DT
F
MedLN T cells
***
***
CD4
CD8

3.4: Discussion

Influenza infection generates lung TRM that can provide cross-strain protective immunity, though the interactions of systemic responses with lung resident immunity are not defined. Here, we reveal how local lung tissue T cell immunity to heterosubtypic challenge is augmented by the enhanced generation and lung homing of peripheral effector T cells. During secondary influenza challenge, increased numbers of T cells in the lung niche early after infection derive from *in situ* TRM proliferation as well as the recruitment of effector cells generated in response to newly encountered influenza epitopes in the medLN. Importantly, prior influenza infection imprints the medLN with greater numbers of cDCs including increased proportions of the $CD103^+$ migratory subset, resulting in more rapid priming of naive T cells. This lymphoid cDC-mediated priming is required for lung-localized protective responses. Our results indicate that the efficacious secondary response to respiratory infection by lung TRM is augmented by the fortified priming environment in the local lymphoid tissue, enabling rapid mobilization of effector T cells to the site of infection.

Prior influenza infection generates high frequencies of memory T cells that reside within the lung and local medLN that are enriched for reactivity to influenza-derived epitopes [104, 173, 174, 182]. Lung TRM can be readily identified by their localization in the lung tissue niche that is inaccessible to circulation and protected by labeling with intravenously administered antibody. Heterosubtypic influenza challenge of memory mice led to protective responses including reduced weight loss morbidity and more rapid viral clearance compared to the primary response, independent of mature B cells, consistent with previous studies showing B cells were not required for memory T cell-directed protection to influenza challenge [175, 183]. This polyclonal T cell-directed response was marked by extensive accumulation of T cells in the lung resident niche, consistent with TRM expansion in other tissue sites following recall challenge [129, 130].

However, the expanding T cells in the lung resident niche did not predominantly exhibit phenotypic features of TRM such as CD103 expression, contrary to findings in skin and female reproductive tract [129, 130]. By contrast, expanded lung T cells were largely CD103-negative for both $CD4^+$ and $CD8^+$ T cells, and derived, in part, from infiltration of effector T cells from local lymphoid sites. The specific and distinct anatomical features of the lung, including extensive vascularization of the tissue and associated lymph nodes, may influence the relative involvement of tissue and systemic responses, which may differ from other sites.

Using a tracking model that monitors the activation and proliferation of OVA-specific T cells, we demonstrate that the environment within the medLN of previously infected mice promotes superior T cell effector generation and lung migration after PR8-OTI/OTII challenge, including for newly encountered influenza epitopes such as OVA. These results indicate a broadening of the early T cell response during a recall challenge. The effect of a previously generated influenza-specific memory response on epitopes introduced during subsequent infections has been examined in mouse lymphoid tissues [184], but not for the early, lung-localized response that is essential for protection. How prior infection impacts a subsequent immune response for humoral immunity is through a phenomenon referred to as “original antigenic sin”, in which antibody production in the recall response favors the original antigens, resulting in a narrowing of the antibody repertoire over repeated pathogen exposures [185-187]. The amplification of new T cell responses during recall suggests that T cell immunity may be more robust than humoral immunity in promoting universal protection, particularly during the critical early period of tissue localized responses.

We identified that enhanced priming in the recall response occurred in local medLN that exhibited a fortified state, being more permissive to maintaining larger numbers of T cells and

increased numbers of cDCs. Recent studies have identified components of the innate immune response that become altered from previous infection and exhibit enhanced responses during recall—a phenomenon known as "trained immunity" [188, 189]. Respiratory infection with adenovirus induced long-term changes in alveolar macrophages (AM), resulting in memory AM with superior functional responses to viral challenge [155]. Here, we describe durable alterations in the local medLN following influenza infection manifested by elevated numbers of T cells and cDC subsets after viral clearance that was not observed in distal lymph nodes. Increased frequencies of $CD103^+$ cDC were localized in the fortified medLN, indicating a migratory phenotype [60, 190, 191] that may also play a role in further promoting both $CD4^+$ and $CD8^+$ T cell priming [192]. However, the medLN cDC in memory mice were otherwise phenotypically and transcriptionally similar to cDC in the medLN of naïve mice, indicating that cDC are not qualitatively altered by the previous infection. Our results indicate that the local LN environment is quantitatively fortified, enabling more efficacious priming.

Our results demonstrating endogenous boosting properties of the local lymphoid environment have implications for generating protective immunity to diverse respiratory infections in vaccines. Protective lung TRM can be generated by diverse respiratory pathogens including RSV, tuberculosis, and pertussis [193-195]. Intranasal routes of immunization can also generate lung TRM and protective immunity to influenza and pertussis in mouse models [174, 193]. We propose that site-specific boosting in the respiratory tract can promote more robust responses to new or heterologous respiratory pathogens through targeting the local fortified LN, and thus augmenting *in situ* T cell-mediated immunity.

Chapter 4: Local lung tissue immunoregulation during heterosubtypic influenza challenge

4.1: Abstract

Although pathogen clearance is a primary objective of the immune response, associated inflammatory responses may damage local tissue during influenza infection. Increased morbidity and mortality caused by influenza infection is correlated with highly upregulated innate inflammatory responses. We demonstrate here that lung tissue resident memory T cells (TRM) exhibit superior production of both antiviral Th1 and immunomodulatory cytokines compared to their circulating counterparts and that lung tissue APCs drive IL-10 family cytokine TRM production. Using a murine heterosubtypic influenza challenge model, we found that compared to a primary infection, the early recall response exhibited a considerably dampened innate immune response, particularly in type I interferon signaling. This dampened recall response includes enhanced *in situ* production of IL-10 by lung $CD4^+$ T cells as compared to a primary response. Using an αIL-10R antibody blockade, we demonstrate that IL-10 signaling modulates inflammatory cytokine production in the airway without inhibiting viral clearance. Our study shows that prior influenza infection generates a lung environment that, during IAV challenge, promotes T cell IL-10 production and limits innate immune responses while maintaining heterosubtypic immunity.

4.2: Introduction

Viral infections elicit protective immune responses that are necessary for viral clearance but may also independently exacerbate disease pathology through the action of pro-inflammatory cytokines and effector T cells. Aberrantly high levels of soluble immune mediators are features of what is known as a "cytokine storm" which causes severe tissue pathology and multi-organ failure [196]. Elevated inflammatory cytokine and cellular responses are correlated with the increased morbidity and mortality of respiratory viruses such as influenza, RSV, and coronaviruses, indicating that maintaining an appropriate immune response is critical for favorable disease outcomes [197-202]. Anti-inflammatory treatments have shown to reduce IAV morbidity and mortality in animal models, suggesting that an endogenous counterbalancing immunoregulatory response is necessary to limit lung tissue injury [162]. Although T cells are critical for viral clearance, both $CD4^+$ and $CD8^+$ T cell inflammatory responses lead to significant morbidity and tissue damage [175, 203]. T-cell derived inflammatory cytokines such as TNF-α have been shown to cause such immunopathology, ostensibly due to increased inflammation and leukocyte recruitment [79, 204].

A counterbalancing immunoregulatory response is a feature of the overall immune response to influenza infection and is mediated by immune cell subsets and their secreted cytokines. Dendritic cells, macrophages, B cells are known producers of immunosuppressive cytokines, as well as various subsets of T lymphocytes including regulatory $CD4^+$ T cells (T_{reg}) which defined by the expression of transcription factor Foxp3. These immunoregulatory cytokines include TGF-β, IL-10, and amphiregulin, which limit tissue damage and mortality during IAV infection [205]. In particular, IL-10 is one of the most highly expressed immunomodulatory cytokines and acts on a broad range of immune cells including lymphocytes, macrophages, and

dendritic cells. IL-10 exerts its immunosuppressive function on virtually all leukocytes by regulating gene transcription in a STAT3 dependent fashion and has been shown to determine viral clearance in animal models [206]. Additionally, IL-10 counteracts many of the proinflammatory signals that are induced by viral PRR activation. While T_{reg} cells are can produce IL-10, effector $CD4^+$ and $CD8^+$ Th1 T cells are the major sources of high levels of IL-10 during active viral infection in mouse models; moreover, IL-10 is necessary to minimize inflammation and disease severity during viral clearance [85, 207, 208].

We demonstrated in Chapter 3 that during a heterosubtypic response, enhanced effector T cell expansion and migration to lung tissue mediated heterosubtypic antiviral protection. In this chapter, we investigate the immunomodulatory role of the T cell response during recall compared to the primary response. We demonstrate that *ex vivo* lung niche $CD4^+$ memory T cells are capable of superior production of both inflammatory and immunomodulatory cytokines that is dependent on the local tissue priming environment. During an early recall infection, lung tissue-wide immune responses are transcriptionally distinct from the primary response, especially reductions of mediators within the type I IFN pathway. Furthermore, lung niche $CD4^+$ effector T cell IL-10 production is enhanced at the site of infection as compared to a primary infection. By blocking IL-10R signaling, we demonstrate that airway IL-10 regulates global local lung and airway innate immunity and that while IL-10 suppresses Th1 cytokine responses in the airway, it does not suppress IAV viral clearance nor disease morbidity. Taken together, we present a model for the lung environment enhanced T cell-mediated IL-10 dependent immunomodulation during a recall response that suppresses inflammatory innate immune responses while maintaining robust viral clearance.

4.3: Results

Enhanced lung TRM cytokine production is modulated by tissue antigen-presenting cells

To define the cytokine profile of lung-localized recall responses, we first assessed the cytokine production of $CD4^+$ lung TRM cells compared to their circulating counterparts, specifically splenic $CD4^+$ TEM cells. Lung TRM were identified by their localization in lung tissue niche, which is defined by a lack of fluorescent staining by an intravenously injected *in vivo* antibody, demonstrating protection from the blood circulation as previously described [104]. $CD4^+$ $CD44^{hi}$ $CD62L^{lo}$ T cells were sorted from both the lung niche and spleen of mice that had been infected with X31 virus 3 weeks previously. These sorted memory $CD4^+$ T cells were stimulated with αCD3/28 activating beads for 24 hours, and the resulting supernatant was analyzed for various Th1, Th2, and Th17 cytokines using a cytometric bead array. Influenza generated TRM produced significantly more Th1-like cytokines IFN-ɣ and TNF-α while simultaneously producing more IL-10 as well. IL-4 was also significantly elevated in the splenic cells compared to the lung niche, perhaps indicative of a role for B cell help that is of greater importance in a lymphoid site such as the spleen compared to the lung (Fig. 4.1). These data suggest that lung niche memory $CD4^+$ T cells have enhanced production of proinflammatory and immunoregulatory cytokines IFN-ɣ, TNF-α, and IL-10, while spleen-derived memory T cells have enhanced IL-4 production. These data suggest that memory T cell cytokine production is adapted to their tissue localization and is consistent with lung TRM being especially important for directly pro-inflammatory antiviral responses whereas splenic T cells play a role in helping B cell differentiation.

We used OT-II $CD4^+$ T cell TCR transgenic T cells to generate antigen-specific T cells in lungs and spleen so that we could analyze the cytokine response to stimulation by their cognate

antigen, the ovalbumin peptide $OVA_{323-339}$. In order to generate substantial numbers of OT-II lung TRM, we used an *in vitro* priming and adoptive transfer model previously used in our laboratory's studies of lung $CD4^+$ TRM [94, 175]. In this model, OT-II $CD4^+$ T cells were stimulated *in vitro* with their cognate antigen $OVA_{323-339}$ peptide, and the resultant activated/effector cells are transferred into $RAG^{-/-}$ mice which lack T lymphocytes. After 3-4 weeks, activated OT-II cells establish themselves as memory T cells in various lymphoid and peripheral tissue niches, including the lung and spleen [94]. Unlike an influenza generated infection model, both TRM and TEM are generated from the same priming event, allowing for more precise interrogation of tissue localization's effects on memory T cell function. OT-II Lung TRM exhibit the same phenotypic markers and localization of TRM as those generated by influenza infection in wild type mice; they are nearly all protected from *in vivo* labeling antibody and are $CD44^{hi}$ $CD62L^{lo}$ and express high levels of CD69 (Fig. 4.2 A).

Whole lung and spleen cells from OT-II $RAG^{-/-}$ memory mice were cultured while normalizing for the number of OT-II memory T cells together with varying concentrations of $OVA_{323-339}$ peptide. In response to antigenic stimulation *ex vivo*, OT-II lung TRM produce robust levels of Th1 and Th2 cytokines in a dose dependent response when co-cultured with total lung homogenate (Fig. 4.2 B). Similar to polyclonal TRM generated by IAV infection (Fig. 4.1), OT-II lung TRM also exhibit enhanced cytokine production compared to their splenic TEM counterparts, particularly for IFN-ɣ and IL-17A (Fig. 4.2 B). Because OT-II cells were co-cultured with their respective non-lymphocyte lung or spleen cells, we wished to further investigate whether the cytokine production by $CD4^+$ memory T cells was dependent on the type of antigen presenting cells located within the tissue environment. Sorted lung OT-II TRM or splenic OT-II TEM were co-cultured with lymphocyte depleted lung or spleen cells to serve as APCs at varying

concentrations of $OVA_{323-339}$ peptide. Both lung and spleen memory T cells produced higher levels of IFN-ɣ when stimulated by spleen-derived APCs compared to lung-derived APCs (Fig. 4.2 C). Although lung APCs seemed to produce increased IL-17A at baseline compared to spleen APCs, the dose response curve itself was unchanged regardless of which APC was used, suggesting that the tissue source of APC was immaterial to $CD4^+$ memory T cell IL-17A responses. Rather, OT-II lung TRM themselves seemed to be intrinsically superior producers of IL-17A compared to OT-II spleen TEM, exhibiting a more responsive IL-17A production profile after peptide stimulation. While IL-10 production itself was uneven in this TRM model (data not shown), IL-22, which is another member of the IL-10 cytokine family and signals through IL-10RB, was produced in high concentrations in our model. IL-22 production reached an inflexion point and began to level off at peptide concentrations between 1 and 10 µg/mL, unlike IFN-ɣ and IL-17A which continued to increase exponentially in the same peptide concentration range. Furthermore, no intrinsic difference in IL-22 production capacity was found between lung TRM and spleen TEM. Rather, the differences in IL-22 production was solely due the APCs in which lung APCs led to significantly greater IL-22 production compared to spleen APCs (Fig. 4.2 C). These data suggest that while lung TRM are intrinsically robust cytokine producers of a wide range of cytokines, the local tissue environment itself, and in particular the APC population, may play a critical role in the determination of which types of cytokines are produced *in situ* during a respiratory infection, particularly of Th1 and IL-10 family cytokines.

Figure 4.1: Cytokine profile of αCD3/28 bead stimulated $CD4^+$ lung niche and splenic memory T cells

$CD44^{hi}$ $CD62L^{lo}$ $CD4^+$ cells were sorted from lung and spleen from mice 4-6 weeks post-infection. Lung cells were sorted from lung niche determined by in vivo labeling technique, and splenic T cells were in vivo label positive. Cells were plated with 1 µL CD3/28 T-cell activator beads in a 96 well plate in 200 µL of media at 2×10^4 cells/well. After 24 hours of stimulation, supernatant was analyzed by cytometric bead array (BD Biosciences). N=3 mice. Data is representative of 2 independent experiments displaying mean and SD. Statistical significance determined by unpaired student's t-test. *p<-0.05. **p<0.01.

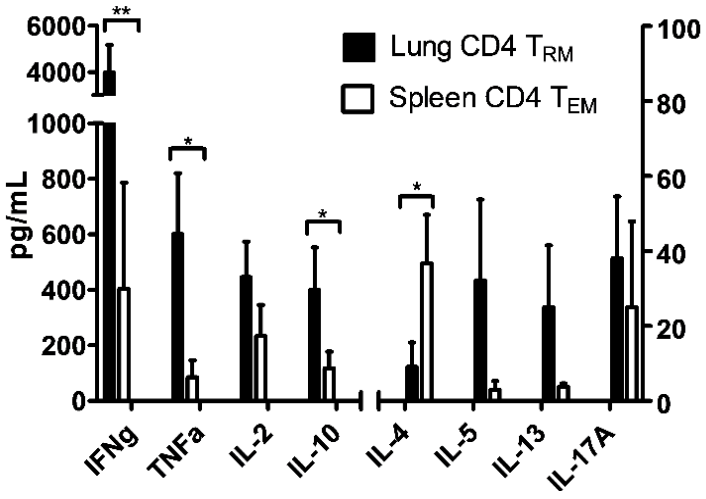
Lung CD4 T_{RM}
Spleen CD4 T_{EM}
pg/mL
6000
4000
1000
800
600
400
200
0
100
80
60
40
20
0
**
*
*
*
IFNg
TNFa
IL-2
IL-10
IL-4
IL-5
IL-13
IL-17A

Figure 4.2 Tissue specificity of lung $CD4^+$ TRM cytokine production dependent on antigen-presenting cells type

(A) OT-II cells were isolated from the lungs of *in vivo* labeled $RAG^{-/-}$ OT-II memory mice. FACS plots are gated on $CD4^+$ T cells and depict CD44 and CD62L expression (left) as well as CD69 expression plotted against in vivo labeling (right). (B) Total lung homogenate from $RAG^{-/-}$ OT-II memory mice was cultured with various concentrations of $OVA_{323-339}$ peptide for 24 hours. Supernatant was measured for cytokine levels using LEGENDplex immunoassay (Biolegend). (C) Lung (black) and spleen (red) OT-II $CD4^+$ memory T cells were sorted from $RAG^{-/-}$ OT-II memory mice and 2×10^4 cells were co-cultured with equal numbers of lung (solid) or spleen (open) cells from $RAG^{-/-}$ mice in a 96 well U-bottom plate. Wells contained various concentrations of $OVA_{323-339}$ peptide, and plate was cultured at 37 ºC for 24 hours. Supernatant was measured for cytokines using LEGENDplex immunoassay. Graphs depict dose response curves for IFN-ɣ (left), IL-17A (middle), and IL-22 (right) production.

A

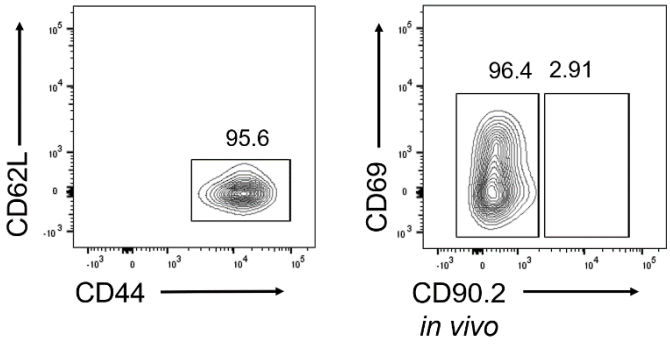
95.6
CD62L
CD44
96.4
2.91
CD69
CD90.2
in vivo

B

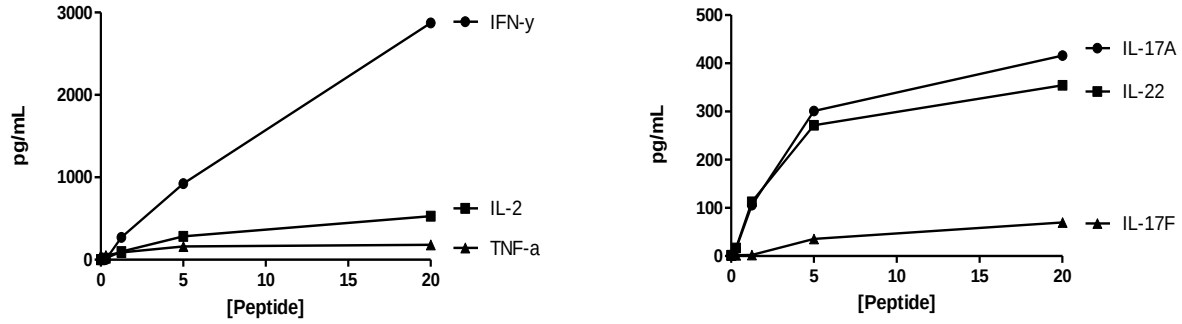
3000
2000
1000
0
pg/mL
0
5
10
15
20
[Peptide]
IFN-y
IL-2
TNF-a
500
400
300
200
100
0
pg/mL
0
5
10
15
20
[Peptide]
IL-17A
IL-22
IL-17F

C

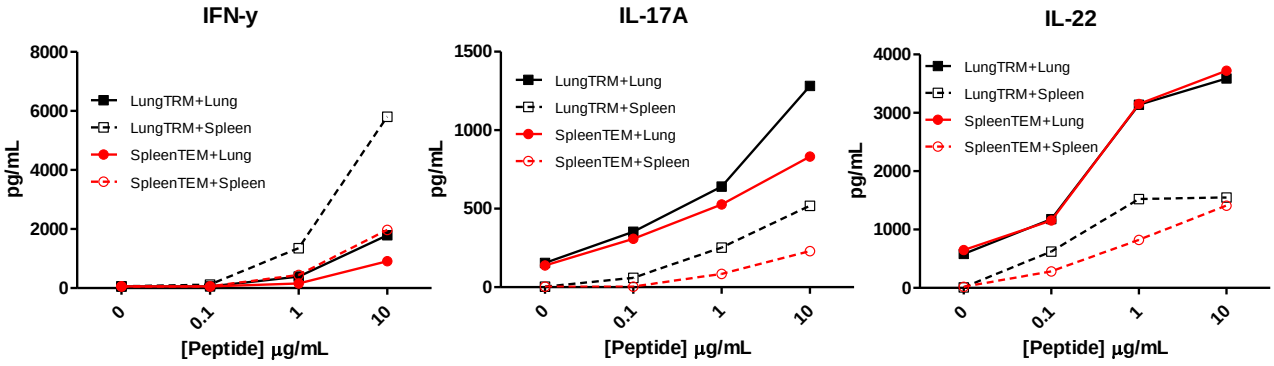
IFN-y
8000
6000
4000
2000
0
pg/mL
LungTRM+Lung
LungTRM+Spleen
SpleenTEM+Lung
SpleenTEM+Spleen
0
0.1
1
10
[Peptide] µg/mL
IL-17A
1500
1000
500
0
pg/mL
LungTRM+Lung
LungTRM+Spleen
SpleenTEM+Lung
SpleenTEM+Spleen
0
0.1
1
10
[Peptide] µg/mL
IL-22
4000
3000
2000
1000
0
pg/mL
LungTRM+Lung
LungTRM+Spleen
SpleenTEM+Lung
SpleenTEM+Spleen
0
0.1
1
10
[Peptide] µg/mL

Lung environment undergoes globally attenuated innate immune response during heterosubtypic challenge

The results above demonstrate that the response in the lung can be influenced by intrinsic differences in the functional capacity of TRM as well as the APC in the lung tissue. We therefore took an unbiased approach to investigate early immunomodulatory effects on the lung by comparing the whole lung transcriptional profiles of the recall and primary responses using RNASeq. To this end, lung tissue was isolated from naïve and memory mice both at their baseline prior to infection and 2 days post-challenge with PR8 IAV challenge. RNASeq analysis revealed that significantly more genes were differentially expressed during a primary infection (1661) compared to a recall infection (160), in which 70 genes were shared (Fig. 4.3 A, B). Differentially expressed genes include many upregulated and downregulated genes; while both recall and primary infection upregulated a number of chemokines including *Ccl2*, *Cxcl11*, *Cxcl10*, and *Cxcl9*, primary infection also upregulated a number of innate antiviral immune genes such as *Tlr9* and interferon signaling genes such as *Ifitm3* and *Irf4* (Fig. 4.3 C).

In order to analyze these data in the context of functional pathways, we performed Gene Set Enrichment Analysis (GSEA) of the differentially expressed genes in primary and secondary infection. Both primary and secondary infection were enriched for genes that were similarly upregulated in studies of DC exposure to Newcastle disease virus [209], demonstrating a non-specific antiviral response (Fig. 4.3 D). While both primary and recall were enriched, the primary response had a larger normalized enrichment score (NES) of 3.22 compared to 2.07. The outsized immune response during primary infection was reflected in its enrichment of upregulated genes (NES score 3.11) after DC exposure to TLR4 and TLR7 agonists which triggered Th1 responses [210], which is consistent with an enhanced antiviral innate immune response by ssRNA which is

a ligand for TLR7 [12] (Fig. 4.3 E). Further pathway analysis using Ingenuity Pathway Analysis (IPA) revealed significant changes during primary infection of EIF2 mediated mRNA translation, metabolic pathways such as mTOR, oxidative phosphorylation, and mitochondrial function, in addition to interferon and leukocyte migration pathways that are upregulated in both recall and primary infection (Fig. 4.3 F). These data demonstrate that the magnitude of the global transcriptional response is significantly larger during a primary infection, particularly with respect to innate immune signaling, while there are fewer innate immune-associated genes induced during the recall response. Together these data suggest an immunomodulatory function inherent within the recall response.

Figure 4.3: Early recall response modulates early innate response of the total lung transcriptome

Whole right lung lobes were isolated from naïve and memory mice as well as naïve and memory mice 2 days after challenge with PR8 influenza virus during FTY720 treatment. Reads were mapped using Salmon and DESeq2 was used to determine significantly differentially expressed genes after a primary infection by comparing transcriptomes of uninfected and infected naïve mice, as well as a recall infection by comparing transcriptomes of uninfected and infected memory mice. (A) Venn diagram illustrating the number of differentially expressed genes in a primary infection versus baseline compared to a recall infection versus baseline, as well as the number of genes which overlap between primary and recall infection. (B) Heat map showing the genes that are differentially upregulated in a primary infection compared to a secondary infection (C) Scatter plot illustrating plotting genes based on their differential expression in a primary (red) and recall response (blue), differentially expressed in both conditions (purple), or not differentially expressed in any condition (black). (D) GSEA of differentially expressed preranked gene list from primary and recall infection compared to independently identified upregulated genes in dendritic cells after Newcastle viral challenge. (E) GSEA of differentially expressed preranked gene list from primary infection compared to independently identified upregulated genes in dendritic cells after LPS and R848 challenge. (F) IPA analysis depicting key differentially expressed pathways in both primary and recall infections. Differential expression in all cases was determined if $P_{adj} < 0.05$ and with an average FPKM count >10 and $\log_2$ fold change >0.5. N=3 mice per group.

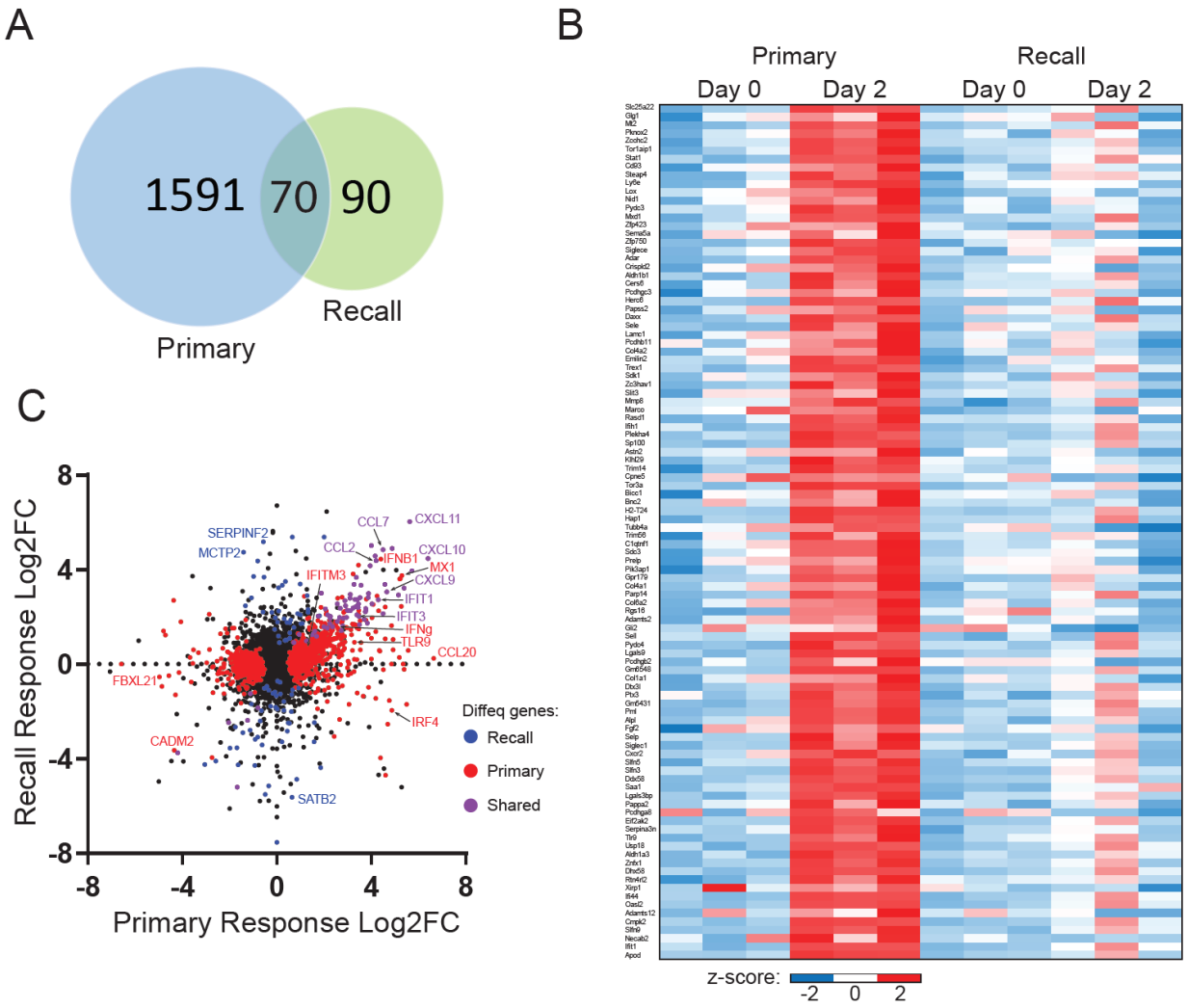
A
1591
70
90
Primary
Recall
B
Primary
Recall
Day 0
Day 2
Day 0
Day 2
z-score:
-2
0
2
C
Recall Response Log2FC
Primary Response Log2FC
8
4
0
-4
-8
SERPINF2
MCTP2
CCL7
CXCL11
CCL2
IFNB1
CXCL10
IFITM3
MX1
CXCL9
IFIT1
IFIT3
IFNg
TLR9
CCL20
FBXL21
IRF4
CADM2
SATB2
Diffeq genes:
Recall
Primary
Shared

D

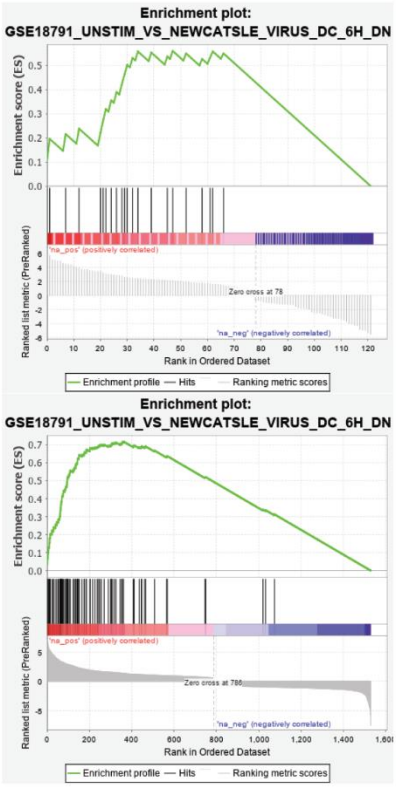

Primary

Recall

E

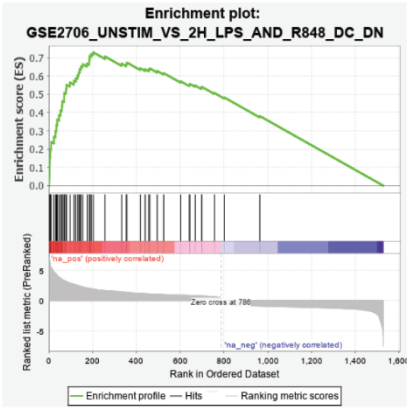

F

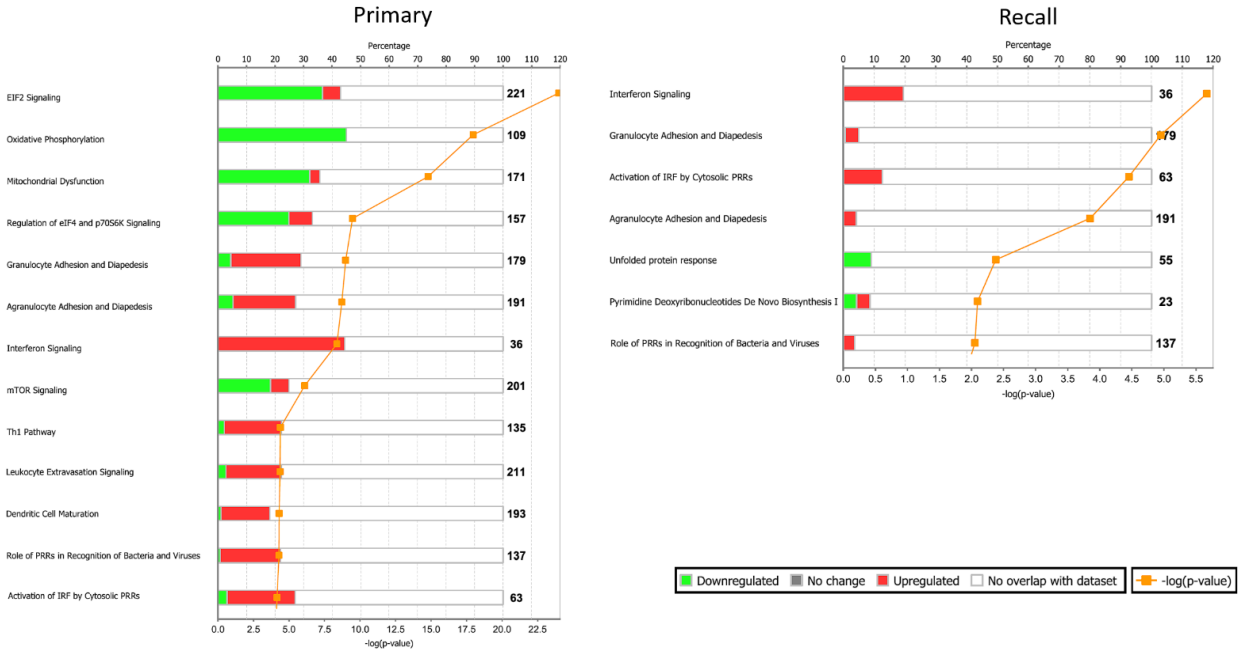

Enhanced IL-10 production by lung niche CD4$^+$ T cells during heterosubtypic influenza challenge

Given the biased production of IL-10 family cytokines by lung TRM and the overall dampened innate immune response in the lung, we sought to determine the extent of *in situ* IL-10 production by lung niche T cells during a recall response compared to a primary response. We used IL-10 GFP-reporter "Tiger" mice to detect *in situ* IL-10 producing T cells. Tiger mice were infected with X31 IAV to generate memory, and both naïve and memory tiger mice were challenged with PR8 IAV, similar to previous influenza challenge models (Fig. 3.3 A). Mice were also treated with FTY720 to sequester circulating cells so as to limit their contributions to the early tissue-localized immune response. Five days after challenge, the lung niche CD4$^+$ CD44^{hi} CD62L^{lo} T cell population during the recall response was significantly enriched for IL-10 producing cells compared to the primary response (Fig. 4.4). On the other hand, the proportion of lung niche CD8$^+$ T cell IL-10 producers was unchanged between the primary and recall responses. In contrast to the lung, while medLN CD4$^+$ CD44^{hi} CD62L^{lo} T cells did produce modest levels of IL-10 (~5% GFP$^+$), we did not observe any enhancement in IL-10 production during the recall response (Fig. 4.4 B), which suggests that the skew toward IL-10 production did not occur within lymphoid sites, but rather, after T cells migrated to the lung tissue niche.

We also observed that during the recall response, non-TRM cells were the primary producers of IL-10. While CD69$^-$ and CD103$^-$ CD4$^+$ T cells were ~30-35% GFP$^+$, their CD69$^+$ or CD103$^+$ TRM counterparts were less than 5% GFP$^+$ (Fig. 4.4 A). This was also true for CD8$^+$ T cells. CD103$^-$ CD8$^+$ T cells comprised the overwhelming majority of CD8$^+$ T cell IL-10 production (~10% GFP$^+$) compared to CD103$^+$ cells (<1% GFP$^+$). Taken together, these data

suggest that effector T cells drive enhanced recall immunomodulatory function upon their migration to the tissue niche.

Figure 4.4: Enhanced lung niche $CD4^+$ IL-10 production during recall response

IL-10-GFP reporter "tiger" memory mice were treated with FTY720 and challenged with PR8 virus. Lung and medLN T cells were isolated after 5 days and analyzed by flow cytometry. (A) Lung niche $CD44^{hi}$ $CD62L^{lo}$ $CD4^+$ (left) and $CD8^+$ (right) $CD44^+$ T cell IL-10 expression is depicted on FACS plots against TRM markers CD69 (top) and CD103 (bottom). Compiled data depicted (right) for IL-10 expression stratified by CD69 expression (top right) and CD103 expression (bottom right). (B) MedLN $CD44^{hi}$ $CD62L^{lo}$ T cell IL-10-GFP is depicted in graphs (right) and on FACS plots against CD69 expression (left). N=2-3 mice per group. Statistical significance determined by unpaired student's t-test. *$p<0.05$.

A

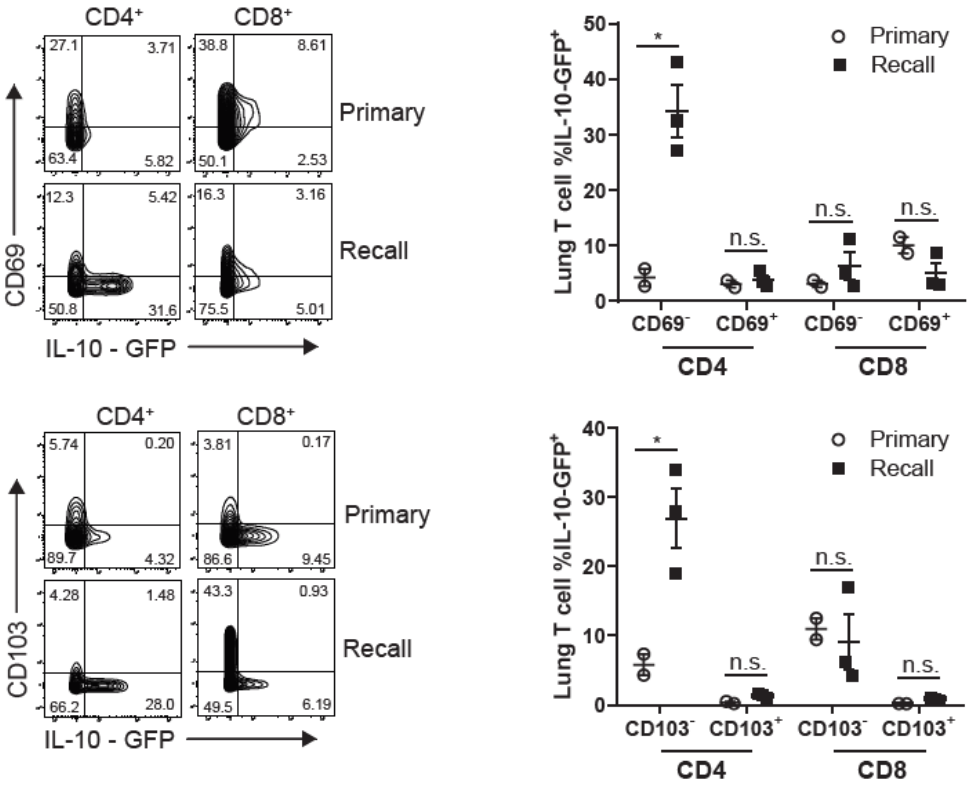
CD4+
CD8+
27.1
3.71
63.4
5.82
38.8
8.61
50.1
2.53
Primary
12.3
5.42
50.8
31.6
16.3
3.16
75.5
5.01
Recall
CD69
IL-10 - GFP
5.74
0.20
89.7
4.32
3.81
0.17
86.6
9.45
Primary
4.28
1.48
66.2
28.0
43.3
0.93
49.5
6.19
Recall
CD103
IL-10 - GFP
Lung T cell %IL-10-GFP+
Primary
Recall
*
n.s.
n.s.
n.s.
CD69-
CD69+
CD69-
CD69+
CD4
CD8
Lung T cell %IL-10-GFP+
Primary
Recall
*
n.s.
n.s.
n.s.
CD103-
CD103+
CD103-
CD103+
CD4
CD8

B

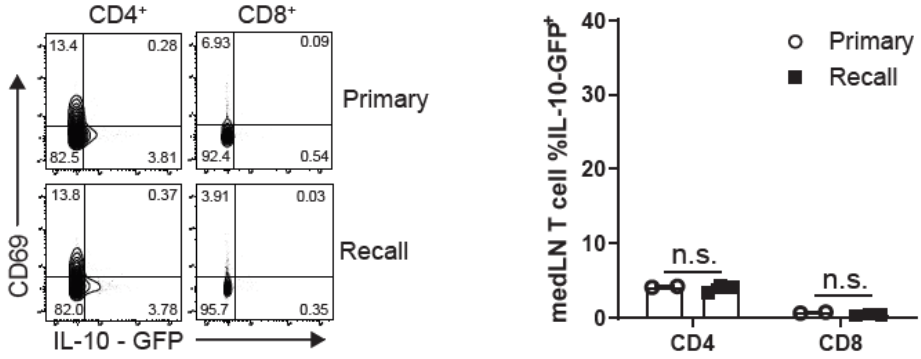
CD4+
CD8+
13.4
0.28
82.5
3.81
6.93
0.09
92.4
0.54
Primary
13.8
0.37
82.0
3.78
3.91
0.03
95.7
0.35
Recall
CD69
IL-10 - GFP
medLN T cell %IL-10-GFP+
Primary
Recall
n.s.
n.s.
CD4
CD8

IL-10 signaling modulates Th1 responses but preserves heterosubtypic immunity

The results above suggest a key role for IL-10 signaling in modulating lung-localized recall responses to influenza challenge. We therefore inhibited IL-10R signaling during heterosubtypic challenge using αIL-10R blocking antibody just prior to and during heterosubtypic influenza challenge. We observed no change in weight loss morbidity in the anti-IL-10R treated group compared to the vehicle control group (Fig. 4.5 A), and no difference in viral clearance was observed six days after challenge as well (Fig. 4.5 B). The cytokine levels in the lung bronchoalveolar lavage (BAL) washes of treated animals contained elevated IL-10 (Fig. 4.5 C), confirming that αIL-10R antibody treatment was sufficient to block IL-10 uptake. However, BAL from treated mice also contained significantly elevated levels of IFN-γ and TNF-α (Fig. 4.5 C), demonstrating that IL-10 signaling is necessary to modulate Th1 antiviral and inflammatory pathways. These changes in cytokine production were not caused by changes in the number of T cells, as no significant difference in the number of $CD4^+$ and $CD8^+$ lung T cells was observed between the αIL-10R blockade and vehicle control groups (Fig. 4.5 D). These results indicate that enhanced lung niche $CD4^+$ effector T cell IL-10 signaling suppress Th1 cytokine production without any deleterious effects on viral clearance or weight loss morbidity.

Figure 4.5: Recall response IL-10 signaling modulates Th1 responses while maintaining antiviral protection

Wild type memory mice were treated with FTY720 and i.p. and i.n. αIL-10R antibody and challenged with PR8 virus. (A) Weight loss as percentage of day 0 body weight compared between treated and vehicle control groups. (B) BAL Viral titers from αIL-10R and vehicle control treated mice 6 days post challenge. (C) Graphs depicting day 6 BAL cytokine concentration as determined by Legendplex cytometric bead array (Biolegend). (D) Graphs depicting lung niche $CD4^{+}$ (left) and $CD8^{+}$ (right) $CD44^{hi}$ $CD62L^{lo}$ T cell counts. All data compiled from 2 independent experiments depicting mean ± SEM. N=11-12 mice. Statistical significance determined by student's unpaired t-test. *$p<0.05$, **$p<0.01$.

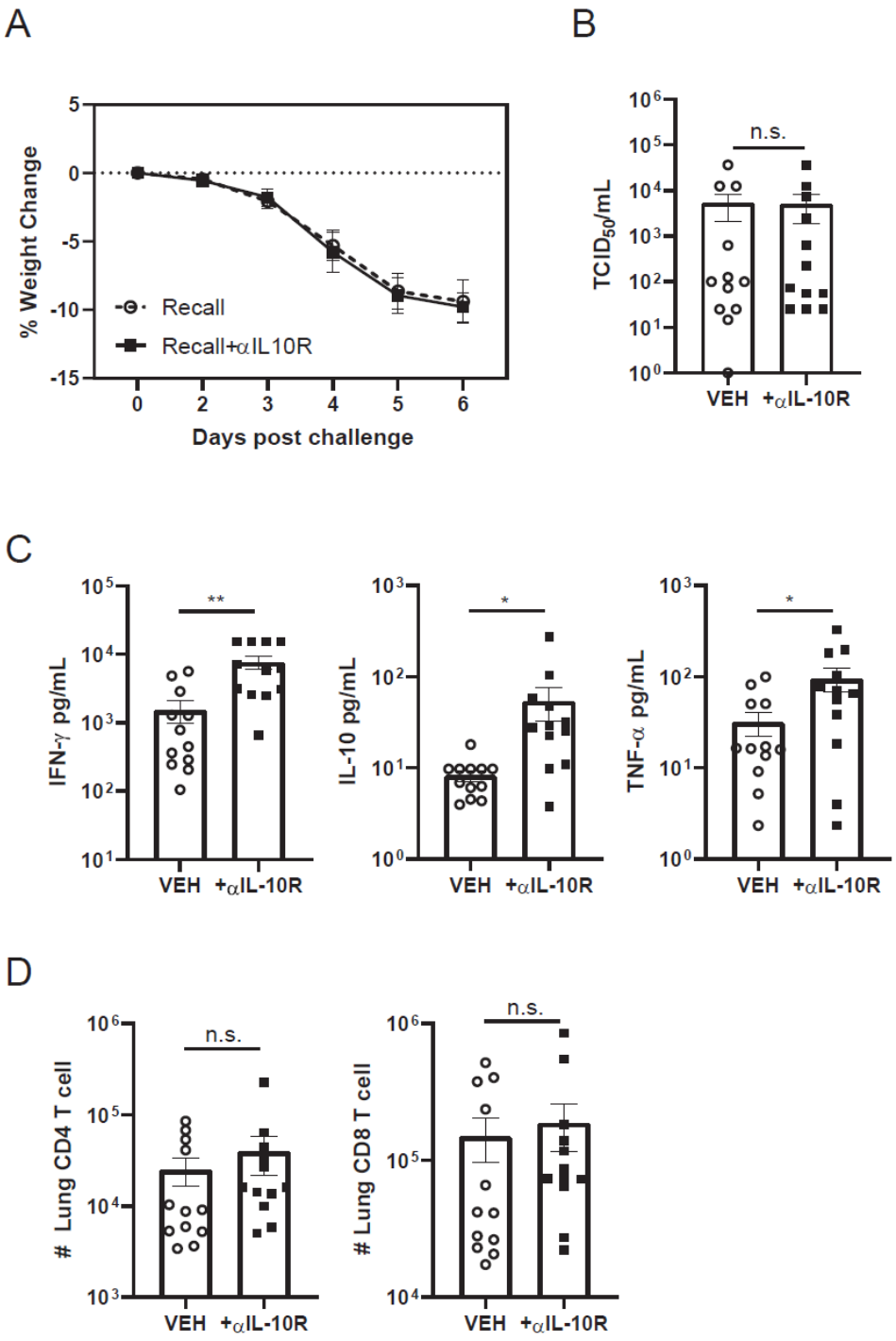
A
% Weight Change
Days post challenge
Recall
Recall+αIL10R
B
TCID50/mL
n.s.
VEH
+αIL-10R
C
IFN-γ pg/mL
IL-10 pg/mL
TNF-α pg/mL
**
*
*
D
Lung CD4 T cell
Lung CD8 T cell
n.s.
n.s.

4.4: Discussion

Recall responses to heterosubtypic influenza challenge provide cross strain protective immunity, but the mechanisms by which inflammatory responses are modulated are not well defined. Here, we reveal that lung $CD4^+$ tissue resident memory T cells have a distinct cytokine profile compared to circulating $CD4^+$ memory T cells that is influenced by the tissue priming environment. Compared to splenic, circulating effector memory $CD4^+$ T cells, $CD4^+$ lung TRM produce more IL-10 after *in vitro* restimulation. Using a heterosubtypic IAV challenge model, we found that early tissue-localized recall responses resulted in globally suppressed inflammatory pathways in the lung at the transcriptional level. Further cellular analysis of the T cell response revealed that enhanced $CD4^+$ lung effector T cell expansion as described in Chapter 3 is concurrent with enhanced IL-10 production which is critical to modulating inflammatory immune responses while preserving viral clearance. These data demonstrate that efficacious antiviral T cell responses during a heterosubtypic IAV response are augmented by an immunomodulatory lung environment that includes IL-10 production by lung niche $CD4^+$ effector and memory T cells.

Lung $CD4^+$ TRM are generated in two models of $CD4^+$ TRM generation: a primary influenza infection to generate polyclonal TRM and the adoptive transfer of *in vitro* activated OT-II T cells into $RAG^{-/-}$ lymphopenic mice to generate OT-II TCR transgenic TRM. In both models, TRM are more potent cytokine producers of IFN-ɣ, TNF-α, IL-17A, and IL-10 after either αCD3/28 or $OVA_{323-339}$ peptide stimulation as compared to their circulating splenic TEM counterparts. Furthermore, we found that the peptide dose response curves of TRM cytokine production were affected by the type of tissue cells used to present antigen; IL-22 production was solely dependent on the use of lung APCs compared to splenic APCs, suggesting that the lung environment itself may have an outsized impact on the production of IL-10 family cytokines.

However, when considering the context of continual environmental exposure, the lung contains unique microbiota that may alter lung T cell responses or contribute to the differential cytokine production when co-cultured with T cells [211], and the lung microbiota may be particularly altered in lymphopenic $RAG^{-/-}$ mice which are the experimental source of tissue APCs. The lung's heterogenous APC population also includes a range of dendritic cells, alveolar macrophages, and interstitial macrophages which may promote more variable cytokine responses compared to lymphoid APCs that promote Th1 cytokines more important in priming and proliferation in response to viral antigens.

By analyzing the transcriptional changes of total lung tissue during primary and recall responses to influenza, we determined that the primary response induces significantly more transcriptional changes, including in innate immune signaling pathways such as interferon signaling, protein translation, and cellular metabolism. These data suggest that after recovery from a primary infection, the lung environment is fundamentally altered to modulate lung niche effector T cell function, which is supported by our finding that effector $CD4^+$ T cells during a recall response produce significantly more IL-10 compared to a primary infection. MedLN $CD4^+$ T cells produce low levels of IL-10 without any difference between primary and secondary infection, suggesting that shift toward IL-10 production is induced by the lung environment. These results support previous observations that lung $CD4^+$ T cells have been shown to be predisposed toward immunomodulatory function compared to systemic $CD4^+$ T cells [212]. However, we observe tissue-wide transcriptional immunoregulation (2 days post challenge) well before the rapid influx of $CD4^+$ T cells (5 days post challenge) even though there are significantly fewer IL-10 producing TRM than non-TRM. We postulate that even though $CD4^+$ and $CD8^+$ TRM produce less IL-10, compared to effector $CD4^+$ T cells, TRM are present in large enough numbers where even modest

IL-10 production in the early stages of infection is sufficient to produce the observed immunomodulatory effects. We further demonstrated with a blockade of enhanced IL-10 signaling that IL-10 suppresses inflammatory IFN-ɣ and TNF-α cytokine levels in the airways without affecting viral clearance during a heterosubtypic IAV infection.

Our findings demonstrate that the resolution of primary influenza infection leads to increased immunoregulation in the lung environment that enhances $CD4^+$ T cell IL-10 production during subsequent viral exposures, which has implications for respiratory antiviral therapies that may seek to reduce excess tissue inflammation and cytokine storms, as well as vaccines which may benefit from site specific delivery methods to induce the immunoregulatory features of local tissue memory generated by a primary infection.

Chapter 5: Conclusions

Defining the features of lung localized T cell immunity that contribute to enhanced cross-strain protection against IAV

Current vaccination strategies that target antibody generation have proven insufficient in generating long-lasting, efficacious protection against seasonal strains of influenza A virus (IAV). On the other hand, T cells react against a wider range of highly conserved influenza epitopes, offering cross-strain protection [166]. A significant body of evidence over the past decade has identified tissue resident memory T cells (TRM) as important mediators of antiviral immunity; TRM localize to a wide variety of tissues such as the in the lung and airways and mediate tissue-localized immune responses against influenza virus (IAV) infection [94, 119, 120, 125]. Understanding the protective mechanisms tissue resident T cell responses will provide insight into immunization strategies that optimize cross-strain immunity and a universal IAV vaccine.

We used a primary H3N2 IAV infection with the X31 strain in order to generate protective, cross-strain immunity against an H1N1 heterosubtypic IAV challenge with the PR8 strain. Memory responses were protective even in B cell-deficient μMT mice as well as in the presence of FTY720 treatment which minimizes peripheral T cell migration, suggesting that a primary infection confers tissue-localized T cell-based immunity. By studying the lung niche T cell in both previously infected and uninfected mice, we identified enhancements in T cell expansion during the recall response. While recent TRM studies of the skin and reproductive tract found TRM proliferation to dominate *in situ* T cell responses [129, 130], our results suggest non-TRM comprised a majority of lung niche T cell expansion during secondary infection and also proliferated *in situ*. Despite the use of FTY720, the possibility also remained that peripheral T cells might also enter the lung niche to further contribute to non-TRM T cell expansion.

By identifying newly generated effector T cells in the lung niche, we could reasonably suppose that those cells must migrate from the periphery, given that the lung is not a recognized site of naïve T cell priming. We transferred naïve OT-II cells and observed that during infection with PR8-OTII, $CD4^+$ OT-II effector T cells migrated to the lung more quickly during a recall response than a primary response, suggesting that increased peripheral T cell migration must be a mechanism for lung T cell expansion. Interestingly, our results showed that the early recall response resulted in a broadening of the T cell repertoire by including newly generated effector T cells against novel IAV epitopes in addition to the reactivation of previously generated cross-reactive memory T cells.

Another benefit of our experimental strategy was that we could also compare the responses of our common transgenic T cell indicator population between a primary and recall response, allowing us to conclude that any differences in the T cell response were due to the local tissue immune environment rather than the T cells themselves. By analyzing both OT-I and OT-II responses to their respective recombinant PR8-OVA viruses, we observed significant enhancements in $CD4^+$ and $CD8^+$ T cell priming and proliferation in the mediastinal lymph node (medLN) that underly the rapid migration to the lung niche during a recall response. At steady state, medLN of memory mice retained significantly more total T cells and $CD103^+$ migratory and $CD11b^+$ LN resident $zbtb46^+$ conventional dendritic cells (cDCs). We created bone marrow chimera mice using donor cells expressing diphtheria toxin receptor (DTR) under the promoter of the cDC-specific Zbtb46 transcription factor. Enhanced T cell proliferation of OT-I and OT-II in chimeric memory mice was abrogated by medLN cDC depletion after diphtheria toxin treatment, demonstrating that increased numbers of cDCs are the underlying mechanism for enhanced $CD4^+$ and $CD8^+$ T cell priming and proliferation during a recall response.

We propose a model for T-cell mediated heterosubtypic immunity in which prior influenza exposure induces durable fortification of local draining lymph nodes with increased numbers of both $CD103^+$ and $CD11b^+$ cDCs that provide increased antigen presentation (Figure 5.1). Upon exposure to a new strain of IAV, lung dendritic cells transport antigen to the medLN where they can share antigen [58] with the increased number of cDCs which activate both pre-existing memory and naïve T cells to mount a rapid and broadened effector T cell response that migrates to the lung resident niche to augment TRM responses. Our results indicate that inoculation at the tissue site may fortify innate immunity in local lymphoid sites to provide enhanced T cell responses in addition to the generation of TRM.

Figure 5.1: Proposed model of lung-localized T cell immune responses to heterosubtypic IAV challenge

We propose a model for tissue-localized lung T cell mediated protection against heterosubtypic IAV challenge. (A) The lung localized recall response to IAV challenge is characterized by an increased number of pre-existing medLN conventional dendritic cells that provide enhanced antigen presentation to lymph node T cells, including naïve T cells. Enhanced medLN $CD4^+$ and $CD8^+$ T cell priming results in the enhanced numbers of T cells that migrate to the lung tissue to augment local TRM responses. Both TRM and effector T cells proliferate within the lung resident niche and provide effector function to clear IAV infection. (B) During primary infection, the medLN contains fewer cDCs and T cells, leading to a more delayed migration of fewer T cells to the lung resident niche. This leads to less effective viral clearance compared to the recall response.

A

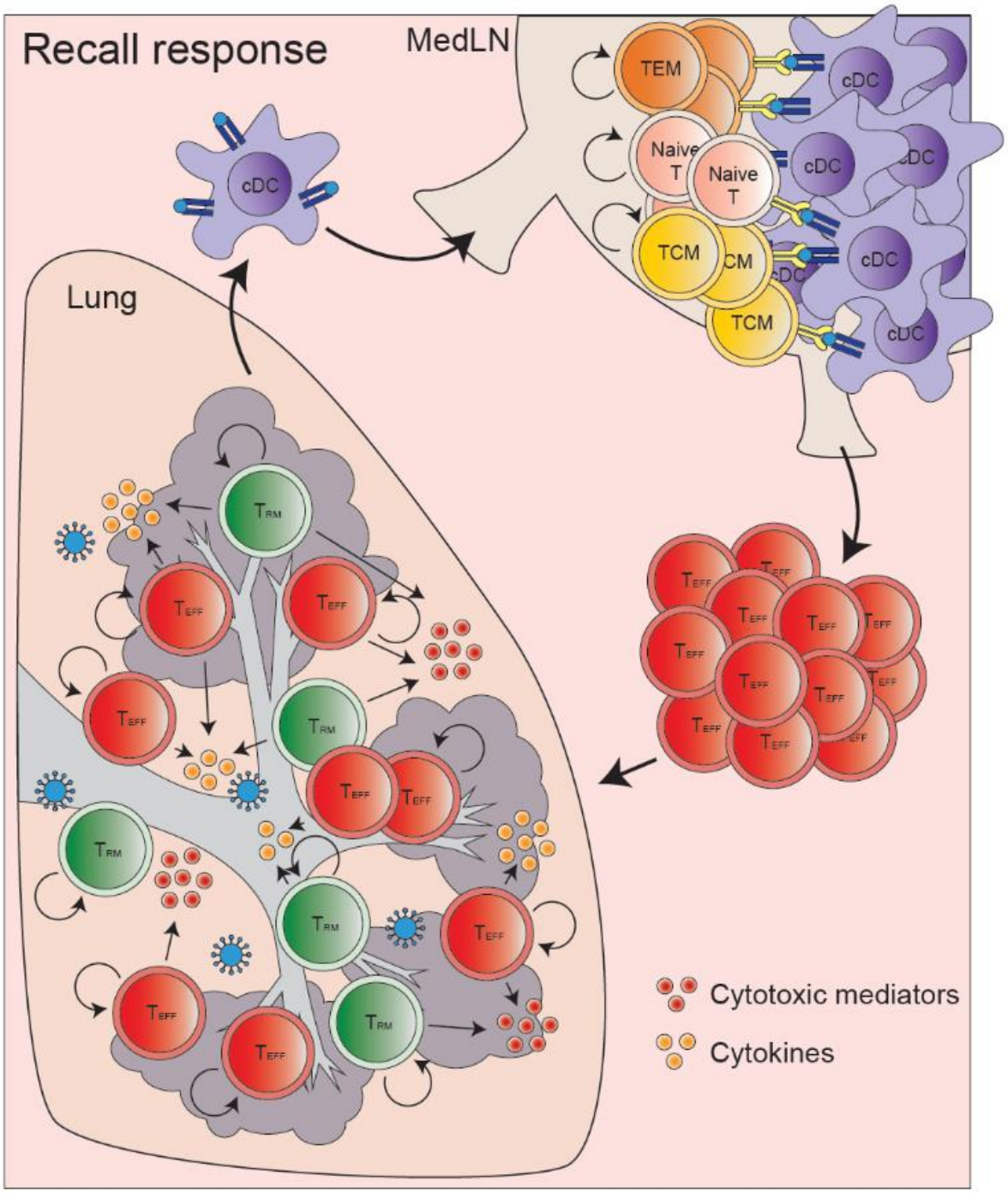
Recall response
MedLN
TEM
cDC
Naive T
Naive T
TCM
CM
TCM
Lung
T_{RM}
T_{EFF}
Cytotoxic mediators
Cytokines

B

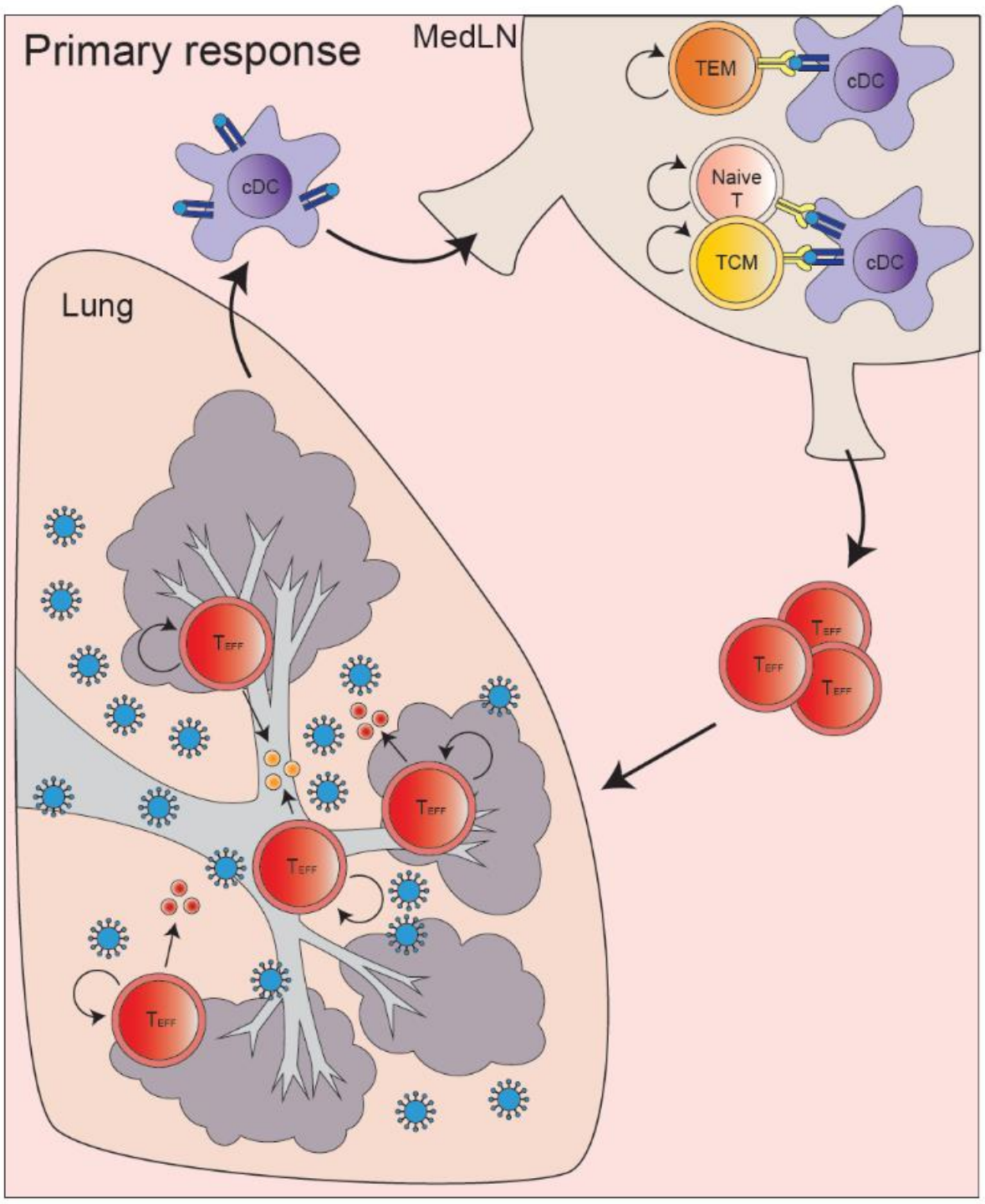
Primary response
MedLN
TEM
cDC
Naive T
TCM
cDC
cDC
Lung
TEFF
TEFF
TEFF
TEFF
TEFF
TEFF
TEFF

Immunomodulatory function of lung localized T cell immunity during heterosubtypic IAV infection

Inflammatory immune responses to respiratory infection are critical to host survival and tissue homeostasis. However, these same inflammatory processes cause non-specific immunopathology that may result in as much morbidity as the infectious disease process itself. Clinical outcomes from respiratory viruses such as coronaviruses and influenza viruses are strongly associated with immunopathology [196-199]. Aberrantly high levels of inflammatory soluble mediators, known as a cytokine storm, mediate the development of immunopathology and are produced by both innate and adaptive T cell responses. During an IAV infection, circulating memory $CD4^+$ T cell responses play a critical role in viral clearance and immunity but also have been shown to increase weight loss morbidity [175]. At the same time, lung effector $CD4^+$ T cells have also been shown to produce the immunomodulatory cytokine IL-10 during IAV infection, suggesting that T cells have self-limiting mechanisms to limit immunopathology [85]. Yet, the role of lung-localized T cell-mediated immunomodulation during a memory response has not been well studied.

In this study we sought to assess the immunomodulatory responses of lung-localized $CD4^+$ T cells during a recall response to IAV challenge. We initially began by determining the cytokine production capacity of lung TRM after *in vitro* reactivation. We found that memory T cells produce cytokines most suitable for their tissue localization. Polyclonal lung $CD4^+$ TRM generated after a primary IAV infection produced significantly more IFN-ɣ, TNF-α, and IL-10 compared to spleen TEM, reflecting enhanced effector function of TRM that may be exposed to future IAV infections. Spleen $CD4^+$ TEM produce greater levels of IL-4, indicative of their role for B cell help within lymphoid sites. We also used a model of memory T cell generation in

which *in vitro* stimulated $CD4^+$ OT-II cells were transferred into $RAG1^{-/-}$ mice to produce antigen-specific lung OT-II TRM and spleen OT-II TEM. Peptide stimulation of lung and spleen OT-II cells indicated that lung TRM are robust producers of Th1 and Th17 cytokines as well as IL-10 family cytokine IL-22. Furthermore, T cell cytokine production was strongly influenced by the tissue localization of the antigen presenting cells; lung APCs induced increased IL-22 production, suggesting that the lung environment drives enhanced IL-10 family cytokine signaling.

We then sought to better assess the tissue-wide effects of the recall response driven immunomodulation. We analyzed transcriptional changes in the whole lung after IAV challenge for both a primary and secondary infection. In a primary infection, significantly more genes were upregulated, including those for innate immune programs such as type I IFN signaling. GSEA analysis revealed significant enrichment for innate antiviral responses such as TLR3 and TLR7 signaling. Given the enhanced T cell responses in a recall response demonstrated in Chapter 3, this paradoxical suppression of transcriptional changes suggest that lung tissue homeostasis is optimally regulated during a recall response.

With the knowledge that the lung environment is highly immunomodulatory, we used IL-10-GFP reporter mice in a heterosubtypic influenza challenge model to assess *in situ* IL-10 production in the lung niche. While $CD4^+$ and $CD8^+$ T cells expressed low levels of IL-10 in the medLN, we observed no difference between a primary and recall response. However, in the lung, $CD4^+$ T cells produced high levels of IL-10 (>25% GFP^+) in a recall response and at significantly greater levels compared to a primary response (<5% GFP^+). $CD8^+$ T cells also produced IL-10, but we observed no difference between a recall and primary response, suggesting that $CD4^+$ T cells are the main drivers of IL-10 mediated immunomodulation in a

memory response. By blocking IL-10R signaling in a recall response, we show that IL-10 signaling dampens production of inflammatory cytokines in the airway such as IFN-ɣ and TNF-α.

In the context of an increased lung cellular response by Th1 polarized T cells (Chapter 3), the body must limit immunopathology during a memory response to IAV. Here we demonstrate using in vitro models that the lung environment predisposes T cells toward immunomodulatory features. This immunomodulation limits inflammatory innate responses that is mediated by IL-10 production by lung T cells, particularly $CD4^+$ T cells, without compromising antiviral function. These results suggest that the enhanced influx of lung T cells may provide a source of IL-10 mediated modulation that limits immunopathology while simultaneously providing enhanced viral clearance.

References

1. Bouvier, N.M. and P. Palese, *The biology of influenza viruses.* Vaccine, 2008. **26 Suppl 4**(Suppl 4): p. D49-D53.
2. Caini, S., et al., *The epidemiological signature of influenza B virus and its B/Victoria and B/Yamagata lineages in the 21st century.* PloS one, 2019. **14**(9): p. e0222381-e0222381.
3. Iwasaki, A. and P.S. Pillai, *Innate immunity to influenza virus infection.* Nature reviews. Immunology, 2014. **14**(5): p. 315-328.
4. Hufford, M.M., et al., *The effector T cell response to influenza infection.* Curr Top Microbiol Immunol, 2015. **386**: p. 423-55.
5. Krammer, F., et al., *Influenza.* Nature Reviews Disease Primers, 2018. **4**(1): p. 3.
6. Trifonov, V., H. Khiabanian, and R. Rabadan, *Geographic dependence, surveillance, and origins of the 2009 influenza A (H1N1) virus.* N Engl J Med, 2009. **361**(2): p. 115-9.
7. Turrell, L., et al., *The role and assembly mechanism of nucleoprotein in influenza A virus ribonucleoprotein complexes.* Nature Communications, 2013. **4**(1): p. 1591.
8. Matrosovich, M.N., et al., *Avian influenza A viruses differ from human viruses by recognition of sialyloligosaccharides and gangliosides and by a higher conservation of the HA receptor-binding site.* Virology, 1997. **233**(1): p. 224-34.
9. Gomez-Puertas, P., et al., *Influenza virus matrix protein is the major driving force in virus budding.* J Virol, 2000. **74**(24): p. 11538-47.
10. Rossman, J.S. and R.A. Lamb, *Influenza virus assembly and budding.* Virology, 2011. **411**(2): p. 229-236.
11. Tecle, T., S. Tripathi, and K.L. Hartshorn, *Review: Defensins and cathelicidins in lung immunity.* Innate Immun, 2010. **16**(3): p. 151-9.
12. Diebold, S.S., et al., *Innate antiviral responses by means of TLR7-mediated recognition of single-stranded RNA.* Science, 2004. **303**(5663): p. 1529-31.
13. Guillot, L., et al., *Involvement of toll-like receptor 3 in the immune response of lung epithelial cells to double-stranded RNA and influenza A virus.* J Biol Chem, 2005. **280**(7): p. 5571-80.
14. Pichlmair, A., et al., *RIG-I-mediated antiviral responses to single-stranded RNA bearing 5'-phosphates.* Science, 2006. **314**(5801): p. 997-1001.
15. Kato, H., et al., *Differential roles of MDA5 and RIG-I helicases in the recognition of RNA viruses.* Nature, 2006. **441**(7089): p. 101-105.
16. Seo, S.U., et al., *MyD88 signaling is indispensable for primary influenza A virus infection but dispensable for secondary infection.* J Virol, 2010. **84**(24): p. 12713-22.
17. Der, S.D., et al., *Identification of genes differentially regulated by interferon α, β, or γ using oligonucleotide arrays.* Proceedings of the National Academy of Sciences, 1998. **95**(26): p. 15623-15628.
18. Chakrabarti, A., B.K. Jha, and R.H. Silverman, *New Insights into the Role of RNase L in Innate Immunity.* Journal of Interferon & Cytokine Research, 2010. **31**(1): p. 49-57.
19. Pindel, A. and A. Sadler, *The Role of Protein Kinase R in the Interferon Response.* Journal of Interferon & Cytokine Research, 2010. **31**(1): p. 59-70.

20. Wang, X., E.R. Hinson, and P. Cresswell, *The interferon-inducible protein viperin inhibits influenza virus release by perturbing lipid rafts.* Cell Host Microbe, 2007. **2**(2): p. 96-105.
21. Brass, A.L., et al., *The IFITM proteins mediate cellular resistance to influenza A H1N1 virus, West Nile virus, and dengue virus.* Cell, 2009. **139**(7): p. 1243-54.
22. Mordstein, M., et al., *Lambda Interferon Renders Epithelial Cells of the Respiratory and Gastrointestinal Tracts Resistant to Viral Infections.* Journal of Virology, 2010. **84**(11): p. 5670-5677.
23. Garcia-Sastre, A., *Induction and evasion of type I interferon responses by influenza viruses.* Virus Res, 2011. **162**(1-2): p. 12-8.
24. Allen, I.C., et al., *The NLRP3 inflammasome mediates in vivo innate immunity to influenza A virus through recognition of viral RNA.* Immunity, 2009. **30**(4): p. 556-65.
25. Thomas, P.G., et al., *The intracellular sensor NLRP3 mediates key innate and healing responses to influenza A virus via the regulation of caspase-1.* Immunity, 2009. **30**(4): p. 566-75.
26. García-Ramírez, R.A., et al., *TNF, IL6, and IL1B Polymorphisms Are Associated with Severe Influenza A (H1N1) Virus Infection in the Mexican Population.* PLOS ONE, 2015. **10**(12): p. e0144832.
27. Dienz, O., et al., *Essential role of IL-6 in protection against H1N1 influenza virus by promoting neutrophil survival in the lung.* Mucosal Immunology, 2012. **5**(3): p. 258-266.
28. Seo, S.H. and R.G. Webster, *Tumor Necrosis Factor Alpha Exerts Powerful Anti-Influenza Virus Effects in Lung Epithelial Cells.* Journal of Virology, 2002. **76**(3): p. 1071-1076.
29. Chan, M.C., et al., *Proinflammatory cytokine responses induced by influenza A (H5N1) viruses in primary human alveolar and bronchial epithelial cells.* Respir Res, 2005. **6**: p. 135.
30. Fujisawa, H., *Neutrophils Play an Essential Role in Cooperation with Antibody in both Protection against and Recovery from Pulmonary Infection with Influenza Virus in Mice.* Journal of Virology, 2008. **82**(6): p. 2772-2783.
31. Gazit, R., et al., *Lethal influenza infection in the absence of the natural killer cell receptor gene Ncr1.* Nature Immunology, 2006. **7**(5): p. 517-523.
32. Amulic, B., et al., *Neutrophil Function: From Mechanisms to Disease.* Annual Review of Immunology, 2012. **30**(1): p. 459-489.
33. Hufford, M.M., et al., *Influenza-infected neutrophils within the infected lungs act as antigen presenting cells for anti-viral CD8(+) T cells.* PloS one, 2012. **7**(10): p. e46581-e46581.
34. Bourdi, M., et al., *Protection against acetaminophen-induced liver injury and lethality by interleukin 10: role of inducible nitric oxide synthase.* Hepatology, 2002. **35**(2): p. 289-98.
35. Morhardt, T.L., et al., *IL-10 produced by macrophages regulates epithelial integrity in the small intestine.* Scientific Reports, 2019. **9**(1): p. 1223.
36. Quiros, M., et al., *Macrophage-derived IL-10 mediates mucosal repair by epithelial WISP-1 signaling.* J Clin Invest, 2017. **127**(9): p. 3510-3520.
37. Sabatel, C., et al., *Exposure to Bacterial CpG DNA Protects from Airway Allergic Inflammation by Expanding Regulatory Lung Interstitial Macrophages.* Immunity, 2017. **46**(3): p. 457-473.

38. Bedoret, D., et al., *Lung interstitial macrophages alter dendritic cell functions to prevent airway allergy in mice.* The Journal of clinical investigation, 2009. **119**(12): p. 3723-3738.
39. Grabiec, A.M. and T. Hussell, *The role of airway macrophages in apoptotic cell clearance following acute and chronic lung inflammation.* Seminars in immunopathology, 2016. **38**(4): p. 409-423.
40. Simpson, J.L., et al., *Impaired macrophage phagocytosis in non-eosinophilic asthma.* Clin Exp Allergy, 2013. **43**(1): p. 29-35.
41. Fitzpatrick, A.M., et al., *Alveolar macrophage phagocytosis is impaired in children with poorly controlled asthma.* J Allergy Clin Immunol, 2008. **121**(6): p. 1372-8, 1378.e1-3.
42. Hodge, S., et al., *Alveolar macrophages from subjects with chronic obstructive pulmonary disease are deficient in their ability to phagocytose apoptotic airway epithelial cells.* Immunol Cell Biol, 2003. **81**(4): p. 289-96.
43. Morimoto, K., W.J. Janssen, and M. Terada, *Defective efferocytosis by alveolar macrophages in IPF patients.* Respir Med, 2012. **106**(12): p. 1800-3.
44. Liu, K., et al., *In vivo analysis of dendritic cell development and homeostasis.* Science (New York, N.Y.), 2009. **324**(5925): p. 392-397.
45. Reizis, B., *Plasmacytoid Dendritic Cells: Development, Regulation, and Function.* Immunity, 2019. **50**(1): p. 37-50.
46. Lund , J., et al., *Toll-like Receptor 9–mediated Recognition of Herpes Simplex Virus-2 by Plasmacytoid Dendritic Cells.* Journal of Experimental Medicine, 2003. **198**(3): p. 513-520.
47. Siegal, F.P., et al., *The Nature of the Principal Type 1 Interferon-Producing Cells in Human Blood.* 1999. **284**(5421): p. 1835-1837.
48. Cella, M., et al., *Plasmacytoid monocytes migrate to inflamed lymph nodes and produce large amounts of type I interferon.* Nature Medicine, 1999. **5**(8): p. 919-923.
49. Stout-Delgado, H.W., et al., *Aging impairs IFN regulatory factor 7 up-regulation in plasmacytoid dendritic cells during TLR9 activation.* J Immunol, 2008. **181**(10): p. 6747-56.
50. Wolf, A.I., et al., *Plasmacytoid Dendritic Cells Are Dispensable during Primary Influenza Virus Infection.* The Journal of Immunology, 2009. **182**(2): p. 871.
51. Kim, T.S. and T.J. Braciale, *Respiratory Dendritic Cell Subsets Differ in Their Capacity to Support the Induction of Virus-Specific Cytotoxic CD8+ T Cell Responses.* PLOS ONE, 2009. **4**(1): p. e4204.
52. Beaty, S.R., C.E. Rose, and S.-s.J. Sung, *Diverse and Potent Chemokine Production by Lung CD11b^{high} Dendritic Cells in Homeostasis and in Allergic Lung Inflammation.* The Journal of Immunology, 2007. **178**(3): p. 1882-1895.
53. Norbury, C.C., *Drinking a lot is good for dendritic cells.* Immunology, 2006. **117**(4): p. 443-451.
54. Platt, C.D., et al., *Mature dendritic cells use endocytic receptors to capture and present antigens.* 2010. **107**(9): p. 4287-4292.
55. Albert, M.L., B. Sauter, and N. Bhardwaj, *Dendritic cells acquire antigen from apoptotic cells and induce class I-restricted CTLs.* Nature, 1998. **392**(6671): p. 86-89.
56. Diebold, S.S., et al., *Viral infection switches non-plasmacytoid dendritic cells into high interferon producers.* Nature, 2003. **424**(6946): p. 324-8.

57. Smed-Sorensen, A., et al., *Influenza A virus infection of human primary dendritic cells impairs their ability to cross-present antigen to CD8 T cells.* PLoS Pathog, 2012. **8**(3): p. e1002572.
58. Gurevich, I., et al., *Active dissemination of cellular antigens by DCs facilitates CD8(+) T-cell priming in lymph nodes.* Eur J Immunol, 2017. **47**(10): p. 1802-1818.
59. Palm, N.W. and R. Medzhitov, *Pattern recognition receptors and control of adaptive immunity.* Immunol Rev, 2009. **227**(1): p. 221-33.
60. Ho, A.W., et al., *Lung CD103+ dendritic cells efficiently transport influenza virus to the lymph node and load viral antigen onto MHC class I for presentation to CD8 T cells.* J Immunol, 2011. **187**(11): p. 6011-21.
61. Russo, E., et al., *Intralymphatic CCL21 Promotes Tissue Egress of Dendritic Cells through Afferent Lymphatic Vessels.* Cell Rep, 2016. **14**(7): p. 1723-1734.
62. Ulvmar, M.H., et al., *The atypical chemokine receptor CCRL1 shapes functional CCL21 gradients in lymph nodes.* Nat Immunol, 2014. **15**(7): p. 623-30.
63. GeurtsvanKessel, C.H., et al., *Clearance of influenza virus from the lung depends on migratory langerin+CD11b- but not plasmacytoid dendritic cells.* J Exp Med, 2008. **205**(7): p. 1621-34.
64. Smith, W.A., CH; Laidlaw PP, *A virus obtained from Influenza patients.* The Lancet, 1933. **222**(5732): p. 66-68.
65. Lewnard, J.A. and S. Cobey, *Immune History and Influenza Vaccine Effectiveness.* Vaccines (Basel), 2018. **6**(2).
66. Krammer, F., *The human antibody response to influenza A virus infection and vaccination.* Nature Reviews Immunology, 2019. **19**(6): p. 383-397.
67. Graham, M.B. and T.J. Braciale, *Resistance to and recovery from lethal influenza virus infection in B lymphocyte-deficient mice.* The Journal of experimental medicine, 1997. **186**(12): p. 2063-2068.
68. Bui, H.-H., et al., *Ab and T cell epitopes of influenza A virus, knowledge and opportunities.* Proceedings of the National Academy of Sciences of the United States of America, 2007. **104**(1): p. 246-251.
69. Schwab, S.R. and J.G. Cyster, *Finding a way out: lymphocyte egress from lymphoid organs.* Nature Immunology, 2007. **8**(12): p. 1295-1301.
70. Lian, J. and A.D. Luster, *Chemokine-guided cell positioning in the lymph node orchestrates the generation of adaptive immune responses.* Current opinion in cell biology, 2015. **36**: p. 1-6.
71. Grigorova, I.L., et al., *Cortical sinus probing, S1P1-dependent entry and flow-based capture of egressing T cells.* Nat Immunol, 2009. **10**(1): p. 58-65.
72. Shiow, L.R., et al., *CD69 acts downstream of interferon-alpha/beta to inhibit S1P1 and lymphocyte egress from lymphoid organs.* Nature, 2006. **440**(7083): p. 540-4.
73. Mandala, S., et al., *Alteration of lymphocyte trafficking by sphingosine-1-phosphate receptor agonists.* Science, 2002. **296**(5566): p. 346-9.
74. Mueller, D.L., M.K. Jenkins, and R.H. Schwartz, *Clonal expansion versus functional clonal inactivation: a costimulatory signalling pathway determines the outcome of T cell antigen receptor occupancy.* Annu Rev Immunol, 1989. **7**: p. 445-80.
75. Chen, L. and D.B. Flies, *Molecular mechanisms of T cell co-stimulation and co-inhibition.* Nat Rev Immunol, 2013. **13**(4): p. 227-42.

76. Boomer, J.S. and J.M. Green, *An enigmatic tail of CD28 signaling.* Cold Spring Harb Perspect Biol, 2010. **2**(8): p. a002436.
77. Kapsenberg, M.L., *Dendritic-cell control of pathogen-driven T-cell polarization.* Nature Reviews Immunology, 2003. **3**(12): p. 984-993.
78. Mikhak, Z., J.P. Strassner, and A.D. Luster, *Lung dendritic cells imprint T cell lung homing and promote lung immunity through the chemokine receptor CCR4.* J Exp Med, 2013. **210**(9): p. 1855-69.
79. Hussell, T., A. Pennycook, and P.J. Openshaw, *Inhibition of tumor necrosis factor reduces the severity of virus-specific lung immunopathology.* Eur J Immunol, 2001. **31**(9): p. 2566-73.
80. Cook, D.N., *The role of MIP-1 alpha in inflammation and hematopoiesis.* J Leukoc Biol, 1996. **59**(1): p. 61-6.
81. Topham, D.J. and P.C. Doherty, *Clearance of an Influenza A Virus by CD4⁺ T Cells Is Inefficient in the Absence of B Cells.* Journal of Virology, 1998. **72**(1): p. 882-885.
82. Boyden, A.W., et al., *Primary and long-term B-cell responses in the upper airway and lung after influenza A virus infection.* Immunol Res, 2014. **59**(1-3): p. 73-80.
83. Bender, B.S., et al., *Transgenic mice lacking class I major histocompatibility complex-restricted T cells have delayed viral clearance and increased mortality after influenza virus challenge.* J Exp Med, 1992. **175**(4): p. 1143-5.
84. Belz, G.T., et al., *Compromised influenza virus-specific CD8(+)-T-cell memory in CD4(+)-T-cell-deficient mice.* J Virol, 2002. **76**(23): p. 12388-93.
85. Sun, J., et al., *Effector T cells control lung inflammation during acute influenza virus infection by producing IL-10.* Nat Med, 2009. **15**(3): p. 277-84.
86. Vos, Q., L.A. Jones, and A.M. Kruisbeek, *Mice deprived of exogenous antigenic stimulation develop a normal repertoire of functional T cells.* J Immunol, 1992. **149**(4): p. 1204-10.
87. Hengel, R.L., et al., *Cutting edge: L-selectin (CD62L) expression distinguishes small resting memory CD4+ T cells that preferentially respond to recall antigen.* J Immunol, 2003. **170**(1): p. 28-32.
88. Sallusto, F., et al., *Two subsets of memory T lymphocytes with distinct homing potentials and effector functions.* Nature, 1999. **401**(6754): p. 708-712.
89. Sathaliyawala, T., et al., *Distribution and compartmentalization of human circulating and tissue-resident memory T cell subsets.* Immunity, 2013. **38**(1): p. 187-97.
90. Thome, J.J., et al., *Spatial map of human T cell compartmentalization and maintenance over decades of life.* Cell, 2014. **159**(4): p. 814-28.
91. Steinert, E.M., et al., *Quantifying Memory CD8 T Cells Reveals Regionalization of Immunosurveillance.* Cell, 2015. **161**(4): p. 737-49.
92. Zhu, J., et al., *Immune surveillance by CD8alphaalpha+ skin-resident T cells in human herpes virus infection.* Nature, 2013. **497**(7450): p. 494-7.
93. Watanabe, R., et al., *Human skin is protected by four functionally and phenotypically discrete populations of resident and recirculating memory T cells.* Sci Transl Med, 2015. **7**(279): p. 279ra39.
94. Teijaro, J.R., et al., *Cutting edge: Tissue-retentive lung memory CD4 T cells mediate optimal protection to respiratory virus infection.* J Immunol, 2011. **187**(11): p. 5510-4.

95. Weisberg, S.P., et al., *Tissue-Resident Memory T Cells Mediate Immune Homeostasis in the Human Pancreas through the PD-1/PD-L1 Pathway.* Cell Rep, 2019. **29**(12): p. 3916-3932.e5.
96. McNamara, H.A., et al., *Up-regulation of LFA-1 allows liver-resident memory T cells to patrol and remain in the hepatic sinusoids.* Sci Immunol, 2017. **2**(9).
97. Mackay, L.K., et al., *Hobit and Blimp1 instruct a universal transcriptional program of tissue residency in lymphocytes.* Science, 2016. **352**(6284): p. 459-63.
98. Sheridan, B.S., et al., *Oral infection drives a distinct population of intestinal resident memory CD8(+) T cells with enhanced protective function.* Immunity, 2014. **40**(5): p. 747-57.
99. Beura, L.K., et al., *T Cells in Nonlymphoid Tissues Give Rise to Lymph-Node-Resident Memory T Cells.* Immunity, 2018. **48**(2): p. 327-338 e5.
100. Zens, K.D., J.K. Chen, and D.L. Farber, *Vaccine-generated lung tissue-resident memory T cells provide heterosubtypic protection to influenza infection.* JCI Insight, 2016. **1**(10).
101. Kumar, B.V., et al., *Human Tissue-Resident Memory T Cells Are Defined by Core Transcriptional and Functional Signatures in Lymphoid and Mucosal Sites.* Cell Rep, 2017. **20**(12): p. 2921-2934.
102. Wakim, L.M., et al., *The molecular signature of tissue resident memory CD8 T cells isolated from the brain.* J Immunol, 2012. **189**(7): p. 3462-71.
103. Anderson, K.G., et al., *Cutting edge: intravascular staining redefines lung CD8 T cell responses.* J Immunol, 2012. **189**(6): p. 2702-6.
104. Turner, D.L., et al., *Lung niches for the generation and maintenance of tissue-resident memory T cells.* Mucosal Immunol, 2014. **7**(3): p. 501-10.
105. Gebhardt, T., et al., *Memory T cells in nonlymphoid tissue that provide enhanced local immunity during infection with herpes simplex virus.* Nat Immunol, 2009. **10**(5): p. 524-30.
106. Snyder, M.E., et al., *Generation and persistence of human tissue-resident memory T cells in lung transplantation.* Sci Immunol, 2019. **4**(33).
107. Mani, V., et al., *Migratory DCs activate TGF-beta to precondition naive CD8(+) T cells for tissue-resident memory fate.* Science, 2019. **366**(6462).
108. Hirai, T., et al., *Keratinocyte-Mediated Activation of the Cytokine TGF-beta Maintains Skin Recirculating Memory CD8(+) T Cells.* Immunity, 2019. **50**(5): p. 1249-1261.e5.
109. Wein, A.N., et al., *CXCR6 regulates localization of tissue-resident memory CD8 T cells to the airways.* J Exp Med, 2019. **216**(12): p. 2748-2762.
110. Takamura, S., et al., *Interstitial-resident memory CD8+ T cells sustain frontline epithelial memory in the lung.* Journal of Experimental Medicine, 2019. **216**(12): p. 2736-2747.
111. Slutter, B., et al., *Dynamics of influenza-induced lung-resident memory T cells underlie waning heterosubtypic immunity.* Sci Immunol, 2017. **2**(7).
112. Hayward, S.L., et al., *Environmental cues regulate epigenetic reprogramming of airway-resident memory CD8(+) T cells.* Nat Immunol, 2020. **21**(3): p. 309-320.
113. Van Braeckel-Budimir, N., et al., *Repeated Antigen Exposure Extends the Durability of Influenza-Specific Lung-Resident Memory CD8(+) T Cells and Heterosubtypic Immunity.* Cell Rep, 2018. **24**(13): p. 3374-3382 e3.

114. Turner, D.L., et al., *Biased Generation and In Situ Activation of Lung Tissue-Resident Memory CD4 T Cells in the Pathogenesis of Allergic Asthma.* J Immunol, 2018. **200**(5): p. 1561-1569.
115. Amezcua Vesely, M.C., et al., *Effector T(H)17 Cells Give Rise to Long-Lived T(RM) Cells that Are Essential for an Immediate Response against Bacterial Infection.* Cell, 2019. **178**(5): p. 1176-1188.e15.
116. Iijima, N. and A. Iwasaki, *T cell memory. A local macrophage chemokine network sustains protective tissue-resident memory CD4 T cells.* Science, 2014. **346**(6205): p. 93-8.
117. Takamura, S., *Niches for the Long-Term Maintenance of Tissue-Resident Memory T Cells.* Front Immunol, 2018. **9**: p. 1214.
118. Zheng, X., et al., *Mucosal CD8+ T cell responses induced by an MCMV based vaccine vector confer protection against influenza challenge.* PLOS Pathogens, 2019. **15**(9): p. e1008036.
119. McMaster, S.R., et al., *Airway-Resident Memory CD8 T Cells Provide Antigen-Specific Protection against Respiratory Virus Challenge through Rapid IFN-gamma Production.* J Immunol, 2015. **195**(1): p. 203-9.
120. Mackay, L.K., et al., *Long-lived epithelial immunity by tissue-resident memory T (TRM) cells in the absence of persisting local antigen presentation.* Proc Natl Acad Sci U S A, 2012. **109**(18): p. 7037-42.
121. Srivastava, R., et al., *CXCL17 Chemokine-Dependent Mobilization of CXCR8(+)CD8(+) Effector Memory and Tissue-Resident Memory T Cells in the Vaginal Mucosa Is Associated with Protection against Genital Herpes.* J Immunol, 2018. **200**(8): p. 2915-2926.
122. Jiang, X., et al., *Skin infection generates non-migratory memory CD8+ T(RM) cells providing global skin immunity.* Nature, 2012. **483**(7388): p. 227-31.
123. Gilchuk, P., et al., *A Distinct Lung-Interstitium-Resident Memory CD8(+) T Cell Subset Confers Enhanced Protection to Lower Respiratory Tract Infection.* Cell Rep, 2016. **16**(7): p. 1800-9.
124. Steinbach, K., et al., *Brain-resident memory T cells represent an autonomous cytotoxic barrier to viral infection.* J Exp Med, 2016. **213**(8): p. 1571-87.
125. Ariotti, S., et al., *T cell memory. Skin-resident memory CD8(+) T cells trigger a state of tissue-wide pathogen alert.* Science, 2014. **346**(6205): p. 101-5.
126. Ariotti, S., et al., *Tissue-resident memory CD8+ T cells continuously patrol skin epithelia to quickly recognize local antigen.* Proc Natl Acad Sci U S A, 2012. **109**(48): p. 19739-44.
127. Zaid, A., et al., *Persistence of skin-resident memory T cells within an epidermal niche.* Proceedings of the National Academy of Sciences, 2014. **111**(14): p. 5307-5312.
128. Dijkgraaf, F.E., et al., *Tissue patrol by resident memory CD8(+) T cells in human skin.* Nat Immunol, 2019. **20**(6): p. 756-764.
129. Park, S.L., et al., *Local proliferation maintains a stable pool of tissue-resident memory T cells after antiviral recall responses.* Nat Immunol, 2018. **19**(2): p. 183-191.
130. Beura, L.K., et al., *Intravital mucosal imaging of CD8(+) resident memory T cells shows tissue-autonomous recall responses that amplify secondary memory.* Nat Immunol, 2018. **19**(2): p. 173-182.

131. Thompson, E.A., et al., *Interstitial Migration of CD8alphabeta T Cells in the Small Intestine Is Dynamic and Is Dictated by Environmental Cues.* Cell Rep, 2019. **26**(11): p. 2859-2867.e4.
132. Fonseca, R., et al., *Developmental plasticity allows outside-in immune responses by resident memory T cells.* Nat Immunol, 2020. **21**(4): p. 412-421.
133. Klicznik, M.M., et al., *Human CD4⁺CD103⁺ cutaneous resident memory T cells are found in the circulation of healthy individuals.* Science Immunology, 2019. **4**(37): p. eaav8995.
134. Fernandez-Ruiz, D., et al., *Liver-Resident Memory CD8(+) T Cells Form a Front-Line Defense against Malaria Liver-Stage Infection.* Immunity, 2016. **45**(4): p. 889-902.
135. Casey, K.A., et al., *Antigen-independent differentiation and maintenance of effector-like resident memory T cells in tissues.* J Immunol, 2012. **188**(10): p. 4866-75.
136. Wakim, L.M., A. Woodward-Davis, and M.J. Bevan, *Memory T cells persisting within the brain after local infection show functional adaptations to their tissue of residence.* Proc Natl Acad Sci U S A, 2010. **107**(42): p. 17872-9.
137. Smolders, J., et al., *Tissue-resident memory T cells populate the human brain.* Nat Commun, 2018. **9**(1): p. 4593.
138. Hombrink, P., et al., *Programs for the persistence, vigilance and control of human CD8(+) lung-resident memory T cells.* Nat Immunol, 2016. **17**(12): p. 1467-1478.
139. Piet, B., et al., *CD8(+) T cells with an intraepithelial phenotype upregulate cytotoxic function upon influenza infection in human lung.* J Clin Invest, 2011. **121**(6): p. 2254-63.
140. Seidel, J.A., et al., *Skin resident memory CD8(+) T cells are phenotypically and functionally distinct from circulating populations and lack immediate cytotoxic function.* Clin Exp Immunol, 2018. **194**(1): p. 79-92.
141. Mackay, L.K., et al., *The developmental pathway for CD103(+)CD8+ tissue-resident memory T cells of skin.* Nat Immunol, 2013. **14**(12): p. 1294-301.
142. Ichikawa, T., et al., *CD103(hi) Treg cells constrain lung fibrosis induced by CD103(lo) tissue-resident pathogenic CD4 T cells.* Nat Immunol, 2019. **20**(11): p. 1469-1480.
143. Oja, A.E., et al., *Trigger-happy resident memory CD4(+) T cells inhabit the human lungs.* Mucosal Immunol, 2018. **11**(3): p. 654-667.
144. Schenkel, J.M., et al., *T cell memory. Resident memory CD8 T cells trigger protective innate and adaptive immune responses.* Science, 2014. **346**(6205): p. 98-101.
145. Khan, T.N., et al., *Local antigen in nonlymphoid tissue promotes resident memory CD8+ T cell formation during viral infection.* J Exp Med, 2016. **213**(6): p. 951-66.
146. Cheuk, S., et al., *CD49a Expression Defines Tissue-Resident CD8(+) T Cells Poised for Cytotoxic Function in Human Skin.* Immunity, 2017. **46**(2): p. 287-300.
147. Schenkel, J.M., et al., *Sensing and alarm function of resident memory CD8(+) T cells.* Nat Immunol, 2013. **14**(5): p. 509-13.
148. Cuburu, N., et al., *Topical herpes simplex virus 2 (HSV-2) vaccination with human papillomavirus vectors expressing gB/gD ectodomains induces genital-tissue-resident memory CD8+ T cells and reduces genital disease and viral shedding after HSV-2 challenge.* J Virol, 2015. **89**(1): p. 83-96.
149. Cuburu, N., et al., *Intravaginal immunization with HPV vectors induces tissue-resident CD8+ T cell responses.* J Clin Invest, 2012. **122**(12): p. 4606-20.
150. Hobbs, S.J. and J.C. Nolz, *Targeted Expansion of Tissue-Resident CD8(+) T Cells to Boost Cellular Immunity in the Skin.* Cell Rep, 2019. **29**(10): p. 2990-2997.e2.

151. Davies, B., et al., *Cutting Edge: Tissue-Resident Memory T Cells Generated by Multiple Immunizations or Localized Deposition Provide Enhanced Immunity.* J Immunol, 2017. **198**(6): p. 2233-2237.
152. Suarez-Ramirez, J.E., et al., *Immunity to Respiratory Infection Is Reinforced Through Early Proliferation of Lymphoid TRM Cells and Prompt Arrival of Effector CD8 T Cells in the Lungs.* Front Immunol, 2019. **10**: p. 1370.
153. Netea, M.G., et al., *Defining trained immunity and its role in health and disease.* Nature Reviews Immunology, 2020.
154. Quintin, J., et al., *Candida albicans infection affords protection against reinfection via functional reprogramming of monocytes.* Cell Host Microbe, 2012. **12**(2): p. 223-32.
155. Yao, Y., et al., *Induction of Autonomous Memory Alveolar Macrophages Requires T Cell Help and Is Critical to Trained Immunity.* Cell, 2018. **175**(6): p. 1634-1650.e17.
156. Benn, C.S., et al., *A small jab - a big effect: nonspecific immunomodulation by vaccines.* Trends Immunol, 2013. **34**(9): p. 431-9.
157. Bull, N.C., et al., *Enhanced protection conferred by mucosal BCG vaccination associates with presence of antigen-specific lung tissue-resident PD-1(+) KLRG1(-) CD4(+) T cells.* Mucosal Immunol, 2019. **12**(2): p. 555-564.
158. Smale, S.T., A. Tarakhovsky, and G. Natoli, *Chromatin contributions to the regulation of innate immunity.* Annu Rev Immunol, 2014. **32**: p. 489-511.
159. Donohoe, D.R. and S.J. Bultman, *Metaboloepigenetics: interrelationships between energy metabolism and epigenetic control of gene expression.* J Cell Physiol, 2012. **227**(9): p. 3169-77.
160. Cheng, S.-C., et al., *mTOR- and HIF-1α–mediated aerobic glycolysis as metabolic basis for trained immunity.* Science, 2014. **345**(6204): p. 1250684.
161. Saeed, S., et al., *Epigenetic programming of monocyte-to-macrophage differentiation and trained innate immunity.* Science, 2014. **345**(6204): p. 1251086.
162. Walsh, K.B., et al., *Quelling the storm: utilization of sphingosine-1-phosphate receptor signaling to ameliorate influenza virus-induced cytokine storm.* Immunol Res, 2011. **51**(1): p. 15-25.
163. Subramanian, A., et al., *Gene set enrichment analysis: A knowledge-based approach for interpreting genome-wide expression profiles.* Proceedings of the National Academy of Sciences, 2005. **102**(43): p. 15545-15550.
164. Mootha, V.K., et al., *PGC-1α-responsive genes involved in oxidative phosphorylation are coordinately downregulated in human diabetes.* Nature Genetics, 2003. **34**(3): p. 267-273.
165. Paules, C.I., et al., *Chasing Seasonal Influenza - The Need for a Universal Influenza Vaccine.* N Engl J Med, 2018. **378**(1): p. 7-9.
166. Liang, S., et al., *Heterosubtypic immunity to influenza type A virus in mice. Effector mechanisms and their longevity.* J Immunol, 1994. **152**(4): p. 1653-61.
167. Richards, K.A., et al., *Cutting edge: CD4 T cells generated from encounter with seasonal influenza viruses and vaccines have broad protein specificity and can directly recognize naturally generated epitopes derived from the live pandemic H1N1 virus.* J Immunol, 2010. **185**(9): p. 4998-5002.
168. Koutsakos, M., et al., *Human CD8(+) T cell cross-reactivity across influenza A, B and C viruses.* Nat Immunol, 2019. **20**(5): p. 613-625.

169. Pizzolla, A., et al., *Influenza-specific lung-resident memory T cells are proliferative and polyfunctional and maintain diverse TCR profiles.* J Clin Invest, 2018. **128**(2): p. 721-733.
170. Marshall, D.R., et al., *Measuring the diaspora for virus-specific CD8+ T cells.* Proc Natl Acad Sci U S A, 2001. **98**(11): p. 6313-8.
171. Schenkel, J.M. and D. Masopust, *Tissue-resident memory T cells.* Immunity, 2014. **41**(6): p. 886-97.
172. Szabo, P.A., M. Miron, and D.L. Farber, *Location, location, location: Tissue resident memory T cells in mice and humans.* Sci Immunol, 2019. **4**(34).
173. Wu, T., et al., *Lung-resident memory CD8 T cells (TRM) are indispensable for optimal cross-protection against pulmonary virus infection.* J Leukoc Biol, 2014. **95**(2): p. 215-24.
174. Zens, K.D., J.-K. Chen, and D.L. Farber, *Vaccine-Generated Lung Tissue-Resident Memory T cells Provide Heterosubtypic Protection to Influenza Infection.* J. Clin. Invest. Insight, 2016. **1** (10): p. e85832.
175. Teijaro, J.R., et al., *Memory CD4 T cells direct protective responses to influenza virus in the lungs through helper-independent mechanisms.* J Virol, 2010. **84**(18): p. 9217-26.
176. Kitamura, D., et al., *A B cell-deficient mouse by targeted disruption of the membrane exon of the immunoglobulin mu chain gene.* Nature, 1991. **350**(6317): p. 423-6.
177. Cunningham, N.R., et al., *Immature CD4+CD8+ thymocytes and mature T cells regulate Nur77 distinctly in response to TCR stimulation.* J Immunol, 2006. **177**(10): p. 6660-6.
178. Ashouri, J.F. and A. Weiss, *Endogenous Nur77 Is a Specific Indicator of Antigen Receptor Signaling in Human T and B Cells.* J Immunol, 2017. **198**(2): p. 657-668.
179. Helft, J., et al., *GM-CSF Mouse Bone Marrow Cultures Comprise a Heterogeneous Population of CD11c(+)MHCII(+) Macrophages and Dendritic Cells.* Immunity, 2015. **42**(6): p. 1197-211.
180. Meredith, M.M., et al., *Expression of the zinc finger transcription factor zDC (Zbtb46, Btbd4) defines the classical dendritic cell lineage.* J Exp Med, 2012. **209**(6): p. 1153-65.
181. Satpathy, A.T., et al., *Zbtb46 expression distinguishes classical dendritic cells and their committed progenitors from other immune lineages.* J Exp Med, 2012. **209**(6): p. 1135-52.
182. Zens, K.D., et al., *Reduced generation of lung tissue-resident memory T cells during infancy.* J Exp Med, 2017. **214**(10): p. 2915-2932.
183. McKinstry, K.K., et al., *Memory CD4+ T cells protect against influenza through multiple synergizing mechanisms.* J Clin Invest, 2012. **122**(8): p. 2847-56.
184. Nayak, J.L., S. Alam, and A.J. Sant, *Cutting edge: Heterosubtypic influenza infection antagonizes elicitation of immunological reactivity to hemagglutinin.* J Immunol, 2013. **191**(3): p. 1001-5.
185. Francis, T., *On the Doctrine of Original Antigenic Sin.* Proceedings of the American Philosophical Society, 1960. **104**(6): p. 572-578.
186. Kim, J.H., et al., *Original antigenic sin responses to influenza viruses.* J Immunol, 2009. **183**(5): p. 3294-301.
187. Zhang, A., et al., *Original Antigenic Sin: How First Exposure Shapes Lifelong Anti–Influenza Virus Immune Responses.* The Journal of Immunology, 2019. **202**(2): p. 335-340.

188. Netea, M.G., et al., *Trained immunity: A program of innate immune memory in health and disease.* Science, 2016. **352**(6284): p. aaf1098.
189. Mitroulis, I., et al., *Modulation of Myelopoiesis Progenitors Is an Integral Component of Trained Immunity.* Cell, 2018. **172**(1-2): p. 147-161.e12.
190. Beauchamp, N.M., R.Y. Busick, and M.A. Alexander-Miller, *Functional Divergence among CD103⁺ Dendritic Cell Subpopulations following Pulmonary Poxvirus Infection.* Journal of Virology, 2010. **84**(19): p. 10191-10199.
191. Kedl, R.M., et al., *Migratory dendritic cells acquire and present lymphatic endothelial cell-archived antigens during lymph node contraction.* Nat Commun, 2017. **8**(1): p. 2034.
192. Hor, J.L., et al., *Spatiotemporally Distinct Interactions with Dendritic Cell Subsets Facilitates CD4+ and CD8+ T Cell Activation to Localized Viral Infection.* Immunity, 2015. **43**(3): p. 554-65.
193. Wilk, M.M., et al., *Lung CD4 Tissue-Resident Memory T Cells Mediate Adaptive Immunity Induced by Previous Infection of Mice with Bordetella pertussis.* J Immunol, 2017. **199**(1): p. 233-243.
194. Sakai, S., et al., *Cutting edge: control of Mycobacterium tuberculosis infection by a subset of lung parenchyma-homing CD4 T cells.* J Immunol, 2014. **192**(7): p. 2965-9.
195. Morabito, K.M., et al., *Intranasal administration of RSV antigen-expressing MCMV elicits robust tissue-resident effector and effector memory CD8+ T cells in the lung.* Mucosal Immunol, 2017. **10**(2): p. 545-554.
196. Teijaro, J.R., *Cytokine storms in infectious diseases.* Seminars in immunopathology, 2017. **39**(5): p. 501-503.
197. Kobasa, D., et al., *Aberrant innate immune response in lethal infection of macaques with the 1918 influenza virus.* Nature, 2007. **445**(7125): p. 319-23.
198. de Jong, M.D., et al., *Fatal outcome of human influenza A (H5N1) is associated with high viral load and hypercytokinemia.* Nat Med, 2006. **12**(10): p. 1203-7.
199. Thiel, V. and F. Weber, *Interferon and cytokine responses to SARS-coronavirus infection.* Cytokine Growth Factor Rev, 2008. **19**(2): p. 121-32.
200. Teijaro, John R., et al., *Endothelial Cells Are Central Orchestrators of Cytokine Amplification during Influenza Virus Infection.* Cell, 2011. **146**(6): p. 980-991.
201. Hogner, K., et al., *Macrophage-expressed IFN-beta contributes to apoptotic alveolar epithelial cell injury in severe influenza virus pneumonia.* PLoS Pathog, 2013. **9**(2): p. e1003188.
202. Perrone, L.A., et al., *H5N1 and 1918 Pandemic Influenza Virus Infection Results in Early and Excessive Infiltration of Macrophages and Neutrophils in the Lungs of Mice.* PLOS Pathogens, 2008. **4**(8): p. e1000115.
203. Moskophidis, D. and D. Kioussis, *Contribution of virus-specific CD8+ cytotoxic T cells to virus clearance or pathologic manifestations of influenza virus infection in a T cell receptor transgenic mouse model.* J Exp Med, 1998. **188**(2): p. 223-32.
204. Peper, R.L. and H. Van Campen, *Tumor necrosis factor as a mediator of inflammation in influenza A viral pneumonia.* Microb Pathog, 1995. **19**(3): p. 175-83.
205. Branchett, W.J. and C.M. Lloyd, *Regulatory cytokine function in the respiratory tract.* Mucosal Immunology, 2019. **12**(3): p. 589-600.
206. Brooks, D.G., et al., *Interleukin-10 determines viral clearance or persistence in vivo.* Nat Med, 2006. **12**(11): p. 1301-9.

207. Loebbermann, J., et al., *IL-10 regulates viral lung immunopathology during acute respiratory syncytial virus infection in mice.* PLoS One, 2012. **7**(2): p. e32371.
208. Sun, J., et al., *Autocrine regulation of pulmonary inflammation by effector T-cell derived IL-10 during infection with respiratory syncytial virus.* PLoS Pathog, 2011. **7**(8): p. e1002173.
209. Zaslavsky, E., et al., *Antiviral Response Dictated by Choreographed Cascade of Transcription Factors.* The Journal of Immunology, 2010. **184**(6): p. 2908-2917.
210. Napolitani, G., et al., *Selected Toll-like receptor agonist combinations synergistically trigger a T helper type 1-polarizing program in dendritic cells.* Nat Immunol, 2005. **6**(8): p. 769-76.
211. O'Dwyer, D.N., R.P. Dickson, and B.B. Moore, *The Lung Microbiome, Immunity, and the Pathogenesis of Chronic Lung Disease.* Journal of immunology (Baltimore, Md. : 1950), 2016. **196**(12): p. 4839-4847.
212. Gerosa, F., et al., *CD4(+) T cell clones producing both interferon-gamma and interleukin-10 predominate in bronchoalveolar lavages of active pulmonary tuberculosis patients.* Clin Immunol, 1999. **92**(3): p. 224-34.

Appendix A: Accepted Abstracts

Oral Presentation: Lung Tissue Resident Memory T cells coordinate effector cell tissue infiltration during influenza infection
Paik DH, Farber DL

American Association of Immunologists (AAI)
Immunology 2018. Austin, TX
Travel Award Recipient

Abstract:

Influenza is a leading cause of hospitalizations and deaths worldwide, and annual vaccinations are required to generate protective antibodies against a narrow range of strains. Lung tissue resident memory (TRM) T cells are a non-circulating memory subset that are generated after infection or live vaccination, and these TRM confer broad cross-strain protection. However, the mechanisms by which they mediate their protective response are not defined. We investigated the tissue specific events during an active murine influenza response, including TRM-mediated protection and effector T cell trafficking. To specifically determine the role of TRM, we treated mice with the drug Fingolimod (FTY720), which sequesters circulating lymphocytes into secondary lymphoid organs, enriching the lung for tissue resident memory cells. During FTY720 treatment, we found that TRM cells confer protection against influenza virus very early in the disease course. Later in the disease course by Day 5, TRM also coordinate the recruitment of influenza-specific effector T cells into the lung resident niche and mediate *in situ* proliferation as measured by BrdU incorporation. Total lung RNA sequencing during active infection and FTY720 treatment reveal candidate TRM-associated chemokine pathways for tissue lymphocyte trafficking. These findings indicate that TRM uniquely influence the cellular dynamics of the lung resident niche to mediate cross-strain protection against influenza.

Appendix B: Abstracts of contributing author manuscripts

Paik DH, Farber DL. Influenza infection imprints local lymphoid sites to promote lung resident heterosubtypic immunity. *Journal of Experimental Medicine*. In review.

Influenza infection generates tissue-resident memory T cells (TRM) that are maintained in the lung and can mediate protective immunity to heterologous influenza strains, though the precise mechanisms of local T cell-mediated protection are not well understood. In a murine heterosubtypic influenza challenge model, we demonstrate that protective lung T cell responses are independent of B cell responses, and derive from *in situ* activation of tissue resident memory T cell (TRM) and the enhanced generation of effector T cells from the local lung draining mediastinal lymph nodes (medLN). Primary infection fortified the medLN with an increased number of conventional dendritic cells (cDC) that mediate enhanced priming of T cells, including those specific for newly encountered epitopes; cDC depletion during the recall response diminished medLN T cell generation and heterosubtypic immunity. Our study shows that during a protective recall response, cDC in a fortified LN environment enhance the breadth, generation, and tissue migration of effector T cells to augment lung TRM responses.

Turner DL, Goldklang M, Cvetkovski F, **Paik D**, Trischler J, Barahona J, Cao M, Dave R, Tanna N, D'Armiento JM, Farber DL (2018). Biased Generation and In Situ Activation of Lung Tissue-Resident Memory CD4 T Cells in the Pathogenesis of Allergic Asthma. *J Immunol*. doi: 10.4049/jimmunol.1700257.

Asthma is a chronic inflammatory disease mediated by allergen-specific CD4 T cells that promote lung inflammation through recruitment of cellular effectors into the lung. A subset of lung T cells can persist as tissue-resident memory T cells (TRMs) following infection and allergen induction, although the generation and role of TRM in asthma persistence and pathogenesis remain unclear. In this study, we used a mouse model of chronic exposure to intranasal house dust mite (HDM) extract to dissect how lung TRMs are generated and function in the persistence and pathogenesis of allergic airway disease. We demonstrate that both CD4+ and CD8+ T cells infiltrate into the lung tissue during acute HDM exposure; however, only CD4+ TRMs, and not CD8+ TRMs, persist long term following cessation of HDM administration. Lung CD4+ TRMs are localized around airways and are rapidly reactivated upon allergen re-exposure accompanied by the rapid induction of airway hyperresponsiveness independent of circulating T cells. Lung CD4+ TRM activation to HDM challenge is also accompanied by increased recruitment and activation of dendritic cells in the lungs. Our results indicate that lung CD4+ TRMs can perpetuate allergen-specific sensitization and direct early inflammatory signals that promote rapid lung pathology, suggesting that targeting lung CD4+ TRMs could have therapeutic benefit in alleviating recurrent asthma episodes.